BERICHTE
aus dem Fachbereich Geowissenschaften
der Universität Bremen

Nr. 134

Draschba, S.

NORTH ATLANTIC CLIMATE VARIABILITY RECORDED IN REEF CORALS FROM BERMUDA

Berichte, Fachbereich Geowissenschaften, Universität Bremen, Nr. 134,
108 Seiten, Bremen 1999

ISSN 0931-0800

Die "Berichte aus dem Fachbereich Geowissenschaften" werden in unregelmäßigen Abständen vom Fachbereich 5, Universität Bremen, herausgegeben.

Sie dienen der Veröffentlichung von Forschungsarbeiten, Doktorarbeiten und wissenschaftlichen Beiträgen, die im Fachbereich angefertigt wurden.

Die Berichte können bei:

Frau Gisela Boelen

Sonderforschungsbereich 261

Universität Bremen

Postfach 330 440

D 28334 BREMEN

Telefon: (49) 421 218-4124

Fax: (49) 421 218-3116

angefordert werden.

Zitat:

Draschba, S.

North Atlantic climate variability recorded in reef corals from Bermuda.

Berichte, Fachbereich Geowissenschaften, Universität Bremen, Nr. 134, 108 Seiten, Bremen, 1999.

ISSN 0931-0800

NORTH ATLANTIC CLIMATE VARIABILITY RECORDED IN REEF CORALS FROM BERMUDA

Dissertation
zur Erlangung des Doktorgrades
am Fachbereich Geowissenschaften
der Universität Bremen

vorgelegt von
Sylke Draschba
Bremen 1998

Tag des Kolloquiums: 12. Februar 1999

Gutachter:

Prof. Dr. G. Wefer

Prof. Dr. R. Henrich

Prüfer:

Priv. Doz. Dr. A. Freiwald

Dr. J. Pätzold

SUMMARY

Climate sensitive proxies can open windows into times, for which instrumental observations are lacking. A strong tool for gaining insight into climate changes through the most recent geological period of the past several centuries, is the use of massive reef coral skeletons. The research reported in this thesis analyzes climate sensitive coral proxy records from Bermuda and is directed at characterizing seasonal, inter-annual and long-term climate fluctuations relevant to the western Sargasso Sea. The type of climate proxies used include skeletal growth parameters, i.e. annual growth rates and density, and the stable oxygen and carbon isotope composition ($\delta^{18}O$ and $\delta^{13}C$, respectively) of coral skeletons.

Chronologies of annual density and growth rate were analyzed in the skeletons of two colonies of *Diploria labyrinthiformis*. The records cover the last 150 years, a period where instrumental climate data are available for comparison and evaluation of the proxy records. Annual values of skeletal density and growth rate reveal response to changes in sea surface temperature and the sea surface convective activity near Bermuda, and large-scale North Atlantic atmospheric mass oscillations. In *D. labyrinthiformis*, skeletal density is the more accurate proxy for climate variations compared to annual growth rates. Skeletal density is high in response to high sea surface temperatures and an enhanced North Atlantic air pressure gradient, i.e. the North Atlantic Oscillation. In general, the coral skeletons portray a most sensitive picture of winter environmental conditions, while the response to the climatic summer regime is minor. The skeletal growth parameters also respond to the extent of Bermuda surface water convection that occurs during winter and reflects both atmospheric and subsurface conditions in the western subtropical gyre. The strength of vertical mixing during winter is interpreted as a gauge for nutrient supply for the corals.

The stable oxygen isotope composition in the skeletons of *D. labyrinthiformis* colonies from Bermuda serves as a proxy for sea surface temperatures. Modern coral $\delta^{18}O$ chronologies, covering periods during the 19^{th} and 20^{th} century, show a strong correspondence with local instrumental temperature data. A specific $\delta^{18}O$ versus temperature relationship, achieved from the modern records, is applied to $\delta^{18}O$ chronologies that extend between AD 1350 and 1630. These records describe periods of the Little Ice Age. Estimates of inter-annual sea surface temperature variations during Little Ice Age, achieved from coral $\delta^{18}O$, indicate a magnitude in the order of modern sea surface temperature variability. The ancient oxygen isotope

temperature proxy records are compared to records of skeletal density from the skeleton slices. Skeletal density time series, which were established to serve as an indicator for sea surface temperatures, reveal a strong similarity with coral $\delta^{18}O$, supporting the credibility of the reconstructed temperature anomaly pattern between the 14th and 17th century.

Stable carbon isotope ratios ($\delta^{13}C$) in three modern (1969 to 1993), high resolution coral records of *D. labyrinthiformis* and *Montastrea cavernosa* monitor changes in the extent of winter convection near Bermuda on both seasonal and inter-annual time-scales. The extent of vertical ventilation in winter largely influences the pattern of sea surface temperatures and nutrient availability in the upper water column. This prerequisite is confirmed by a strong correspondence between coral $\delta^{13}C$ and $\delta^{18}O$ in both the modern and three ancient stable isotope records (AD 1350 to 1630), indicating a process that generates both proxies. The three stable isotope records that span periods between the 14th and 17th century represent a contribution to elucidate the history of the hydrographic circulation pattern in the western subtropical gyre and can deliver implements for the reconstruction of large-scale North Atlantic pressure alterations.

ACKNOWLEDGEMENTS

Prof. Dr. Gerold Wefer gave me the opportunity to pursue this Ph.D.. I would like to express my gratitude for this chance and his support throughout the work.

Special thanks also belong to Prof. Dr. Rüdiger Henrich for being a referee to this thesis.

A large part of what I learned about corals, I owe to Dr. Jürgen Pätzold, my advisor. Without his help and support, this work would not have been possible and he deserves my grateful and heartfelt thanks.

I would like to thank my Ph.D. colleagues, Yaser Moustafa, my office mate, and Henning Kuhnert and Tomas Felis, from next-door, for the very easy-going and comfortable atmosphere in our lab. Especially, I want to mention the constant readiness for help of Henning, in both scientific and computer questions, without the latter I sometimes probably would have gone insane, or alternatively, wrecked my PC.

Notably, I would like to acknowledge the pleasant atmosphere in the working group Meeresgeologie, which made for an appreciable working ambience. Elemental support in technical questions came from Dr. Volker Ratmeyer and Dr. Ursula Röhl, which was of great benefit for this work. Respectful thanks also belong to Dr. Monika Segl and the team from the stable isotope laboratory, who cope with the huge amounts of stable isotope samples.

The valuable discussions with Prof. Dr. Wolfgang H. Berger, Dr. Jelle Bijma, Dr. André Freiwald and Dr. Christoph Waldmann have been most enriching for my knowledge and they deserve great acknowledge for their interest in my work. Dr. Torsten Bickert, Dr. Burkhard Flemming and Dr. Hannes Grobe provided help during the sample collection in Bermuda.

I would also like to thank my precious circle of friends, who always lend me a patient ear and shared my preference for a certain French red wine. My parents have supported me along my educational way and it's to them, I owe my sincere thanks. My beloved partner Robert Huber has always been there for me. His endearing encouragement and faith in me makes my day, and I want to express him my deep gratitude and love.

This study was conducted as part of the Research Project "Paläoklima, Klimavariabilität im Spätquartär", funded by the German Ministry for Education, Science, Research and Technology (BMBF).

TABLE OF CONTENTS

1 INTRODUCTION

The climate of our planet is expected to change significantly within the next century due to the increasing greenhouse effect. In order to reach an early prediction how climate may change in the future, whether as a consequence of human activities or of natural variability, we first need to understand the true nature of climate variations. Current approaches, used to predict future climate development, are mainly based on model calculations. An alternative and promising approach to assess the responses of the global climate system to disturbances, is to investigate past global changes.

High frequency climate variations that occurred during the last several centuries are of particular relevance but unfortunately, sufficient detailed instrumental records are scarce and rarely span more than a few decades. Especially low latitudes which play an important role in the global climate system, are rarely monitored by climate observation instruments. Furthermore, large areas of the oceans are similarly devoid of instrumental observations. In order to fill these temporal and spatial gaps, indirect information on past climate conditions can be deduced from climate-sensitive proxies. Such proxy extensions that have the potential to accurately portray climate variations, are needed to provide background data to distinguish natural variability from anthropogenic change. Especially, climate variability on decadal to century time-scales is of most relevance to today's social and political concerns (IPCC [Intergovernmental Panel on Climate Change], 1992; 1996; 1998).

Excellent resources, which can give us insights on climate changes over the last few centuries, are large colonies of massive reef corals. Taxonomically, corals belong to the phylum Coelenterata and the class Anthozoa. Present day coral reefs are dominated by colonies of the reef-building (hermatypic) order of scleractinians (stony corals). The coral polyps form only a thin living tissue layer, covering the aragonitic skeleton (Barnes and Lough, 1993). In their tissue the polyps host photosynthesizing endosymbionts (unicellular dinoflagellates), the zooxanthellae (Schuhmacher, 1988).

In numerous studies, skeletons of massive scleractinian reef corals have been proven to sensitively monitor changes of their marine environment on a seasonal to century time-scales (e.g. Pätzold, 1984; Cole and Fairbanks; 1990; Pätzold *et al.*, 1998; Dunbar *et al.*, 1994; Quinn *et al.*, 1996; Crowley *et al.*, 1997). Skeletal growth parameters, and trace element and

stable isotopic composition of coral skeletons can reveal a detailed history of past environmental conditions. Among other environmental parameters, these proxy indicators monitor changes in sea surface temperature ($\delta^{18}O$, Sr/Ca, U/Ca, skeletal growth parameters), sea surface salinity ($\delta^{18}O$, U/Ca), insolation ($\delta^{13}C$, skeletal growth parameters), and upwelling ($\delta^{13}C$).

The valuable combination of abundant geochemical tracers and skeletal growth indices, and the applicability to both recent and past climate changes establishes massive reef corals as one of the most potential natural marine environmental proxies. Since hermatypic reef corals flourish in the shallow water of the tropics and subtropics, they can provide proxy climate information for regions, partly devoid of instrumental climate observations. An exceptionally high temporal resolution of climate proxy information is given by rapid skeletal growth, that typically ranges between several millimeters (e.g. *Diploria, Montastrea*) and a centimeter (e.g. *Porites*) per year. Accordingly, several studies have even been able to deduce coral time series as records for transient climate events with weekly or biweekly resolution (Gagan *et al.*, 1994, 1996; McCulloch *et al.*, 1994; Gagan and Chivas, 1995; Leder *et al.*, 1996). Meanwhile, large colonies can contain a record of several centuries (Pätzold *et al.*, 1998). An excellent dating capacity is given by annual skeletal density banding (Knutson *et al.*, 1972), which can be used comparable to tree rings. These annual alternating bands of high and low skeletal density provide the strong stratigraphic backbone by counting annual band-pairs backward from the top of the colony, and thus allow the determination of calendric years for certain skeletal layers.

The analyses of stable oxygen and carbon isotopic compositions ($\delta^{18}O$ and $\delta^{13}C$, respectively) and of skeletal growth parameters in coral skeletons, as investigated in this thesis, are the most established approaches in coral paleoclimate studies. Detailed descriptions of the coral climate proxy indicators, used in this study, are given in Chapter 1.3. The data were obtained from the skeletons of the hermatypic reef corals *Diploria labyrinthiformis* and *Montastrea cavernosa* from Bermuda. Both species belong to the most abundant reef-building coral genus at Bermuda (Thomas and Logan, 1991).

1.1 MAIN OBJECTIVES

In this thesis, the skeletons of massive reef corals from Bermuda are examined to record and portray changes in the climatic and environmental conditions of their surrounding marine habitat. The general aim of this work concentrates on the development of coral skeletal climate proxy time series on different time-scales. A coral based proxy record, such as from Bermuda, which remained mainly unaffected by local coastal and terrestrial processes, is relevant to clearly relate local changes in the surface hydrography, to atmospheric and oceanic processes that operate on much larger spatial scales in the North Atlantic (e.g. North Atlantic Oscillation).

One part of this study examines skeletal growth parameters, i.e. annual skeletal density and growth rate, in coral skeletons over the last 150 years. The investigation was undertaken with the goal of deciphering the main physical processes that yield an influence on growth parameters in the skeletons of *D. labyrinthiformis*. An additional question which is addressed, is if the response of skeletal growth parameters is seasonally dependent. With these prerequisites, a sclerochronological approach on the reconstruction of changes in pattern of hydrographic and atmospheric circulation variability in the western North Atlantic shall be supported.

Another aspect dealt with in this thesis, is the stable oxygen isotopic composition ($\delta^{18}O$) in coral skeletons. The $\delta^{18}O$ signal is used to reconstruct temperature changes during the Little Ice Age. This period describes an era in the current millenium, for which an extension of the climate proxy archive is most desirable. A further issue addressed at this point is the possibility to combine the proxy information, obtained from both coral $\delta^{18}O$ and skeletal growth parameters.

A third topic of concern, is the stable carbon isotopic composition in coral skeletons. Various factors can potentially generate the $\delta^{13}C$ signal in coral skeletons. Therefore, it is important to determine the main environmental influence on $\delta^{13}C$ in the investigated skeletons. Furthermore, possible growth-depth or species related differences in coral $\delta^{13}C$ are considered. A further aim of this investigation is directed at the development of $\delta^{13}C$ time series that cover periods during the Little Ice Age. These records are sought to deliver implements for the reconstruction of the low-latitude North Atlantic hydrographic circulation pattern.

1.2 ENVIRONMENTAL SETTING OF BERMUDA

The Bermuda Islands are located in the western Sargasso Sea, in the northwestern Atlantic Ocean at 32° 20'N and 64° 50'W. It lies at approximately 1000 km distance from the U.S. coast (Figure 1.1). Bermuda is composed of an archipelago of over 120 islands. The archipelago is supported on a volcanic seamount, rising from depths of about 4000m, and capped by limestone sediments and reefs.

From a biological point of view, an interesting feature of the islands is the northerly extension of the subtropical climate system to this latitude. This is due to warm water masses which are transported north by the Gulf Stream. Thanks to this fact, the Bermuda reefs represent the northernmost limit of reef coral distribution (Thomas and Logan, 1991). Hermatypic reef corals that grow at the edge of the latitudinal range of 30°N are strongly affected by changes in climate, i.e. they will most sensitively monitor those conditions, which form some type of environmental limit. Besides various limiting factors, such as light and nutrients, water temperatures below 18°C can impede the development of hermatypic coral growth (Wood, 1983). Sea surface temperatures in Bermuda can approach such low figures during winter (Bermuda Biological Station for Research, 1993). Consequently, the proxy signals of the investigated corals can be expected to display a most sensitive picture of conditions outside the optimum range of coral growth.

Furthermore, the Bermuda reefs are among the only ones that grow in typical open-ocean conditions in the North Atlantic, and hence preserve a record of them. Indeed, within the broad region of the Sargasso Sea subtropical gyre the hydrographic properties show large geographic uniformity (Joyce and Robbins, 1996), and Bermuda can well serve as a representative for a broad western Atlantic region.

In general, the North Atlantic gyre has an overriding influence on the oceanography of Bermuda. The Antilles Current dominates the hydrography during summer and autumn and the Gulf Stream gains influence on the islands during winter and spring months (Figure 1.1). Climatic and oceanographic information on Bermuda is detailed in the Bermuda Environmental Scenario (Anonymous, 1974).

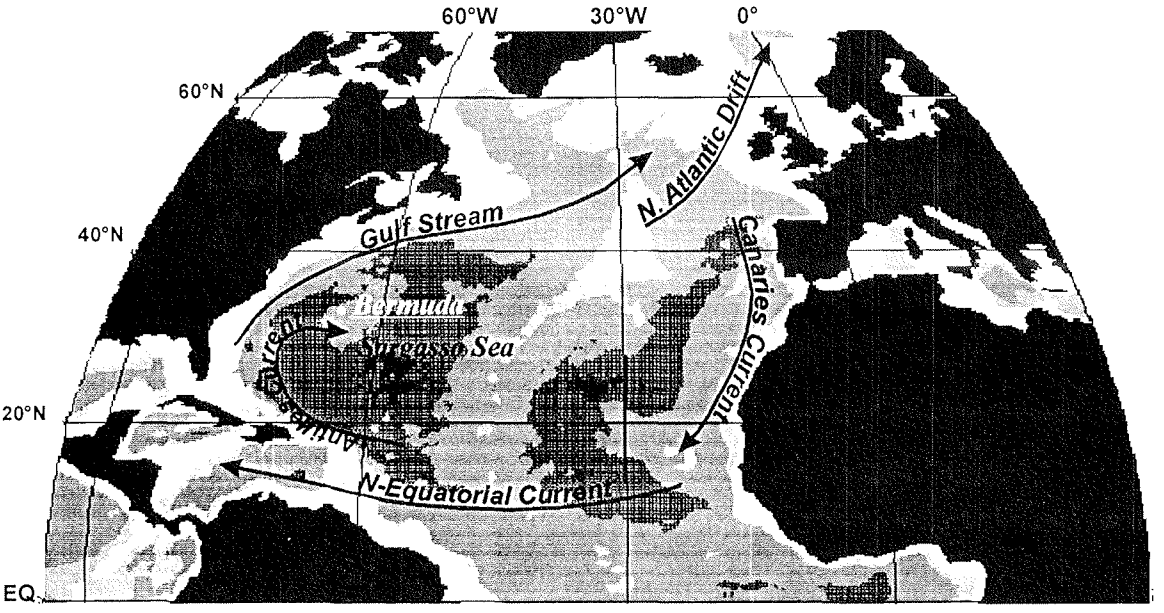

Figure 1.1 Major components of the North Atlantic surface current system and the location of the Bermuda islands in the western Sargasso Sea.

1.2.1 Climatic conditions

The subtropical climate of Bermuda is largely controlled by the surrounding ocean. Air and sea surface temperatures are closely linked in Bermuda. Seasonally, average sea surface temperatures range between 19°C in February and 26°C in August. The dominant atmospheric feature in Bermuda is the Azores-Bermuda High. The influence of the subtropical high pressure ridge is strongest during summer, coinciding with slight southerly winds and low cloud cover and rainfall (Bermuda Environmental Scenario, 1974). A strong stratification of the upper water column leads to oligotrophic conditions in the surface layer in summer (Menzel and Ryther, 1960, 1961).

The region is characterized by a strong seasonality in mixed layer depths. Convective mixing of the upper 50 to 400m with deeper, colder, and nutrient richer waters is confined to winter and early spring (Spitzer and Jenkins, 1989; Siegel *et al.*, 1990; Michaels *et al.*, 1994). This is due to an increase in the westerly wind component and decreasing atmospheric pressure. Light availability is reduced during winter due to higher cloud cover and decreased net insolation. Sea surface salinity shows little variation around 36.5‰, on both seasonal (36.20‰ in August to 36.70‰ in April) and inter-annual time-scales (general range between

36.35‰ and 36.60‰) (Bermuda Environmental Scenario, 1974, Bermuda Biological Station for Research, 1993). In the following, particular attention shall be directed to the role of the North Atlantic Oscillation.

1.2.2 North Atlantic Oscillation

The North Atlantic Oscillation (NAO) describes the mutual north-south oscillation in atmospheric mass, centered near the semi-permanent Icelandic Low and the Subtropical High (Bjerknes, 1964), i.e. when pressure is below normal near Iceland, it is generally above normal in the Subtropical High, and vice versa. Large amplitude fluctuations in the inter-annual to decadal modes of the NAO are increasingly recognized for their impact on the weather conditions in the North Atlantic sector and adjacent continents (e.g. Marshall and Kushnir, 1997).

An index of the atmospheric mass alteration was first given by using the difference of normalized winter (December to February) atmospheric sea level pressures between Ponta Delgada, Azores, and Akureyri, Iceland (Rogers, 1984). Hurrell (1995; 1996) could temporally extend the index into 1864 by using data from Lisbon, Portugal and Stykkisholmur, Iceland. Influenced by the Subtropical High, Bermuda was proposed to serve as a representative for the Azores/Lisbon Station by Molinari *et al.* (1997). Based on COADS (Comprehensive Ocean-Atmosphere Data Set), a Bermuda-Iceland pressure-index can be calculated back to 1847.

The NAO is held responsible for generating systematic, large zonal patterns in the anomalies of wind speed, heat fluxes, and therefore influences sea surface temperatures over much of the extratropical North Atlantic (Deser and Blackmon, 1993; Kushnir, 1994; Hansen and Bezdek, 1996; Sutton and Allen, 1997; Mc Cartney, 1997). Among a wide range of coherencies with Atlantic climate indices, it has recently been noticed that the NAO is an important factor in controlling the path and intensity of the Atlantic storm track (Rogers, 1990; Hurrell, 1995; 1996) and propagating sub-surface temperature anomalies that move from the western subtropical gyre downstream along the gyres' circulation pathways (Hansen and Bezdek, 1996; Sutton and Allen, 1997; Molinari *et al.*, 1997).

Kushnir (1994) identified the Sargasso region as one of the centers of action of the NAO. Two extreme modes of winter conditions in Bermuda are related to the NAO's atmospheric circulation changes: During high index years, westerly wind stress across the Atlantic Ocean

increases but the zone of maximum wind stress is shifted northward from the Sargasso Sea (Hurrell, 1996). This shift yields a reduction of wind stress at the Bermuda latitude. Consequently, heat-loss to the atmosphere is reduced (Molinari *et al.*, 1997) and periods of low convection of the surface layers in winter were noted near Bermuda (Michaels *et al.*, 1994; Dickson *et al.*, 1996). Low NAO index years are characterized by a southwestward shift in the wind track, into the western Sargasso region (Hurrell, 1996). Synchronous cooling of the surface waters (Molinari *et al.*, 1997) can be attributed to wind induced latent heat flux (Deser and Blackmon, 1993; Cayan, 1992) and to surface mixing with deeper and thus colder waters (Dickson *et al.*, 1996; Reverdin *et al.*, 1997), resulting in increased pumping of nutrients to the sea surface (Michaels *et al.*, 1994).

Although present studies are trying to answer the numerous questions arising from the current picture of the NAO, observational evidence draws a very complex scenario, in which the ocean and atmosphere interact on a wide range of temporal frequencies. One of the major questions concerns possible active coupling between the atmosphere and the ocean. While for example Marshall and Molteni (1993) argue that the NAO arises mostly from atmospheric processes, a coupled ocean-atmospheric mechanism has been proposed by Latif *et al.* (1996). Another important interest regards to the NAO's future impact on climate variability (CLIVAR, 1997). With the basis of a better understanding of the spatial and temporal properties of the NAO, it might be possible to make future predictions for the recurring atmospheric patterns (Griffies and Bryan, 1997). For such purpose, the NAO must be characterized on a longer term basis as it has been presently (Marshall and Kushnir, 1997).

While longest meteorological records extent to the mid 19th century, there is only limited proxy information on the history of the NAO. A terrestrial reconstruction is based on circum-Atlantic tree-ring chronologies from North America and Europe (Cook *et al.*, 1998), but marine proxy records, which can elucidate the response and the role of the ocean, are lacking so far. In this study, a composite record of annual skeletal density of two Bermuda corals is shown to yield a signal of changes in the hemispherical pressure gradient, and hence, deliver a tool to expand the archive of marine data sets for the reconstruction of the NAO. The corals investigated in this thesis could be demonstrated to primarily portray a picture of winter conditions. This seasonally specific respond corresponds to the season when the NAO pattern is best defined in amplitude and spatial coverage (Marshall *et al.*, 1993).

1.3 CORAL CLIMATE PROXY INDICATORS

1.3.1 Stable oxygen isotopes

The most commonly used parameter in coral paleoceanography studies is the oxygen isotopic composition of the aragonite skeletons. The interpretation of the stable oxygen isotope ratio is relatively straightforward and measurements can be developed in quantity. Stable oxygen isotope ratios (and analogously stable carbon isotope ratios) are reported in the δ-notation:

$$\delta^{18}O[‰] = \left[\frac{\left(\frac{^{18}O}{^{16}O}\right)_{Sa} - \left(\frac{^{18}O}{^{16}O}\right)_{St}}{\left(\frac{^{18}O}{^{16}O}\right)_{St}} \right] * 1000 \qquad \begin{matrix} Sa = Sample \\ St = Standard \end{matrix} \qquad (1)$$

The ratios of stable oxygen isotopes in coral skeletons reflect a combination of changes in sea surface temperature and the isotopic composition of the ambient seawater. During temperature dependent kinetic fractionation, $\delta^{18}O$ of biogenic carbonate decreases by 0.22‰ for every 1°C increase in water temperature (Epstein *et al.*, 1953). The $\delta^{18}O$ of the seawater, in turn, varies as a result of the hydrologic balance and can be deduced from changes in sea surface salinity (Fairbanks *et al.*, 1992).

Unlike many other marine organisms, such as many foraminifera and most mollusk species, stony corals precipitate aragonite with an offset from isotopic equilibrium. In scleractinian corals, the isotopic offset accounts for approximately -2 to -3‰ $\delta^{18}O$, but was reported to be consistent within scleractinian coral genera (Weber and Woodhead, 1972), and along the rapidly growing portions of the skeleton (Pätzold, 1986; McConnaughey, 1989).

In regions where seawater isotopic composition remains reasonably constant, skeletal $\delta^{18}O$ can be converted into estimates of past sea surface temperatures, with a resolution down to about 0.5°C (e.g. Fairbanks and Dodge, 1979; Pätzold, 1984, Wefer and Berger, 1991; Winter *et al.*, 1991; Dunbar *et al.*, 1994; Crowley *et al.*, 1997). Alternatively, regions that reveal little variation in sea surface temperature allow the detection of variations in the input of isotopically lighter rainfall of runoff (Cole and Fairbanks, 1990; Linsley *et al.*, 1994; Tudhope *et al.*, 1995). The interpretation of coral $\delta^{18}O$ is complicated in regions, which are characterized by variability of both parameters (Carriquiry *et al.*, 1993). In Bermuda, changes

in salinity are small (see Chapter 1.2) and the coral $\delta^{18}O$ signals reported here are interpreted to dominantly reflect changes in sea surface temperature.

1.3.2 Stable carbon isotopes

Though the literature on carbon isotopic composition in coral skeletons suggests a very complex system (Aharon, 1991; Wefer and Berger, 1991; McConnaughey, 1996), two key mechanisms are held responsible for stable carbon isotope fractionation: kinetic and metabolic fractionation effects (McConnaughey, 1989). The kinetic disequilibrium results in simultaneous depletion of ^{18}O and ^{13}C. While $\delta^{18}O$ is largely affected by temperature (as described above) this effect only accounts for a decrease of 0.035‰ $\delta^{13}C$ per degree Celsius (Grossman and Ku, 1986).

Metabolic fractionation effects on coral $\delta^{13}C$ are much more complex. Radioactive tracer experiments showed that algal photosynthesis enhances coral calcification and that metabolic carbon is incorporated into the coral skeleton (Goreau, 1963). The skeleton calcification takes place from an internal carbon pool which consequently is fed by varying rates of carbon derived from both seawater and metabolism (Goreau, 1963, 1977a, b; Weber and Woodhead, 1970; Erez, 1978). The most commonly held opinion is that, at high rates of skeletal accretion, coral $\delta^{13}C$ is dominantly controlled by varying rates of symbiotic photosynthesis and respiration (Swart, 1983; Swart *et al.*, 1996).

Two competing theories, plead by Goreau (1977a, b) and Erez (1978), concentrate on the role of zooxanthellae photosynthesis: The prevalent theory by Goreau (1977a, b) is based on the observation that there is a corresponding increase in skeletal $\delta^{13}C$ with increased photosynthesis of algal symbionts, which preferentially fix isotopically light $^{12}CO_2$ (Weber and Woodhead, 1970; 1972). As a result, the corals' internal carbon pool, and subsequently the deposited carbonate, are argued to become relatively enriched in ^{13}C (Goreau 1977a, b; Land *et al.*, 1977; Weber *et al.*, 1976; Fairbanks and Dodge, 1979; Cole and Fairbanks, 1990; Bosscher, 1992). The alternative theory introduced by Erez (1978) suggests that increasing rates of photosynthesis, relative to respiration, provide a generally higher concentration of metabolic CO_2, and hence ^{12}C in the internal carbon pool and act to isotopically deplete the coral skeleton.

In general, coral $\delta^{13}C$ is interpreted in terms of changes in the environment, which either have the capacity to influence the metabolism of the coral-symbiont system, or reflect changes in the carbon isotopic composition of the seawater (Nozaki, 1978; Winter *et al.*, 1991). Often, variations in coral $\delta^{13}C$ were explained by changes in photosynthetic activity, i.e. variations in light intensity (Fairbanks and Dodge, 1979; Weil *et al.*, 1981; Pätzold, 1984; Cole and Fairbanks, 1990; Shen *et al.*, 1992; Klein *et al.*, 1992). Other studies suggest that coral $\delta^{13}C$ should indicate the trophic capacity, i.e. if the internal carbon pool derives more carbon from either allochthonous sources (e.g. zooplankton, dissolved organic carbon) or from zooxanthellae photosynthesis, since both sources have distinctive $\delta^{13}C$ values (Swart, 1983; Swart *et al.*, 1996). Gagan *et al.* (1996) found a signal of reproductive activity in their coral $\delta^{13}C$. Other studies concentrated on tracing changes of the isotopic composition of the global carbon pools (Nozaki, 1978; Winter *et al.*, 1991). The release of carbon into the atmosphere since the beginning of the 19th century, due to anthropogenic activities, has caused an increase in concentration, as well as a decrease in the isotopic composition of atmospheric carbon dioxide (e.g. Friedli *et al.*, 1986).

1.3.3 Skeletal growth parameters

The skeletons of hermatypic reef corals contain an intriguing growth structure. Horizontal skeleton growth increments are characterized by alternating layers of high and low bulk density (Figure 1.2). This density banding is mainly manifested in the varying size and space of the skeletal elements (Pätzold, 1986; Barnes and Devereux, 1988; Dodge *et al.*, 1992). A pair of such high and low density bands was first reported to be of annual nature by Knutson *et al.* (1972). They suggested that coral skeletal banding may function as the tropical marine analogue for tree-rings in paleoclimate studies.

Two parameters define linear skeletal growth rate: Skeletal bulk density and accumulation rate of new carbonate, i.e. calcification rate (Dodge and Brass, 1984):

$$linear\ growth\ rate = \frac{calcification\ rate}{bulk\ density} \qquad (2)$$

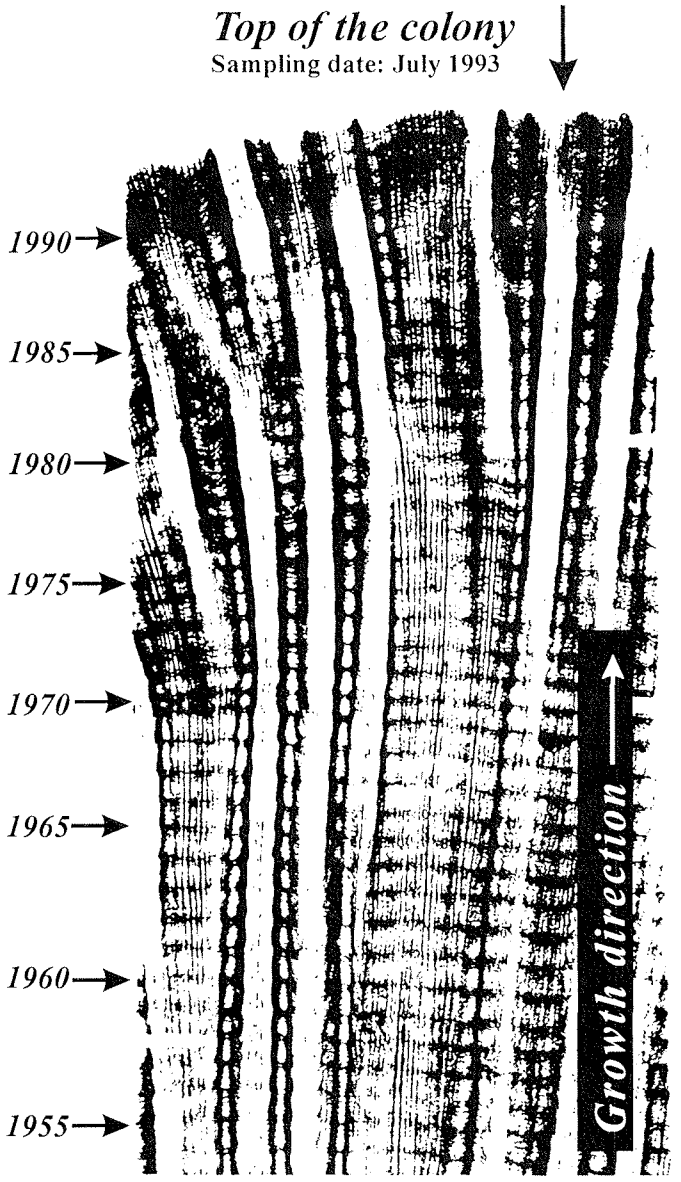

Figure 1.2 X-radiograph positive of a 6 mm skeleton slice of *Diploria labyrinthiformis*, showing clear horizontal annual density banding. The colony was sampled in July 1993. The last density band that has been secreted is a complete high density band.

Skeletal growth parameters were shown to reveal variance across environmental gradients (e.g. Logan and Tomascik, 1991; Bosscher, 1992; Klein *et al.*, 1993; Logan *et al.*, 1994), and in response to changes in environmental conditions with time (e.g. Dodge, 1981; Dullo *et al.*, 1993; Dunbar *et al.*, 1994; Lough and, 1997). Most commonly, records of annual linear extension rates where analyzed (e.g. Dodge and Vaisnys, 1975; Pätzold *et al.*, 1998), but the literature also contains proxy-records of coral skeletal density (Lough and Barnes, 1990) and calcification rate (Lough and Barnes, 1997).

Often, temporal variability in skeletal growth parameters was found to be linked to changes in water temperature (Dodge and Vaisnys, 1975; Gladfelter *et al.*, 1978), or light intensity (Weber *et al.*, 1976; Taylor *et al.*, 1993). Other environmental factors discussed to influence skeletal growth include nutrient availability (Pätzold *et al.*, 1998; Dullo, 1993), wave energy (Logan *et al.*, 1994), factors affecting gametogenesis of polyps (Wellington and Glynn, 1983), and anthropogenic disturbances, such as water pollution, commercial fishery, and extensive tourism (Dodge and Lang, 1983; Tomascik and Logan, 1990; Eatkin *et al.*, 1993).

However, controversy exists about a common environmental control. For example, Dodge (1981) reported that skeletal growth rate of an individual of *Diploria spp.* from Puerto Rico varied positively with changes in sea surface temperature. In contrast, in this thesis, results on *Diploria labyrinthiformis* from Bermuda include that annual growth rate is inversely related to temperature. This contradiction vividly shows that skeletal growth parameters are likely to reveal varying responses at different locations, each characterized by a different combination of milieu components. The large variety of triggering environmental influences on skeletal growth, leads to the understanding that individual coral skeletons contain records that do reflect multi-causative climatic and environmental influences. Furthermore, the sensitivity of different coral species to the surrounding influences may not be uniform (Lough and Barnes, 1997).

1.3.4 Application of independent proxies

In any climate proxy interpretation, the specific limitations of particular proxies have to be kept in mind. For example, tree ring records, ice core records, and historical records of flowering dates differ in their seasonal sensitivity. One season may be over-represented in the proxy series, while other seasons may not be reflected in the record at all. This might be the case in coral proxy studies, where for example, skeletal growth is stunted by extreme temperatures. For an appropriate interpretation, it is essential to clarify the degree, to which relationships between the coral proxy information and instrumental climate data are seasonally dependent. For example, in this thesis, coral skeletal growth parameters were found to be strongly affected by winter conditions in Bermuda. This can be considered a benefit, since in their analysis of 20th century global temperature variations, Briffa and Jones (1993) point out that winter season indices are the most typical of seasonal averages, especially in the Northern Hemisphere.

Furthermore, spatial limitations may occur where local influences are strong enough to override responses to large-scale climate elements (Briffa and Jones, 1993). Therefore it is important to critically consider the specific environmental features and stress factors at a particular sampling location. To avoid possible biases, proxy climate information can gain considerable reliability by the support of corroborating evidence from another independent proxy source.

1.4 MATERIALS AND ANALYTICAL METHODS

1.4.1 Material collection and preliminary laboratory work

The corals investigated in this thesis were collected during two sampling-campaigns of Bremen University, in June and July 1984 and in July 1993. The colonies were recovered at northern Bermuda fore-reef locations from 20 to 40m water depth (Figure 1.3).

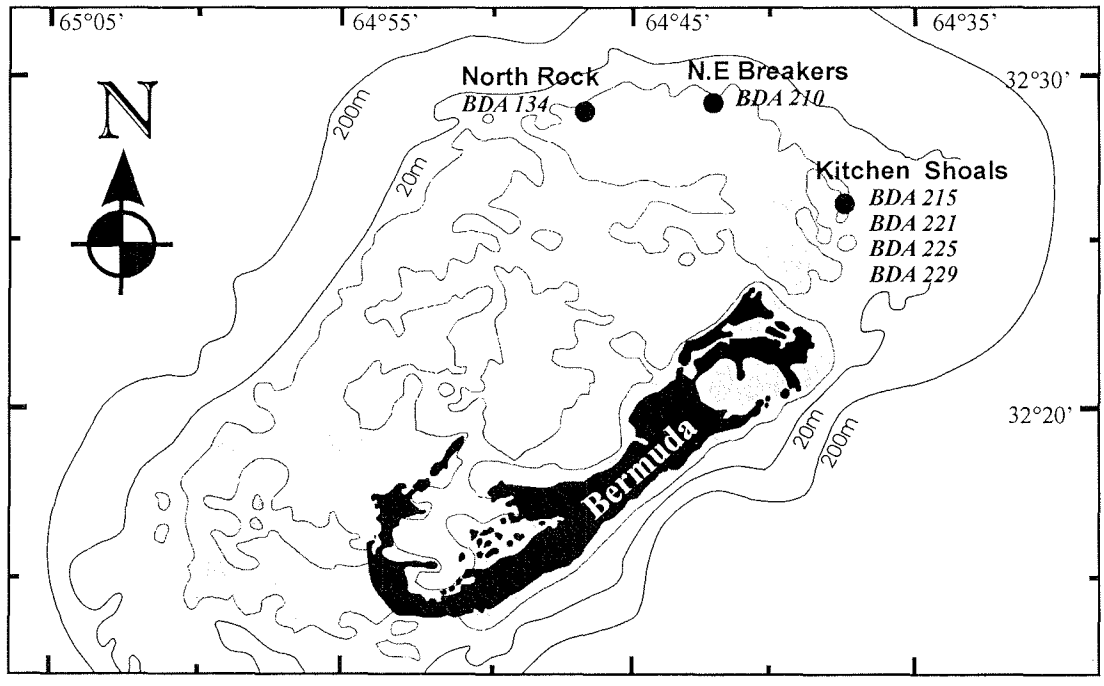

Figure 1.3 Map of the Bermuda Islands, including North Lagoon and the northern fore-reef. The sampling locations of the coral colonies, examined in this study are shown. Shaded areas are shallower than 5m.

Living coral tissue was removed instantaneously. In the laboratories of the Department of Geosciences, University of Bremen, the coral heads were cut perpendicular to density banding with a high speed, water-cooled blade-saw and sectioned into slabs of 4 to 6mm thickness, equally following the growth axis. The skeleton slices were cleaned with deionized water and X-rayed under a Faxitron Cu-k-α-Source, at 45kV exposure condition. The chronologies are based on skeletal banding, visualized in the X-radiographs. The development of several parallel skeleton slices improves the reliability of the temporal assignment of certain layers, especially in areas where skeletal banding is poorly developed and ambiguous. The carbonate skeletons were carefully inspected to ensure the absence of calcareous boring or encrusting organisms.

1.4.2 Stable isotope sampling

Two different approaches were used in stable isotope sampling, depending on the desired temporal resolution. For very high resolution isotope records, small sticks with a cross-sectional area of approximately 2mm were cut from the skeleton slices. In intervals of 150μm, 12 to 17 sub-annual samples were collected by low-speed milling of the cross sections. The carbonate sampling-sticks are very delicate and therefore require particular care when high resolution sampling is performed.

For isotope sampling with several-year resolution, bulk sampling was applied. Analogue to high resolution sampling, thin sticks were sawn from the skeleton slabs. These sticks were sectioned into segments, comprising three years of skeletal growth. The segments were subsequently ground and homogenized.

Isotopic analysis were obtained in an automated carbonate reaction (Kiel) device, coupled with a Finnigan MAT-251 mass spectrometer. Stable isotope results are reported as per mil (‰) deviations relative to PDB and were calibrated via the NBS-19 standard (-2.20‰ $\delta^{18}O$). Average reproducibility for $\delta^{18}O$ and $\delta^{13}C$ is ±0.06‰ and 0.03‰, respectively.

1.4.3 Limits of stable isotope sampling methods

Inaccuracies of stable isotope climate estimates may result from the temporal demarcation of $\delta^{18}O$ samples by the employment of skeletal density banding. It is possible that the seasonal timing of band formation is slightly variable with time (Swart *et al.*, 1996). In combination with strong seasonal cycles of the environment, a time-displacement of the isotope signal in the order of weeks to months can arise from sampling a density band that did not exactly coincide at the assumed period of band formation (Leder *et al.*, 1996; Bryant *et al.*, 1998).

Another potential source for uncertainties, using coral isotopic signatures, can result from small skeletal annual growth rates, paired with a marked relief and spines on the skeleton surface. For example, the skeletons of *D. labyrinthiformis* and *M. cavernosa* show a surface relief between thecae and exothecae, which accounts for about half of the average annual growth rate (i.e. 3-4mm). Consequently, different generations of carbonate are adjacent in a horizontal level (Barnes and Lough, 1993; Leder *et al.*, 1996; Bryant *et al.* 1998). Therefore sampling has to be restricted to one skeletal element. Furthermore, Juillet-Leclerc *et al.* (1997)

and Bryant *et al.* (1998) showed that distinct skeletal layers do not necessarily yield an instantaneous response to the forcing environmental conditions. They described prolonged and secondary calcification mechanisms during skeletogenesis. Hence, integrative sampling over larger cross-sections will temporally average different carbonate generations. For example, in high resolution sampling approaches, this will lead to attenuate the range of the seasonal signal. The cross-section of the exothecae of *D. labyrinthiformis* and *M. cavernosa* is 3 to 4mm. Therefore, the 2mm cross-section of the sampling strip is a deliberate compromise between minimizing time-averaging of the isotope signal, and avoiding the integration of various skeletal elements into the sample.

In annual bulk sampling strategies, distortions may appear where seasonal skeletal growth rates are constant and skeletal banding produces different carbonate accumulation rates throughout the year (Kuhnert, 1998). Such integration sampling approach will over-represent carbonate that was deposited during the season of high density band formation.

1.4.4 Measurement of skeletal growth parameters

In this thesis, a combination two methods for the assessment of coral skeletal density has been applied for the first time. The first method is based on optic density measurements on X-radiographs, yielding relative skeletal density and providing accurate annual growth rates. The second method uses gamma densitometry, providing absolute skeletal density measurements:

Relative optic density can be obtained from X-radiographs or from their contact prints by the image analysis software OPTIMAS (Bioscan Inc., UK). The system allows the measurement of optic densities in scanned pictures, providing exceptionally high resolution. 15 to 20 gray values were registered per annual growth band, depending on annual skeletal growth rate. These optic density measurements are qualitative. Annual density banding was clearly developed in the optic density profiles and hence delivered an excellent time-control when combined with gamma-densitometry. Mean annual optic density could be calculated from the average optic density counts of an annual cycle. These records could later be used to allocate a time axis on absolute gamma-densitometry profiles by cross-correlation of both series.

Absolute skeletal densities can be determined from the attenuation of a beam of gamma photons by a known thickness of the coral skeleton slice (Chalker and Barnes, 1990). The gamma densitometry system MSCL [Multi Sensor Core Logger] was equipped with a ^{137}Cs-

Source. The end window of the ^{137}Cs-capsule (emission 662 keV, activity 10mCi, capsule type 225; GEOTEK Ltd. Haslemere, UK) was centered beneath a 1mm diameter collimator tunnel, drilled through a lead shielding. The coral slabs were placed on a computer-controlled conveyer belt underneath the collimator and moved in steps of 1mm. Calibrations involved 20 seconds to 5 minute counts, whereas 2 minute counts were used when tracking across skeletal slabs. For calculation of bulk density values from gamma-counts, there exists a log-linear relationship between the attenuation of counts and the mass thickness, defined as skeletal density x slice thickness. A specific mass attenuation coefficient was calibrated by a shell-cube of the giant clam *Tridacna*. The shell of *Tridacna* is constructed of aragonite, like coral skeletons, but is a massive secretion without porous architecture.

Analogous to tree-ring studies, the most promising way is to integrate more than one coral record. Such approach will suppress individual signals, triggered by local influences, and enhance the common superordinated climatic signal. For this purpose, each skeleton slice was measured on six to seven parallel tracks, and these records were averaged. Furthermore, the density records of two colonies of *D. labyrinthiformis* from different fore-reef locations in Bermuda, were averaged into a single composite record. This procedure suppresses noise and purely local signals. Another important fact is that different skeletal elements reveal significant differences in density. Appropriate averaging of skeletal chronologies can minimize distortion of the proxy record, resulting from the complex three dimensional skeletal architecture.

1.4.5 Investigated periods of time

The coral chronologies investigated in this thesis are divided into modern records that cover periods for which relevant climate data are available (early 19th to early 20th century), and past time series, unsupported by instrumental climate data (mid 14th to early 17th century). The modern records, extending back to the mid 19th century, represent the background for the calibration between coral proxy information and instrumental climate data sets, available for Bermuda. The past time series includes three long coral chronologies. These ancient records cover a major part of the period referred to as the Little Ice Age (LIA) (Lamb, 1982; Grove, 1988).

Since LIA was the most recent and drastic era of rapid Holocene climate changes, it represents a period of major relevance for the understanding of modern natural climate variability

(Bradley and Jones, 1992). With its demise, it ushered in the age of global warming by 0.3 to 0.6°C, coincident with the extensive burning of fossil fuels since the mid 19th century (Folland *et al.*, 1990). LIA occurred well before the Industrial Revolution and therefore its climatic convulsions are believed to have been caused by purely natural forcing.

Although globally distributed, the LIA was not a multi-century span of spatially and temporally uniform cold conditions. It is generally agreed that the impact of LIA varied geographically (Lamb, 1982; Grove, 1988). However, the global pattern of these climate fluctuations and the mechanisms behind these changes are still elusive. Possible causes for LIA were solar activity variations (Stuiver and Braziunas, 1989) and explosive volcanic eruptions (Bradley and Jones, 1992). As well, there is disagreement surrounding the onset and the duration of the LIA. For example, Porter (1986) indicates the duration of Little Ice Age between AD 1250 and 1920, whereas Lamb (1977) defines it from 1550 to 1850, with its main phase between 1550 and 1700.

There is some historical (Lamb, 1977) and proxy evidence (Druffel, 1982; Pätzold *et al.*, 1998; Keigwin, 1996) for the LIA in the subtropical North Atlantic, which indicate that temperatures were cooler by 1 to 1.5°C, compared to recent annual average conditions. For example, Pätzold *et al.* (1998) introduced an 800-year Bermuda record of coral growth that has been interpreted in terms of cooling of this magnitude, which was induced at least partly by an enhancement of wind-driven vertical mixing and heat flux changes in the surface waters. To the west, in the Florida Straits, coral $\Delta^{14}C$ and stable oxygen isotope values also indicated that temperatures were comparably lower during LIA (Druffel, 1982).

It is conceivable that the century-scale climate changes in sea surface temperatures in the Sargasso Sea are part of a much larger climate system (Keigwin, 1996) and may also have influenced climate downstream in widespread regions east to the Atlantic (Folland *et al.*, 1986). The past coral proxy records, recording changes in sea surface temperature and vertical mixing, as analyzed in this thesis, can contribute to our understanding of key climate variables during this important period.

1.4.6 Climate data

Compared to other areas of the low-latitude world oceans, Bermuda offers a rich archive of meteorological and hydrographic data. Available records of various lengths include air and sea surface temperature, sea surface salinity, winter mixing depth, atmospheric pressure, humidity, precipitation, wind and hurricanes (Table 1.1).

Table 1.1 Selection of climate data available for Bermuda. All data can be retrieved via Internet. The addresses are given in the reference section.

Parameter	Period	Source
Air temperature	1856-1947	Bermuda Botanical Gardens
"	1909-1991	COADS
Sea surface temperature	1888-1991	COADS
"	1856-1991	MOHSST5
"	1954-1991	Hydrostation S
Sea surface salinity	1954-1991	Hydrostation S
Sea level pressure	1836-1953	Bermuda Meteorological Office
"	1847-1991	COADS
Wind speed	1885-1991	COADS
Humidity	1932-1956	Bermuda Meteorological Office
Rainfall	1852-1942	Bermuda Meteorological Office
Hurricanes	1932-1953	Bermuda Meteorological Office

Earliest measurements of air temperatures, atmospheric pressure and rainfall in Bermuda began in the mid 19th century, conducted by the Bermuda Meteorological Office and Bermuda Botanical Gardens. Intensive survey of hydrographic parameters near Bermuda, including temperatures and salinity in various water depths, started in 1954 with the initiation of Hydrostation S, southeast of the archipelago (Bermuda Biological Station for Research, 1993). From this data set, a record of surface water mixing depth was calculated by Michaels *et al.* (1994).

Furthermore, Bermuda owes long continuous sets of hydrographic data to it's position beside one of the world's busiest shipping routes. In 1981, a program was initiated to create a

consistent historical record of global surface marine data, the Comprehensive Ocean-Atmosphere Data Set (COADS) (Woodruff *et al.*, 1987). Hydrographic data, such as sea surface temperature and sea level pressure, have been collected by trade-ships and have been monthly summarized by averaging data from 2° latitude by 2° longitude geographical grid boxes. Each monthly value consists of a large number of single measurements. Sufficiently continuos COADS data for Bermuda are available since 1888. Kaplan *et al.* (1997) corrected the COADS data set for the „bucket effect" and used it to create the MOHSST5 data set, containing sea surface temperatures for 5° latitude by 5° longitude grids. For Bermuda, the data set extends back to 1856.

For comparison with the Bermuda coral proxy records, sea surface temperature and atmospheric pressure data from COADS were preferably used, instead of Hydrostation S data. First, COADS data deliver a longer continuous record. Second, monthly values summarized by COADS were calculated from a much higher quantity of single values, compared to approximately bimonthly measurements at Station S. However, there exists a high statistical correspondence between the locally representative Hydrostation S data and spatially averaged data from COADS, on both monthly and annual time-scales.

1.5. OVERVIEW OF SUBMITTED MANUSCRIPTS

The main body of this thesis consists of three manuscripts (Chapter 2 to 4). They are submitted to scientific journals. The following gives a short overview of the thematic content addressed in the manuscripts.

CHAPTER 2

North Atlantic climate variability recorded in growth chronologies of hermatypic corals from a high latitude reef of Bermuda

S. Draschba, J. Pätzold, G. Wefer

This manuscript evaluates the suitability of annual skeletal density and growth rate of *D. labyrinthiformis* from Bermuda, as climate proxy indicators in the low-latitude North Atlantic. Time series of annual skeletal bulk density and growth rate, covering the last 150 years, are correlated to seasonal and inter-annual figures of sea surface temperatures and winter mixing depth in Bermuda, and a Bermuda-Island atmospheric pressure index, i.e. the NAO. The main focus of this study is to demonstrate the potential of variations in skeletal density in *D. labyrinthiformis* to monitor changes in the inter-annual to decadal pattern of hydrographic and atmospheric circulation variability in the North Atlantic.

CHAPTER 3

North Atlantic climate variability since AD 1350 recorded in $\delta^{18}O$ and skeletal density of Bermuda corals

S. Draschba, J. Pätzold, G. Wefer

The subject of this manuscript is the examination of coral $\delta^{18}O$ time series with triennial temporal resolution and the combination with annual skeletal density time series. Two modern skeletal $\delta^{18}O$ chronologies of *D. labyrinthiformis*, covering periods in the 19th and 20th century are compared to instrumental temperature data. A modern $\delta^{18}O$/ temperature calibration serves to calculate sea surface temperature anomalies from coral $\delta^{18}O$ records that cover the period between 1350 and 1630. These time series, that describe parts of the Little Ice Age, are

compared to parallel records of skeletal density and to previously published proxy records for Bermuda and the Northern Hemisphere.

CHAPTER 4

Winter mixing processes recorded by $\delta^{13}C$ in Bermuda corals

S. Draschba, J. Pätzold, G. Wefer

The third manuscript is concerned with the analysis of coral skeletal $\delta^{13}C$ time series. The first part focuses on three modern $\delta^{13}C$ records (1969 to 1993) with a high temporal resolution, where one sample represents approximately three weeks. The modern $\delta^{13}C$ records were obtained from skeletons of *D. labyrinthiformis* and *M. cavernosa*. They reveal clear seasonal cycles and are compared to the seasonal cycling in $\delta^{18}O$. Annual mean $\delta^{13}C$ of the modern time series is related to a time series of maximum winter mixing depth near Bermuda, which is interpreted as a gauge for nutrient supply. The second part of the study analyses ancient coral $\delta^{13}C$ records of *D. labyrinthiformis* with triennial resolution, covering parts of the Little Ice Age (AD 1350 to 1630). The records are compared to triennial coral $\delta^{18}O$. This allows to transfer interpretations for modern coral $\delta^{13}C$ to the proxy information yielded by the Little Ice Age $\delta^{13}C$ records.

1.6. REFERENCES

Aharon, P. 1991: Recorders of reef environment histories: Stable isotopes in corals, giant clams, and calcareous algae. *Coral Reefs* 10, 71-90.

Barnes, D.J. and Devereux, M.J. 1988: Variations in skeletal architecture associated with density banding in the hard coral *Porites*. *J. Exp. Mar. Biol. Ecol.* 121, 37-54.

Barnes, D.J. and Lough, J.M. 1992: On the nature and causes of density banding in massive coral skeletons. *J. Exp. Mar. Biol. Ecol.* 167, 91-108.

Bermuda Environmental Scenario 1974: *US Naval Weather Service Detachment,* Asheville, New York, 199pp.

Bermuda Biological Station for Research 1993: Bermuda Atlantic Time-Series Study. U.S. Joint Global Ocean Flux Study, *BATS Data Report, B-2* Oct. 1989 - Sept. 1990; B-3 Oct. 1990 - Sept. 1991. 339pp.

Bjerknes, J. 1964: Atlantic air-sea interaction. *Adv. Geophys.* 10, 1-82.

Bosscher, H. 1992: Growth potential of coral reefs and carbonate platforms. *Ph.D. Dissertation, Vrije Universiteit Amsterdam*, Vrije University Press, 160pp.

Bradley, R.S. and Jones, P.D. 1992: Climatic variations in the longest instrumental records. In: Bradley, R.S. and Jones, P.D. [Eds.], *Climate since A.D. 1500*. Routledge, London, 248-290.

Bradley, R.S. and Jones, P.D. 1993: Little Ice Age summer temperature variations: their nature and relevance to

recent global warming trends. *The Holocene* 3, 367-376.

Briffa, K.R. and Jones, P.D. 1993: Global surface air temperature variations during the twentieth century. Part 2: Implications for large-scale, high frequency paleoclimatic studies. *The Holocene* 3, 82-93.

Bryant, D.J., Schrag, D.P. and Moore, M.D. 1998: Origin and smoothing of environmental signals in the stable isotope composition in an Indonesian *Porites* coral. Palaeogeogr., Palaeoclimatol., Palaeoecol., in press.

Carriquiry, J.D., Risk, M.J. and Schwarcz, H.P. 1993: Stable isotope geochemistry of corals from Costa Rica as proxy indicator of the El Nino/ Southern Oscillation (ENSO). *Geochim. Cosmochim. Acta* 58, 335-351.

Cayan, D. 1992: Latent and sensible heat flux anomalies over the northern oceans: Driving the sea surface temperature. *J. Phys. Oceanogr.* 22, 859-881.

Chalker, B.E. and Barnes, D.J. 1990: Gamma-densitometry for measurement of skeletal density. *Coral Reefs* 9, 11-23.

CLIVAR, 1997: The North Atlantic Oscillation. http://www.clivar.ucar.edu/iplan/pd1.html.

Cole, J.E. and Fairbanks, R.G.1990: The Southern Oscillation recorded in the $\delta^{18}O$ of corals from Tarawa Atoll. *Paleoceanography* 5, 669-683.

Cook, E.R., D'Arrigo, R.D. and Briffa, K.R. 1998: A reconstruction of the North Atlantic Oscillation using tree-ring chronologies from North America and Europe. *The Holocene* 8, 9-17.

Crowley, T.J., Quinn, T.M., Taylor, F.W., Henin, C. and Joannot, P. 1997: Evidence for a volcanic cooling in a 335-year coral record from New Caledonia. *Paleoceanography* 12, 633-639.

Deser, C. and Blackmon, M.L. 1993: Surface climate variations over the North Atlantic Ocean during winter 1900-1989. *J. Clim.* 6, 1743-1753.

Dickson, R., Lazier, J., Meincke, J., Rhines, P. and Swift, J. 1996: Long-term coordinated changes in the convective activity of the North Atlantic. *Progr. Oceanogr.* 37, 207-262.

Dodge, R.E. and Vaisnys, J.R. 1975: Hermatypic coral growth banding as an environmental recorder. *Nature* 258, 706-708.

Dodge, R.E. 1981: Growth characteristics of reef-building corals within and external to a naval ordnance range: Vieques, Puerto Rico. *Proc. 4th Int. Coral Reef Symp.*, Manila 2, 241-248.

Dodge, R.E. and Lang, J.C. 1983: Environmental correlates of hermatypic coral (*Montastrea annularis*) growth on the East Flower Gardens Bank, northwest Gulf of Mexico. *Limnol. Oceanogr.* 28, 228-240.

Dodge, R.E. and Brass, G.W. 1984: Skeletal extension, density and calcification of the reef coral Montastrea annularis: St. Croix, Virgin Islands. *Bull. Mar. Sci.* 34, 288-307.

Dodge, R.E., Szmant, A.M., Garcia, R., Swart, P.K., Forester, A. and Leder, J.J. 1992: Skeletal structural basis of density banding in the reef coral *Montastrea annularis*. *Proc. 7th Int. Coral Reef Symp.*, Guam 1, 24 (abstract).

Druffel, E.M. 1982: Banded corals: Changes in oceanic carbon-14 during the Little Ice Age. *Science* 218, 13-19.

Dullo, W.C., Heiss, G.A. and de Vries, E. 1993: Comparison of linear growth rates in *Porites* between undisturbed and stressed environments. Gulf of Aqaba, Red Sea. In: Ginsburg, R.N. [Ed.], *Proc. Colloq. on Global Aspects of Coral Reefs: Health, Hazards and History*. Rosenstiel School of Marine and Atmospheric Sciences, University of Miami, 34-37.

Dunbar, R.B., Wellington, G.M., Colan, M.W. and Glynn, P.W. 1994: Eastern Pacific sea-surface temperatures since 1600 AD: The $\delta^{18}O$ record of climate variability in Galapagos corals. *Paleoceanography* 9, 291-315.

Eatkin, C.M., Feingold, J.S. and Glynn, P.W. 1993: Oil refinery impacts on coral reef communities in Aruba, N.A. In: Ginsburg, R.N. [Ed.], *Proc. Colloq. on Global Aspects of Coral Reefs: Health, Hazards and History*. Rosenstiel School of Marine and Atmospheric Sciences, University of Miami, 139-145.

Epstein, S., Buchsbaum, R., Lowenstam; H. and Urey, H.C. 1953: Revised carbonate-water isotopic temperature scale. *Geol. Soc. Am. Bull.* 64, 1315-1325.

Erez, J. 1978: Vital effect on stable-isotope composition seen in foraminifera and coral skeletons. *Nature* 273, 199-202.

Fairbanks, R.G. and Dodge, R.E. 1979: Annual periodicity of the $^{18}O/^{16}O$ and $^{13}C/^{12}C$ ratios in the coral *Montastrea annularis*. *Geochim. Cosmochim. Acta* 43, 1009-1020.

Fairbanks, R.G., Charles, C.D. and Wright, J.D. 1992: Origin of global meltwater pulses. In: Taylor, R.E. [Ed.], *Radiocarbon after four decades*. Springer Verlag, New York, 473-500.

Folland, C.K., Palmer, T.N. and Parker, D.E. 1986: Sahel rainfall and worldwide sea temperatures, 1901-1985. *Nature* 320, 602-607.

Folland, C.K., Karl, T.R. and Vinnikov, K.Y. 1990: Observed climate variations and change. In: Houghton, J.T., Jenkins, G.J. and Ephraums, J.J. [Eds.], *Climate Change. The IPCC Climate Assessment*. Cambridge University Press, Cambridge, 194-238.

Friedli, H., Lötscher, H., Oeschger, H., Siegenthaler, U. and Stauffer, B. 1986: Ice core record of the $^{13}C/^{12}C$ ratio of atmospheric CO_2 in the past two centuries. *Nature* 324, 237-238.

Gagan, M.K., Chivas, A.R. and Isdale, P.J. 1994: High resolution isotopic records from corals using ocean temperature and mass-spawning chronometers. *Earth Planet. Sci. Lett.* 121, 549-558.

Gagan, M.K. and Chivas, A.R. 1995: Oxygen isotopes in corals reveal Pinatubo aerosol-induced cooling in the Western Pacific Warm Pool. *Geophys. Res. Lett.* 22, 1069-1072.

Gagan, M.K., Chivas, A.R. and Isdale, P.J. 1996: Timing coral-based climatic histories using ^{13}C enrichments driven by synchronized spawning. *Geology* 24, 1009-1012.

Gladfelter, E.H., Monahan, R.K. and Gladfelter, W.B. 1978: Growth rates of five reef building corals in the Northeastern Caribbean. *Bull. Mar. Sci.* 28, 728-734.

Griffies, S.M. and Bryan, K. 1997: Predictability of North Atlantic multi-decadal climate variability. *Science* 275, 181-184.

Goreau, T.F. 1963: Calcium carbonate deposition by coralline algae and corals in relation to their role as reef builders. *Ann. NY Acad. Sci.* 109, 127-167.

Goreau, T.J. 1977a: Coral skeleton chemistry: physiological and environmental regulation of stable isotopes and trace metals in *Montastrea annularis*. *Proc. Royal Soc. London*, B196, 291-315.

Goreau, T.J. 1977b: Carbon metabolism in calcifying and photosynthetic organisms: theoretical models based on stable isotopic data. *Proc. 3rd Int. Coral Reef Symp.*, Miami 2, 359-401.

Grossman, E.L. and Ku, T. 1986: Oxygen and carbon isotope fractionation in biogenic aragonite: temperature effects. *Chem. Geol.* 59, 59-74.

Grove, J.M. 1988: *The Little Ice Age*. Menthuen, London, 498pp.

Hansen, D.V. and Bezdek, H.F. 1996: On the nature of decadal anomalies in North Atlantic sea surface temperature. *J. Geophys. Res.* 101, C4, 8749-8758.

Hurrell, J.W. 1995: Decadal trends in the North Atlantic Oscillation: Regional temperature and precipitation. *Science* 269, 676-679.

Hurrell, J.W. 1996: Influence of variations in extratropical wintertime teleconnections on Northern Hemisphere temperature. *Geophys. Res. Lett.* 23, 6, 665-668.

IPCC 1992: Climate Change 1992: *The supplementary report to the IPCC Scientific Assessment*. Houghton, J.T., Callander, B.A. and Varney, S.K. [Eds.]. Cambridge University Press, Cambridge, 198pp.

IPCC 1996: Climate Change 1995. *The Science of Climate Change*. Houghton, J.T., Meira Filho, L.G., Callander, B.A., Harris, N., Kattenberg, A. and Maskell, K. [Eds.]. Cambridge University Press, Cambridge, 572pp.

IPCC 1998: Summary for Policymakers. *The regional impacts of climate change: an assessment of vulnerability*. http://www.usgcrp.gov/ipcc/html/RISPM.html.

Joyce, T.M. and Robbins, P. 1996: The long-term hydrographic record at Bermuda. *J. Clim.* 96, 001-0011.

Juillet-Leclerc, A., Montaggioni, L.F., Pichon, M. and Gattuso, J.P. 1997: Effects of calcification patterns on the oxygen isotope composition of the skeleton of the scleractinian coral *Acropora formosa*. *Oceanol. Acta* 20, 1-14.

Keigwin, L.D. 1996: The Little Ice Age and Medieval Warm Period in the Sargasso Sea. *Science* 274, 1504-1508.

Klein, R., Pätzold, J., Wefer, G. and Loya, Y. 1992: Seasonal variations in the stable isotopic composition and the skeletal density pattern of the coral *Porites lobata* (Gulf of Eilat, Red Sea). *Mar. Biol.* 112, 259-263.

Klein, R., Pätzold, J., Wefer, G. and Loya, Y. 1993: Depth related timing of density band formation in *Porites* spp. corals from the Red Sea inferred from X-ray chronology and stable isotope composition. *Mar. Ecol. Progr. Ser.* 97, 99-104.

Knutson, D.W., Buddemeier, R.W. and Smith, S.V. 1972: Coral chronometers: Seasonal growth bands in reef corals. *Science* 177, 270-272.

Kuhnert, H. 1998: Aufzeichnung des Klimas vor Westaustralien in stabilen Isotopen in Korallenskeletten. *Berichte, FB Geowissenschaften, Univ. Bremen*, 117, 109pp.

Kushnir, Y. 1994: Interdecadal variations in North Atlantic sea surface temperature and associated atmospheric conditions. *J. Clim.* 7, 141-157.

Lamb, H.H. 1977: *Climate, Present Past and Future.* Menthuen, London, 835pp.

Lamb, H.H. 1982: *Climate History and the Modern World.* Menthuen, London, 387pp.

Land, L.S., Lang, J.C. and Smith, B.N. 1977: Preliminary observations on the carbon isotopic composition of some reef coral tissues and symbiotic zooxanthellae. *Limnol. Oceanogr.* 20, 283-287.

Latif, M. and Barnett, T.P. 1996: Causes of decadal climate variability over the North Pacific and North America. *Science* 266, 634-637.

Leder, J.J., Swart, P.K., Szmant, A.M. and Dodge, R.E. 1996: The origin of variations in the isotopic record of scleractinian corals: 1 Oxygen. *Geochim. Cosmochim. Acta* 60, 2857-2870.

Linsley, B.K., Dunbar, R.B., Wellington, G.M. and Mucciarone, D.A. 1994: A coral-based reconstruction of Intertropical Convergence Zone variability over central America since 1707. *J. Geophys. Res.* 99, 9977-9994.

Logan, A. and Tomascik, T. 1991: Extension growth rates in two coral species from high latitude reefs of Bermuda. *Coral Reefs* 3, 155-160.

Logan, A. Yang, L. and Tomascik, T. 1994: Linear skeletal extension rates in two species of *Diploria* from high latitude reefs in Bermuda. *Coral Reefs* 13, 225-230.

Lough, J.M. and Barnes, D.J. 1990: Possible relationships between variables and skeletal density in a coral colony from the central Great Barrier Reef. *J. Exp. Mar. Biol. Ecol.* 134, 221-241.

Lough, J.M. and Barnes, D.J. 1997: Several centuries of variation in skeletal extension, density and calcification in massive *Porites* colonies from the Great Barrier Reef: A proxy for seawater temperature and a background of variability against which to identify unnatural change. *J. Exp. Mar. Biol. Ecol.* 211, 29-67.

Marshall, J.C. and Molteni, F. 1993: Towards a dynamical understanding of weather regimes. *J. Atmos. Sci.* 50, 1792-1818.

Marshall, J.C., Nurser, A.J.G. and Williams, R.G. 1993: Inferring the subduction rate and period over the North Atlantic. *J. Phys. Oceanogr.* 23, 1315-1329.

Marshall, J. and Kushnir, Y. 1997: Atlantic climate variability. Science Plan for NAO and Tropical Dipole. http://geoid.mit.edu/accp/avehtml.html.

Mc Cartney, M. 1997: Is the Ocean at the helm? *Nature* 388, 521-522.

McConnaughey, T. 1989: ^{13}C and ^{18}O isotopic disequilibrium in biological carbonates. 2: In vitro simulation of kinetic isotope effects. *Geochim. Cosmochim. Acta* 53, 163-171.

McConnaughey, T., Burdett, J., Whelan, J.F. and Paul, C.K. 1996: Carbon isotopes in biological carbonates: Respiration and photosynthesis. *Geochim. Cosmochim. Acta* 61, 611-622.

McCulloch, M.T., Gagan, M.K., Mortimer, G.E., Chivas, A.R. and Isdale, P.J. 1994: A high resolution Sr/Ca and $\delta^{18}O$ coral record from the Great Barrier Reef, Australia, and the 1982-1983 El Nino. *Geochim. Cosmochim. Acta* 58, 2747-2754.

Menzel, D.W. and Ryther, J.H. 1960: The annual cycle of primary production in the Sargasso Sea off Bermuda. *Deep-Sea Res.* 6, 351-367.

Menzel, D.W. and Ryther, J.H. 1961: Annual variation in primary production of the Sargasso Sea off Bermuda. *Deep Sea Res.* 7, 282-288.

Michaels, A.F., Knap, A.H., Dow, R.L., Gundersen, K., Johnson, J.J., Sorensen, J., Close, A., Knauer, G.A., Lohrenz, S.E., Asper, V.A., Tuel, M. and Bidigare, R. 1994: Seasonal patterns of ocean biogeochemistry at the JGOFS Bermuda Atlantic Time-Series Study Site. *Deep-Sea Res.* 41, 7, 1013-1038.

Molinari, R.L., Mayer, D.A., Festa, J.F. and Bezdek, H.F. 1997: Multi-year variability in the near surface temperature structure of the midlatitude western North Atlantic Ocean. *J. Geophys. Res.* 102, C2, 3267-3278.

Morris, B., Barnes, J., Brown, F. and Markham, J. 1977: The Bermuda Marine Environment. A report of the Bermuda inshore waters, Investigations 1976-1977. *BBSR Special Publication* 15, 120pp.

Nozaki, Y., Rye, D.M., Turekian, K.K. and Dodge, R.E. 1978: A 200-year record of carbon-13 and carbon-14 variations in a Bermuda coral. *Geophys. Res. Lett.* 5, 825-828.

Pätzold, J. 1984: Growth rhythms recorded in the stable isotopes and density bands in the reef coral *Porites lobata* (Cebu, Philippines). *Coral Reefs* 3, 87-90.

Pätzold, J. 1986: Temperatur- und CO_2-Änderungen im tropischen Oberflächenwasser der Philippinen während der letzten 120 Jahre: Speicherung in stabilen Isotopen hermatyper Korallen. *Reports, Geol.-Paläont. Inst. Univ. Kiel* 12, 92pp.

Pätzold, J., Bickert, T., Flemming, B., Grobe, H. and Wefer, G. 1998: Holozänes Klima des Nordatlantiks rekonstruiert aus massiven Korallen von Bermuda. *Natur und Museum*, in press.

Porter, S.C. 1986: Pattern and forcing of Northern Hemisphere glacier variations during the last millennium. *Quatern. Res.* 26, 27-48.

Quinn, T.M., Crowley, T.J. and Taylor, F.W. 1996: New stable isotope results from a 173-year coral from Espiritu Santo, Vanuatu. *Geophys. Res. Lett.* 23, 3413-3416.

Reverdin, G., Cayan, D.R. and Kushnir, Y. 1997: Decadal variability of hydrography in the upper North Atlantic, 1948-1990. *J. Geophys. Res.* 102, C4, 8505-8531.

Rogers, J.C. 1984: The Association between the North Atlantic Oscillation and the Southern Oscillation in the Northern Hemisphere. *Mon. Weath. Rev.* 112, 1999-2015.

Rogers, J.C. 1990: Patterns of low-frequency monthly sea-level pressure variability (1899-1986) and associated wave cyclone frequencies. *J. Clim.* 3, 1364-1379.

Schumacher, H. 1988: *Korallenriffe, Verbreitung Tierwelt und Ökologie*. BLV, München, 275pp.

Shen, G.T., Cole, J.E., Lea, D.W., Linn, L.J., McConnaughey, T.A. and Fairbanks, R.G. 1992: Surface ocean variability at Galapagos from 1936-1982: Calibration of geochemical tracers in corals. *Paleoceanography* 7, 563-588.

Siegel, D.A., Itturiaga, R., Bidigare, R.R., Smith, R.C., Pak, H., Dickey, T.D., Marra, J. and Baker, K.S. 1990: Meridional variations in the spring time phytoplankton community in the Sargasso Sea. *J. Mar. Res.* 48, 379-412.

Spitzer, W.S. and Jenkins, W.J. 1989: Rates of vertical mixing, gas exchange and new production: Estimates from seasonal gas cycles in the upper ocean near Bermuda. *J. Mar. Res.* 47, 169-196.

Stuiver, M. and Braziunas, T.F. 1989: Atmospheric ^{14}C and century-scale solar oscillations. *Nature* 338, 405-408.

Sutton, R.T. and Allen, M.R. 1997: Decadal predictability of North Atlantic sea surface temperature and climate. *Nature* 388, 563-567.

Swart, P.K. 1983: Carbon and oxygen isotope fractionation in scleractinian corals: a review. *Earth-Sci. Rev.* 19, 51-80.

Swart P.K., Leder, J.J., Szmant, A.M. and Dodge, R.E. 1996: The origin of variations in the isotopic record of scleractinian corals: 2. Carbon. *Geochim. Cosmochim. Acta* 60, 2871-2885.

Taylor, R.B., Barnes, D.J. and Lough, J.M. 1993: Simple models of density band formation in massive corals. *J. Exp. Mar. Biol. Ecol.* 167, 109-125.

Thomas, M.L.H. and Logan, A. 1991: A guide to the ecology of shoreline and shallow water marine communities of Bermuda. *BBSR Special Publication* 30, 345pp.

Tomascik, T. and Logan, A. 1990: A comparison of peripheral growth rates in the recent solitary coral *Scolymia cubensis* from Barbados and Bermuda. *Bull. Mar. Sci.* 46, 799-806.

Tudhope, A.W., Shimmield, G.B., Chilcott, C.P., Jebb, M., Fallick, A.E. and Dalgleish, A.N. 1995: Recent changes in climate in the far western equatorial Pacific and their relationship to the Southern Oscillation; oxygen isotope records from massive corals, Papua New Guinea. *Earth Planet. Sci. Lett.* 136, 575-590.

Weber, J.N. and Woodhead, P.M.J. 1970: Carbon and oxygen isotope fractionation in the skeletal carbonates of reef building-corals. *Chem. Geol.* 6, 93-117.

Weber, J.N. and Woodhead, P.M.J. 1972: Temperature dependence of oxygen-18 concentration in reef coral carbonates. *J. Geophys. Res.* 77, 463-473.

Weber, J.N., Deines, P., White, E.W. and Weber, P.H. 1976: Seasonal high and low density bands in reef coral skeletons. *Nature* 255, 697-698.

Wefer, G. and Berger, W.H. 1991: Isotope paleontology: growth and composition of extant calcareous species. *Mar. Geol.* 100, 207-248.

Weil, S.M., Buddemeier, R.W., Smith, S.V. and Kroopnick, P.M. 1981: The stable isotopic composition of coral skeletons: control by environmental variables. *Geochim. Cosmochim Acta* 45, 1147-1153.

Wellington, G.M. and Glynn, P.W. 1983: Environmental influences on skeletal banding in Eastern Pacific (Panama) corals. *Coral Reefs* 1, 215-222.

Winter, A., Goenaga, C. and Maul, G.A. 1991: Carbon and oxygen isotope time series from a 18 year Caribbean reef coral. *J. Geophys. Res.* 96, 16673-16678.

Wood, E.M. 1983: *Corals of the world.* T.F.H. Publications Ltd., New Jersey, 256pp.

Woodruff; S.D., Slutz, R.J., Jenne, R.L. and Steurer, P.M. 1987: A Comprehensive Ocean-Atmosphere Data Set. *Bull. Am. Meteorol. Soc.* 68, 1239-1250.

2.6.1 Climate data references from Internet

COADS: http://ingrid.ldgo.columbia.edu/SOURCES/.COADS/

Hydrostation S and BATS: http://www.bbsr.edu/users/ctd/nisklist.html

MOHSST5: http://ingrid.ldgo.columbia.edu/SOURCES/.KAPLAN/

Bermuda Botanical Gardens and Meteorological Office:

http://ingrid.ldgo.columbia.edu/SOURCES/.NOAA/.DCDC/.GCPS/.MONTHLY/.STATION/

2 NORTH ATLANTIC CLIMATE VARIABILITY RECORDED IN GROWTH CHRONOLOGIES OF HERMATYPIC CORALS FROM A HIGH LATITUDE REEF OF BERMUDA

S. DRASCHBA, J. PÄTZOLD, G. WEFER

Fachbereich Geowissenschaften

Universität Bremen

Postfach 330 440

D-28334 Bremen

Germany

Submitted to 'The Holocene'

2.1 ABSTRACT

Skeletal density and annual growth rate histories of two coral colonies of *Diploria labyrinthiformis* from Bermuda were analyzed and correlated to instrumental climatic data over the last 150 years. Relative optic density measurements, made on X-radiographs of skeleton slices, revealed qualitative, highly resolved density profiles and allowed accurate assessment of annual growth rates.

Absolute skeletal density was measured by gamma-densitometry. Seasonal timing of band formation is that high density bands were secreted during summer, and low density increments were deposited in winter. On inter-annual time-scales, mean annual density and growth rates show a strong inverse relationship. Annual skeletal density shows stronger correlation to climate variables than annual growth rates and is positively related to sea surface temperature and hemispherical pressure index anomalies. Furthermore, correlations between skeletal growth parameters and seasonal climatic regimes indicate that the corals respond most sensitively to their environment during the winter months. Especially, variations of annual skeletal density is an excellent indicator of winter climatic conditions at Bermuda. High correlation is also found between skeletal growth parameters and the depth of the mixed layer, which is produced during overturning events in winter and reflects both, atmospheric and subsurface water conditions. Characterized by meteorological and oceanographic properties that are influenced by the North Atlantic Oscillation system (NAO), Bermuda represents a key site for the reconstruction of natural climate variability of low latitudes in the North Atlantic.

2.2 INTRODUCTION

Instrumental climate records are the basis for the detection of both, natural climatic variability and anthropogenic impacts on climate. Unfortunately, historical records are limited in geographic distribution and time. High quality proxy data that are calibrated to physical components of the climate system can help fill gaps in geographic coverage. Furthermore, they can provide permanent climate proxy information of earlier times, for which anthropogenic modification of climate can be excluded.

The skeletons of massive reef corals are characterized by alternating bands of high and low bulk density. These increments were first reported to be seasonal by Knutson *et al.* (1972). They allow an accurate dating of coral chronologies. Furthermore, the density and growth rate histories of reef-building corals have been widely examined to reveal responses to environmental influences. Ecological factors discussed include temperature (e.g. Dodge and Vaisnys, 1975) and light (e.g. Taylor *et al.*, 1993). Other possible controls on skeletal growth are related to sedimentation rates (e.g. Dodge *et al.*, 1974), growth depth (e.g. Logan and Tomascik, 1991; Klein *et al.*, 1993), the latitude of the reef location, nutrient supply and wave energy (Logan *et al.*, 1994), and factors affecting gametogenesis of polyps (Wellington and Glynn, 1983).

For the use of coral skeletal growth parameters as climate proxies it is confusing to attempt to find a common environmental signal among a wide range of coral species from different locations. Obviously, different limiting environmental influences can variously dominate the skeletal growth of scleractinian corals, and the predominance of these factors can vary with location. Hence, for the use of skeletal growth parameters as a climate-proxy, calibration against instrumental climate data is fundamental to the interpretation of skeletal growth features.

In this study, we present validation data of skeletal density and growth rate histories of the scleractinian reef coral *D. labyrinthiformis* from Bermuda as potential climate proxy-indicators. Variations of sea surface temperature (SST) at Bermuda, the atmospheric sea level pressure difference between Bermuda and Iceland, and the depth of the mixed layer in winter at Bermuda are tested to reveal influence on coral growth.

Presumably, the climate variables that are compared to the coral growth histories reflect integral aspects of the North Atlantic Oscillation system (Bjerknes, 1964; Kushnir, 1994; Dickson *et al.*, 1996; Sutton and Allen, 1997). Because of its location with respect to this system, Bermuda can be considered a subtropical key-site for climatic reconstruction by a high-resolution coral proxy.

2.3 OCEANOGRAPHY AND CLIMATE

The Islands of Bermuda, near the western edge of the Sargasso Sea, represent the northernmost limit of coral reef distribution. Warm waters brought by the Gulf Stream allow certain hermatypic corals to grow at such high latitude. The subtropical climate and water properties at Bermuda are marked by strong seasons, with average seasonal SST of 19°C in February and March and 28°C in August (Bodungen *et al.*, 1982). Winter temperature minima occur in response to convective mixing with colder subsurface water. The underlying 18° mode water mass is a nutrient-enriched layer of almost isothermal water between 250 and 400 m depth, which puts a lower limit on surface water temperatures in winter. Wind-induced mixing persists from November until March (Michaels *et al.*, 1994) and nutrients are supplied to the oligotrophic surface layers, consequently enhancing the productivity (Menzel & Ryther, 1961; Siegel *et al.*, 1990). Furthermore, several storms occur during winter and support vertical mixing. During the transition to summer, decreasing wind speed and enhanced irradiance lead to a strong thermal stratification of the surface waters (Bodungen *et al.*, 1982).

The water clarity on the outer fore-reef sites is high due to low sedimentation and resuspension rates throughout the year. Atmospheric pressure is highest in July and lowest in February. The cloud cover is considerably enhanced during winter. Consequently, the amount of sunlight that reaches the water surface is further reduced to an average of 240 gcal cm^{-2} day^{-1} in December, compared to average insolation in July of 670 gcal cm^{-2} day^{-1}. Salinity, humidity and evaporation are fairly uniform throughout the year (Morris *et al.*, 1977).

Bermuda lies in the sphere of influence of the North Atlantic subtropical high pressure zone. The interaction between the Iceland Low and the subtropical high pressure zone dominate the weather in the North Atlantic. These large-scale changes in atmospheric conditions are defined as the North Atlantic Oscillation (Bjerknes, 1964; Hurrell, 1995). An index of the atmospheric mass alteration was first given by using the difference of normalized winter (December to February) atmospheric sea level pressures between Ponta Delgada, Azores, and Akureyri, Iceland (Rogers, 1984). Influenced by the Subtropical High, Bermuda was proposed to serve as a representative for the Azores/Lisbon Station by Molinari *et al.* (1997). Based on COADS (Comprehensive Ocean-Atmosphere Data Set), a Bermuda-Iceland pressure-index can be calculated back to 1847.

The Bermuda-Iceland index tracks atmospheric flow affecting the distribution of wind stress fields and hence the ocean-atmosphere heat exchange and details in the oceanic gyre circulation (Kushnir, 1994; Hansen and Bezdek, 1996; Sutton and Allen, 1997; Mc Cartney, 1997). The index also is related to characteristic spatial and temporal patterns in SST anomalies on inter-annual time-scales, as well as to inter-decadal fluctuations (Deser and Blackmon, 1993; Hurrell, 1995; Molinari *et al.*, 1997).

Kushnir (1994) identified the western Sargasso region as one of the centers of action of the NAO. Two extreme modes of winter conditions in Bermuda are related to the NAO's atmospheric circulation changes: During high index years, westerly wind stress across the Atlantic Ocean increases but the zone of maximum wind stress is considerably shifted northward (Hurrell, 1996). This shift yields a reduction of wind stress at the Bermuda latitude. Consequently, heat-loss to the atmosphere is reduced and periods of lower than normal ventilation of the surface layers in winter were noted at Bermuda (Michaels *et al.*, 1994). As typical attributes of low index years enhanced zonal winds arise in the western parts of the Sargasso Sea paired with an intensified activity of storms over mid-latitudes (Hurrell, 1996). Synchronous chilling of surface waters can be attributed to wind induced latent heat flux (Cayan, 1992; Deser and Blackmon, 1993) and to the mixing of deeper and thus colder waters (Dickson *et al.*, 1996), resulting in strong vertical ventilation at Bermuda (Michaels *et al.*, 1994).

2.3.1 Climate data

For correlation with the coral chronologies we chose SST at Bermuda, the Bermuda-Iceland atmospheric pressure difference and the maximum depth of the winter mixed layer at Bermuda.

Instrumental climate data of SST (1889-1991) and sea level pressure (1854-1991) for grid box areas of 2° latitude by 2° longitude are available from COADS (Comprehensive Ocean-Atmosphere Data Set, Woodruff *et al.*, 1987). Bermuda lies close to the demarcation line of two grid boxes (center at 32°N, 65°W; 32°N, 63°W) and the mean of both grid areas was used. The sea-level pressure index is calculated as the difference of normalized winter (December to February) sea level pressure between Bermuda and Iceland (Stykkisholmur).

Monthly hydrographic measurements are obtained at the Hydrostation S approximately 22 km

south of the archipelago (WOODS Hole Oceanographic Institute and Bermuda Biological Station for Research, 1988). A time series of the mixed layer depth since 1957 was calculated from this data set by Michaels *et al.* (1994).

2.4 MATERIALS AND METHODS

Two large colonies of *D. labyrinthiformis* were collected in summer 1993 on the outer fore-reef rim of the Bermuda platform at North East Breakers (BDA 210) and Kitchen Shoals (BDA 221) (Figure 2.1). Both flourished in approximately 25 m water depth in comparable open-water conditions with negligible island effect. Both colonies were approximately 70 cm high and revealed a columnar shape with dead and encrusted flanks.

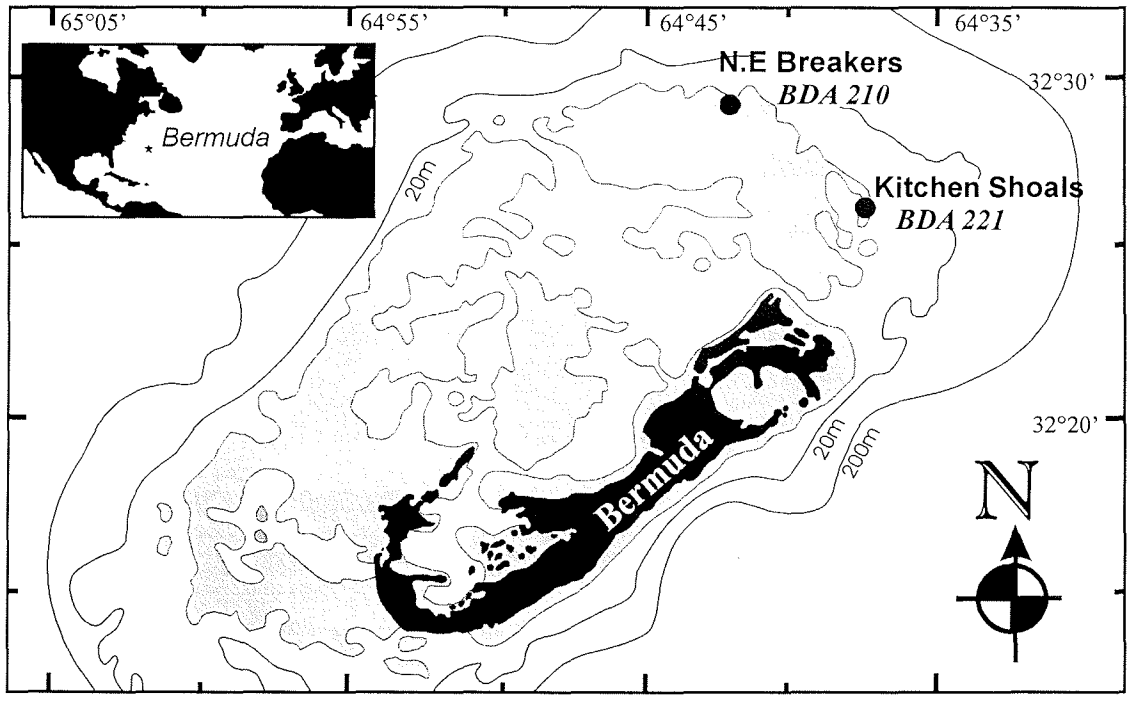

Figure 2.1 Map of the Bermuda Islands and sampling sites of the two large coral colonies of *D. labyrinthiformis* at North East Breakers (BDA 210, 32°30′2′′N/ 64°42′0′′W) and Kitchen Shoals (BDA 221, 32°28′2′′N/ 64°34′5′′). Shaded areas mark water depths ≤ 5m.

After sampling, residual organic matter was removed from the colony surfaces. The skeletons were sectioned longitudinally, parallel to the axis of maximum growth, into slabs of 5-6 mm. The slabs were X-rayed on an industrial X-ray machine and radiographs were developed on Agfa Strukturix D 4 film. Contact prints of the X-radiographs were made to choose suitable profiles of growth patterns and to provide templates. Annual growth bands were assigned appropriate years of formation by counting couplets of density bands from the known date of collection at the top of the colonies.

Two approaches were combined to analyze skeletal density and growth rate history:

1. Relative optic density measurements were obtained from contact prints of X-ray images. The radiographs were scanned, and brightness and contrast effects were optimized with the image analysis software OPTIMAS (Bioscan Inc., UK). Optic grey values of the X-ray image were measured on profiles from the colony surface, following tracks of exothecal increments. A single measurement covered 0.2 mm in heights and 0.5 mm in width, resulting in 15 to 20 gray values per annual growth band. The method does not yield absolute density values but grants high resolution to extract annual growth rates. In the optic density profiles, high density bands are recorded by narrow and sharp peaks while low density portions are significantly extended and grey values vary strongly. Therefore, we determined the linear growth of one year and average annual optic density between two optic density maxima.

2. Absolute bulk density was measured by gamma-densitometry along the growth-axis of skeleton slices with 1-2 cm thickness. The method is based upon the attenuation of a gamma photon beam, depending on the thickness and density of the skeletal material (Evans, 1965). The application on coral skeleton density was introduced by Chalker and Barnes (1990). The gamma-ray beam (emission 662 keV) of the Cs^{137} MSCL-source (Multi Sensor Core Logger, Geotek Ltd., UK) was collimated by a 2 mm collimator, measurement steps were 1 mm and counting time was 120 seconds. Absolute bulk density ρ (g/cm^3) is defined as:

$$\rho = \ln\left[\frac{I}{Io}\right] \cdot \left[\frac{I}{-\mu d}\right] \qquad (1)$$

where Io is the incident gamma-ray intensity (counts per second), and I is the attenuated gamma-ray intensity (counts per second) after passing through an object with the Compton mass attenuation coefficient μ and the thickness d (cm). The mass attenuation coefficient was

calibrated by measuring solid marine aragonite cubes (cut from a giant clam *Tridacna*) with density of 2.92 g cm^{-3} and known edge-length. Our experimental value for mass attenuation coefficient of 0.0778 cm^2 g^{-1} is identical to the value given in literature for marine aragonitic materials with a strontium content of 0.8% (Whitmarsh, 1971).

Gamma-densitometry profiles were assigned to years by peak-to-peak assignment with the time series of mean annual optic density values. Due to considerable small growth rates of 3-4 mm in *D. labyrinthiformis,* the method by gamma-densitometry does not clearly detect seasonal cycles of skeletal density variation but displays variability, integrated over a time-span exceeding one season.

In order to test the seasonal assignment of sub-annual density variations, a short profile of optic density measurements was compared to a high-resolution parallel track of oxygen isotope data. Stable oxygen isotope measurements were carried out on a Finnigan MAT 251 mass spectrometer with an automatic carbonate preparation device (Kiel Device). The results were calibrated against NSB-19 standard and are given in the δ notation relative to PDB isotopic standard. Measurement precision was ±0.06‰ for $\delta^{18}O$.

The density and growth rate time series of the two corals, that both cover the period since 1855, were correlated to instrumental time series of SST, the winter pressure index between Bermuda and Iceland and the depth of winter mixed layer by linear and multiple regression analysis.

2.5 RESULTS

2.5.1 Seasonal timing of band formation

In Figure 2.2, a profile of optic density values is compared to a high resolution profile of coral $\delta^{18}O$ in BDA 210. The stable oxygen isotope composition of the coral skeleton serves as a measure of seasonal variations in SST (Epstein *et al.*, 1953) and hence offers a scale for the seasonal timing of band formation.

Seasonally, the position of high density bands occurs relative to low $\delta^{18}O$ values, which are indicators for high seasonal water temperatures in summer.

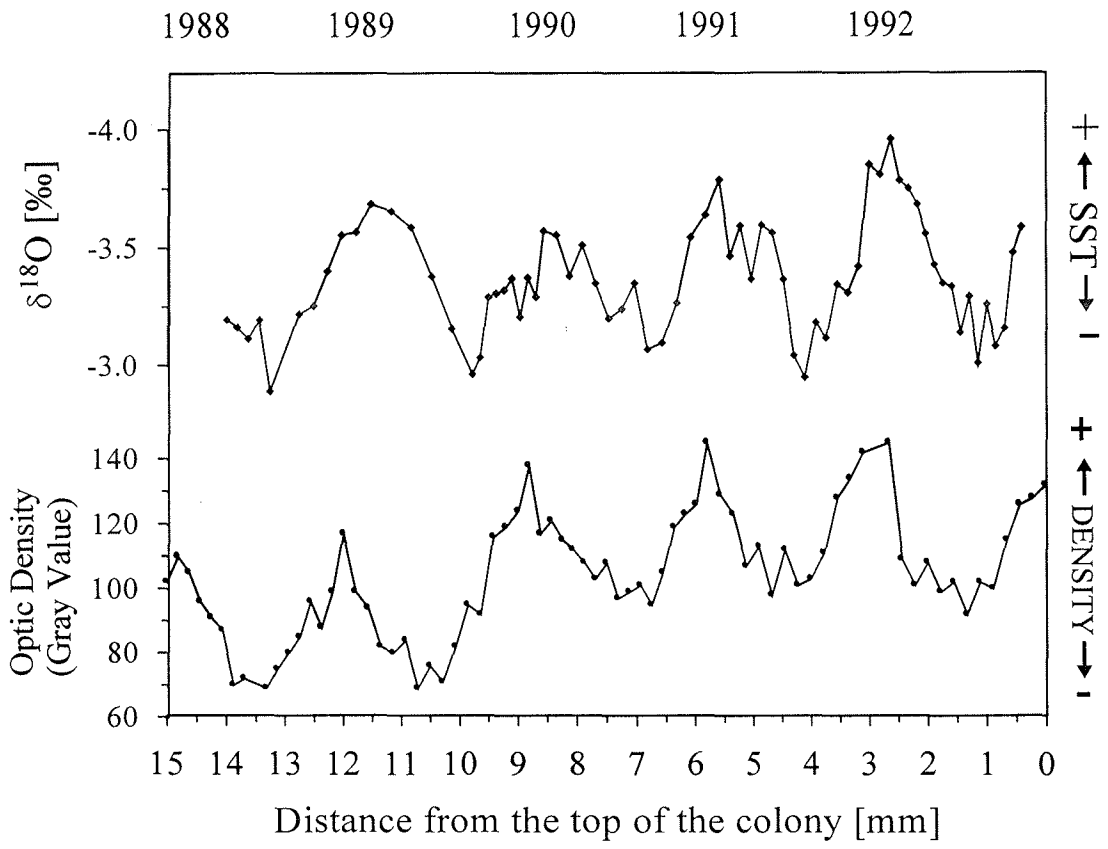

Figure 2.2 High resolution profile of optic skeletal density and a parallel track of stable oxygen isotope composition in the skeleton of *D. labyrinthiformis* (BDA 210). The chronologies cover the period between 1988 and 1993. The positions of sub-annual high density bands are indicated by shaded bars.

In a general pattern, seasonal variations of skeletal density are characterized by a positive relationship to seasonal SST variations. However, high and low density extremes temporally lead extremes in water temperature. The phase shift between optic density and $\delta^{18}O$ extremes accounts for approximately one to two months. Hence, high and low density bands are most probable to center in June to July and December to January, respectively, and do not exactly coincide to SST extremes that occur in August and February. Therefore, we suggest that high and low density bands in BDA 210 occur in response to maximum and minimum light intensities, respectively, which analogously lead extremes in water temperature by about one month (Bodungen *et al.*, 1982). The thesis that light, rather than temperature, is the primary triggering influence for seasonal variations of skeletal density, can deliver further implements for the interpretation of long-term density variability.

2.5.2 Correlation to climate data

Time series of annual skeletal bulk density and annual growth rate of BDA 210 and BDA 221 are displayed in Figure 2.3a, b. Annual density values were calculated by the average of three to four bulk density values that were attributed to one years growth by the linear share they represent.

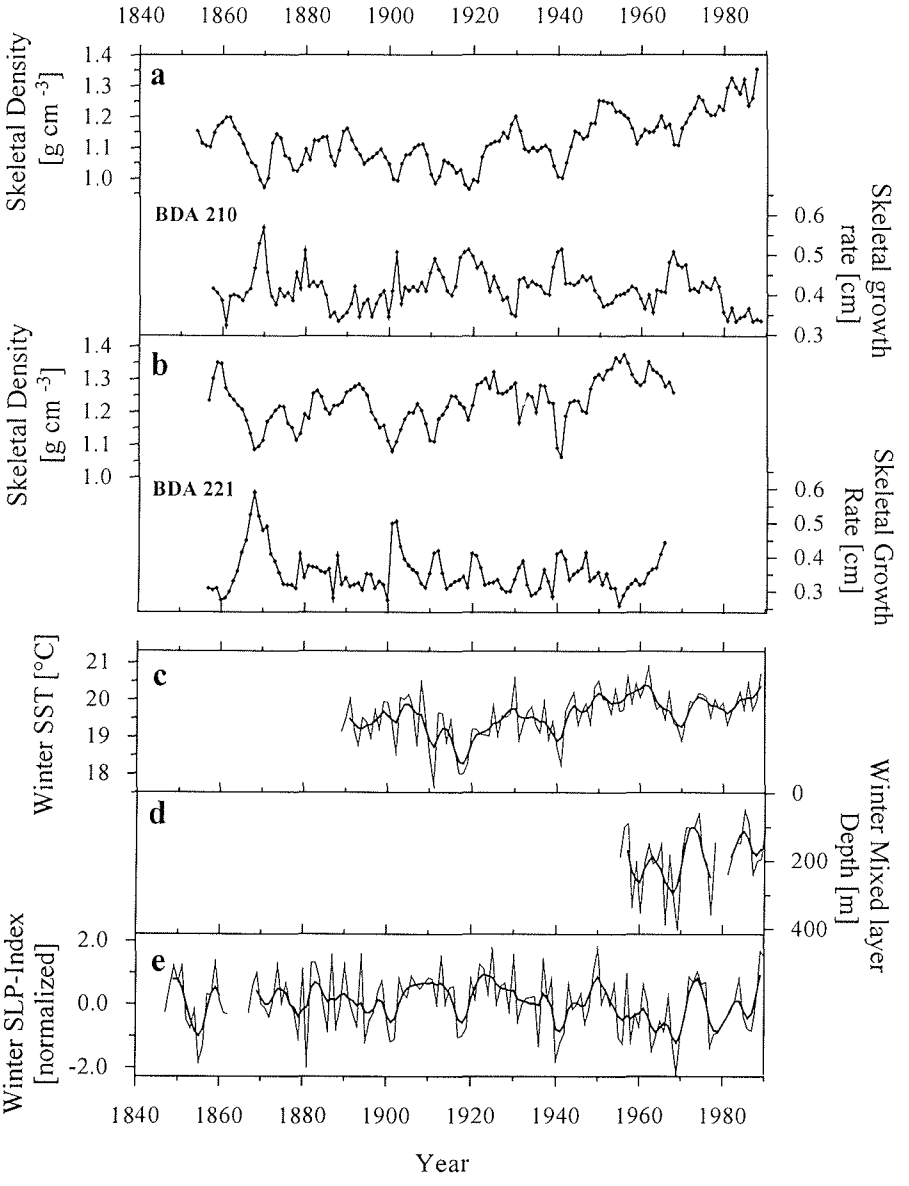

Figure 2.3 Time series of skeletal bulk density and growth rates of two colonies of *D. labyrinthiformis* (BDA 210 and BDA 221) between 1855 and 1990 (Figure 2.3a, b). Instrumental records of mean winter (December-February) SST (Figure 3c), and winter mixing depth at Bermuda (Figure 3d) (after Michaels *et al.*, 1994), and winter sea-level pressure index between Bermuda and Iceland (Figure 3e). Climatic data are additionally smoothened by a symmetric 3-point Gauss-filter.

In BDA 210, average bulk density is 1.126 g cm^{-3} and mean growth rate is 0.39 cm $year^{-1}$. Density ranges from 0.97 g cm^{-3} to 1.29 g cm^{-3} and band width totally varies between 0.31 cm $year^{-1}$ and 0.47 cm $year^{-1}$. The skeleton of BDA 221 is denser with an average bulk density of 1.24 g cm^{-3} but characterized by smaller mean growth rate of 0.35 cm $year^{-1}$. Total variation of density is between 1.06 g cm^{-3} and 1.43 g cm^{-3} and growth rate varies between 0.26 cm $year^{-1}$ and 0.59 cm $year^{-1}$.

On inter-annual time-scales, skeletal density is strongly inverse related to growth rate. In BDA 210 the reciprocity between annual values of density and linear growth is given by r = -0.64 (n = 131) and in BDA 221 by r = -0.62 (n = 111).

The most striking feature of the annual skeletal density time series of both corals is the strong resemblance. The correlation between both density time series is r = 0.81 (n = 105) (Figure 2.4). Growth rate chronologies of both corals on the other hand yield a significant but inferior similarity with r = 0.46 (n = 105).

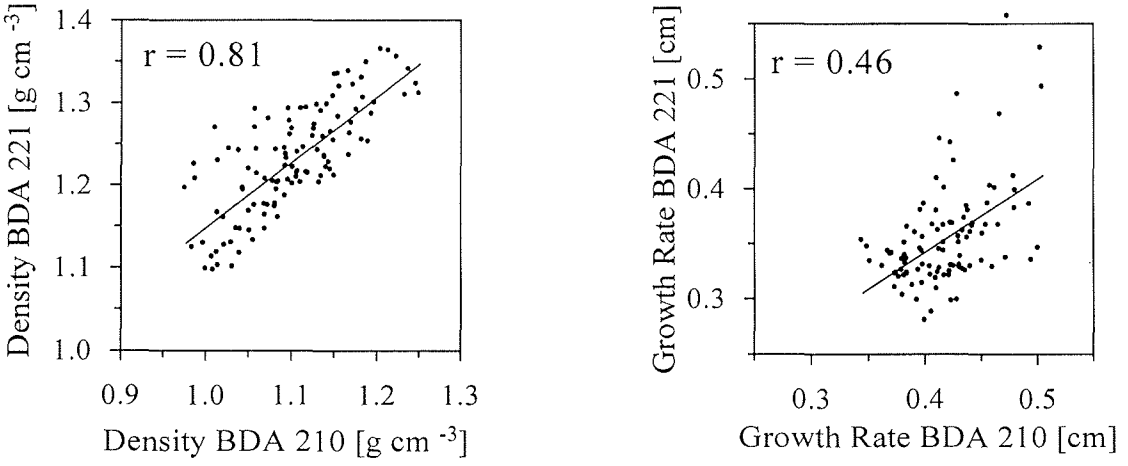

Figure 2.4 Scatter plots and correlation coefficients (r) of annual skeletal density of BDA 210 versus density of BDA 221 and annual growth rate of BDA 221 versus growth rate of BDA 221 for the period between 1865 and 1970 (n = 105). The lines indicate the geometric mean regression of the variables.

The time series of skeletal bulk density and growth rates of the two corals (Figure 2.3a, b) show an evident convariation with instrumental records of winter SST (Figure 2.3c) and mixed layer depth (Figure 2.3d) at Bermuda and the winter atmospheric pressure index between Bermuda and Iceland (Figure 2.3e). The dependence of skeletal growth parameters

on seasonal climate regimes was tested. We calculated linear correlation coefficients between annual bulk density and growth rate versus seasonal values of SST and sea level pressure index where winter is December to February, spring is March to May, summer is June to August and fall is September to November (Table 2.1).

Table 2.1 Correlation coefficients (r) of annual skeletal density and growth rate versus seasonal values of sea surface temperature (SST) at Bermuda and sea-level pressure difference between Bermuda and Iceland (SLP-Ind.). Bold marked coefficients are statistically valid at the 95% confidence level. Level of significance for BDA 210 is 0.17 and for BDA 221 0.19

Climatic season	Skeletal Density		Growth Rate	
	BDA 210	BDA 221	BDA 210	BDA 221
SST Winter	**0.59**	**0.56**	**-0.46**	**-0.31**
SST Spring	**0.29**	**0.28**	**-0.27**	-0.13
SST Summer	**0.18**	0.11	**0.19**	-0.01
SST Fall	**0.45**	**0.49**	**-0.32**	**-0.19**
SLP-Ind. Winter	**0.35**	**0.31**	**-0.29**	-0.18
SLP-Ind. Spring	0.03	0.01	-0.03	0.01
SLP-Ind. Summer	0.04	-0.04	-0.12	-0.08
SLP-Ind. Fall	0.14	-0.03	-0.13	0.02

Annual skeletal density of both corals shows a positive and statistically significant association to SST in all seasons. The correlation is highest in winter, diminishes in transition to spring and summer and again is moderate during fall. A similar pattern can be examined for yearly growth rates. In both corals linear growth rate is significantly related to winter SST at Bermuda. In BDA 210 the correlation between annual growth rates and spring and summer SST is statistically valid but weaker, while growth rate of BDA 221 reveals no significant correspondence to spring and summer SST. Annual skeletal density is positively related to the winter atmospheric pressure index between Bermuda and Iceland while growth rate exhibits a negative relationship. However, growth rate is only matched significantly to the sea-level pressure index in BDA 210.

Convincingly high correlations between skeletal growth parameters and environmental data are exclusively revealed to temperature and atmospheric pressure differences of the winter seasons. In both corals, annual skeletal density generally reveals a stronger correlation to seasonal climate variables, compared to annual growth rate.

We Gauss-filtered both time series of skeletal density and instrumental climate time series of the winter quarter (December to February). Moreover, we calculated an average composite time series of both skeletal density chronologies, justified by the strong similarity, and compared this composite density record to the filtered climate variables (Figure 2.5). From visual comparison with Figure 2.3 it can be stated that the agreement between Gauss-filtered time series of skeletal density and winter climate variables is higher than for unfiltered time series.

Superimposed on the records is the trend of second polynomial order. There is a strong similarity between the filtered composite skeletal density record and winter SST data (Figure 2.5a). The trend in skeletal density closely matches the increasing SST trend recorded since the late nineteenth century. The linear correlation coefficient between both time series is $r = 0.68$ ($n = 96$). There is also an evident convariation between the skeletal density composite record and the winter SLP index but the trends of the instrumental data series and the proxy record are opposite in sign (Figure 2.5b). The records match with a correlation of $r = 0.36$ ($n = 127$). Figure 2.5c illustrates the increased coincidence between the composite density record and the winter SLP index after subtraction of the polynomial trend. The detrended time series reveal a linear correlation of $r = 0.47$ ($n = 127$). In a multiple regression analysis between detrended time series of the composite skeletal density and the environmental variables, SST variations account for 32% and SLP index for 23% of inter-annual skeletal density variations.

Most sensitively, the corals record cold year events, connected to an extreme negative state of the atmospheric pressure difference, such as occurred in 1902, 1918, 1941 and 1969. On the other hand, extraordinary warm years in which a high SLP index was measured, like 1904, and 1961, result in a less characteristic response by skeletal density. This finding is supported by the fact that correlation graphs of linear regression analysis between skeletal growth parameters and climate variables generally reveal a strong scatter in the upper range of values and show better correlation in the low range of values.

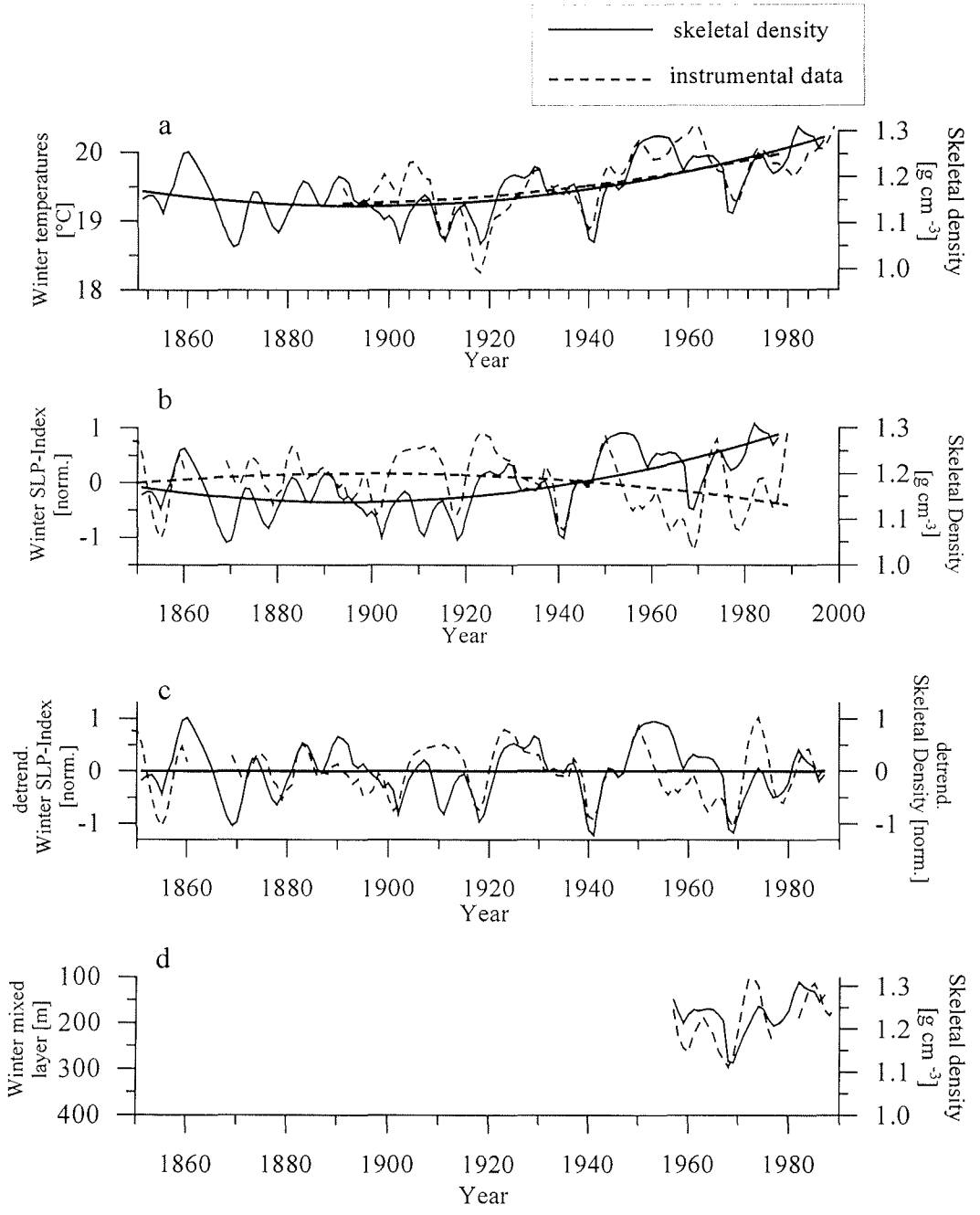

Figure 2.5a-d Gauss-filtered time series of composite skeletal density (solid lines) versus (a) normalized winter SST (dashed line), (b) versus winter SLP index (dashed line), (c) detrended record of composite skeletal density (solid line) versus detrended winter SLP index (dashed line) and (d) composite record of skeletal density versus mixed layer depth (dashed line). The trends (2^{nd} polynomial order) are indicated by bold curves.

The time series of winter mixed layer is too short to integrate the environmental variable into the multiple regression analysis. However, the skeletal density composite record reveals a

close association to winter mixing depth (Figure 2.5d). Skeletal density is negatively related to the time series of the maximum depth of the mixed layer in winter since 1957 with r =-0.56 (n = 31). Hence, a deep winter mixing that is indicating an extensive supply with nutrients to the upper layer causes a reduction of skeletal density of the corals.

2.6 DISCUSSION

2.6.1 Interrelations of coral growth

The aim of this study was to evaluate the suitability of skeletal growth parameters of *D. labyrinthiformis* as climate proxy-indicators for the low-latitude North Atlantic during the last 150 years. Significant correlations are evident between coral growth chronologies and instrumental time series of SST at Bermuda, for atmospheric pressure differences between Bermuda and Iceland and for the depth of mixed layer in winter. The correspondence between skeletal density and environmental variables, however, is slightly different between the two coral colonies.

Principally, skeletal density reveals a stronger correlation to climate variables in both colonies than observed for annual growth rate. Furthermore, the density chronologies of the two colonies show a higher resemblance than both time series of growth rates. We therefore suggest that skeletal density is the more sensitive and dependent proxy for the environmental parameters studied, while annual linear growth rate varies more individually and probably reflects a larger proportion of differences in the microhabitat. Furthermore, the highly inverse correlation between skeletal density and growth rate observed in both exemplars is a hint that both parameters are closely coupled, and possibly one parameter is governed by the other. Here, skeletal density was earlier suggested to be influenced by variations in growth rate (Barnes & Devereux, 1988).

As possible environmental influences on skeleton growth parameters of Bermuda corals we suggest temperature, light and nutrients. At the Bermuda off-shore locations, mainly in winter inorganic nutrients are provided by the overturning of the surface water layer (Siegel *et al.*, 1990), because sewage and land runoff are negligible (Morris *et al.*, 1977). The extent of vertical winter mixing is responsible for the timing and intensity of phytoplankton blooms and

in turn of zooplankton blooms (Menzel and Ryther, 1961). The later form the heterotrophic food source of the coral polyps. Several studies provided evidence that enhanced zooplankton and allochthonous nutrient levels promote increasing growth rates of coral skeletons (e.g. Dodge and Vaisnys, 1975; Tomascik and Sander, 1985). Supporting this thesis, we find an increase in linear extension during winters with high heterotrophic food supply, indicated by deep vertical mixing. Presumably, the sources and supply with food for hermatypic corals is different between the seasons. During winter, when sufficient supply with zooplankton is given, the heterotrophic diet might be dominating. In contrast, during summer, when light supply is sufficient but zooplankton levels are diminished, the corals might predominantly show autotrophic behaviour, deriving photosynthetically produced matter from their symbiotic zooxanthellae. Light intensity (Muscatine *et al.*, 1989) and temperature (Highsmith, 1979) control the photosynthetic activity of the zooxanthellae and hence are dominating the supply of autotrophic energy for the coral polyps.

Seasonal light intensity varies considerably at Bermuda. During winter, high cloud cover adds to a decrease in net insolation by 65% relative to average insolation in June. Here, atmospheric pressure can act as an indicator for seasonal and long-term light levels, where periods of low pressure are usually accompanied by cloudy conditions, and high pressure by sunshine. The colonies that grew in relatively deep habitats of approximately 25 m, revealed a high columnar growth shape with dead and encrusted flanks. Probably, the angular entering light was not substantial in guaranteeing survivorship of the peripheries of the colonies. This is a hint that light is a limiting environmental factor. Furthermore, during strong winters, the reduction of skeletal density might be a necessity in order to cope with a diminished metabolic turnover. In comparison, increased skeletal growth rates might be an indicator for competitive behavior and the urgent need to grow upwards into levels were light and temperature are more likely to secure survivor of the community.

The skeletal density and growth rate records of both colonies of *D. labyrinthiformis* from Bermuda are predominantly reflecting a particular season of the year. Correlations between skeletal growth parameters and seasonal climate regimes show that the corals respond most sensitively to wintertime conditions. Summer conditions are most probable to be favorable for coral growth. Therefore, variations within the optimum range of environmental parameters will only result in minor effects of skeletal growth. Furthermore, the autotrophic behavior

during the warm and bright summer season might provide independence from the heterotrophic food supply and in turn act like a buffer to the environment. During winter, on the other hand, both temperature and light intensity might be reduced to a limiting level for coral growth. Correspondingly, the corals reveal lesser reaction during years when wintertime conditions were mild but show a strong skeletal signal during years that were characterized by severe winters. This most probably reflects that the corals are close to some form of climatic limit and hence they reveal clear correlations with limiting and unfavorable climatic conditions.

2.6.2 Correlation with climate variables

The low density bands are formed in early winter, and high density bands are secreted during early summer, as found also by Dodge and Thompson (1974) for inshore colonies of *D. labyrinthiformis* in Bermuda. Here, light is believed to be the primary environmental control on skeletal density variations on seasonal time-scales. On inter-annual time-scales, skeletal density is characterized by a positive relationship to SST. For inter-annual variations of skeletal density, it cannot be clarified whether density is a function of light intensity, which is important for the photosynthesizing symbionts, or a function of water temperature. The impact of temperature on coral growth parameters has been reported (e.g. Highsmith, 1979) but the explicit vindication for a causative relation is lacking. Still, the temperature of the uppermost water column certainly is strongly dependent on the amount of sunlight, which in turn varies with the seasonal netto insolation and cloud cover. Hence, we suggest that SST could serve as an indicator for light intensity.

In this study, high correlations are registered between skeletal density and the depth of the homogenous mixed surface layer, the connection between atmospheric and subsurface water conditions that occur during overturning events in winter (Dickson *et al.*, 1996; Sutton and Allen, 1997). Furthermore, skeletal density reveals a significant response to atmospheric pressure differences between Bermuda and Iceland that act as the North Atlantic Oscillation. Not surprisingly, both phenomena are coupled. Michaels *et al.* (1994) reported significant variations in the depth and strength of winter mixing that are attributed to changes in strength of the North Atlantic Oscillation (Dickson *et al.*, 1996).

Skeletal density and growth rate records of *D. labyrinthiformis* from Bermuda are predominantly reflecting winter conditions. Hence, the strongest impact on coral growth is given during the season when the connecting patterns of the North Atlantic hydrographic and atmospheric circulation modes are best defined (Bjerknes, 1964). Furthermore, the maximum response of the corals is observed during years of prevailing unfavorable winter conditions. The unique value of skeletal density of *D. labyrinthiformis* from Bermuda as a proxy indicator for climatic variability in the North Atlantic can therefore be given by the strong response to inter-annual events of cold water anomalies connected to extreme low index states of the North Atlantic Oscillation system.

During the twentieth century, Bermuda exhibits a strong annual correspondence between annual mean SST and annual winter SST ($r = 0.76$, $n = 91$). Despite the dominance of a seasonal response of skeletal growth parameters, the reconstructed SST conditions, to a certain extent, can be extrapolated to the climatic year as a whole and skeletal density may well be representative for annual average conditions in most years.

2.7 CONCLUSIONS

On coral colonies of *D. labyrinthiformis* it could be shown that mean annual skeletal density and annual growth rates are strongly but inversely correlated. However, skeletal density generally reveals a closer statistical correspondence between two different colonies and to environmental parameters, compared to annual growth rate. Therefore, we consider density as the more sensible and reliable predictor for the climate variables observed in our study. The coral skeletons reveal a most effective response to their environment during winter. Density is positively related to winter temperature and to hemispherical pressure anomalies. We suggest that light is a fundamental limiting factor. High inverse correlation is also recorded between skeletal growth and the depth of the homogeneous mixed layer, which is interpreted as a gauge for heterotrophic food supply.

The apparent impact of Atlantic atmospheric and hydrographic changes on skeletal growth supports a sclerochronological approach to skeletal density of *D. labyrinthiformis* as a high-

resolution marine analogue to the study of tree rings. Coral chronologies have the capacity to yield incessant proxy data to reconstruct climate for the last several centuries.

2.8. ACKNOWLEDGEMENTS

We thank T. Bickert, B. Flemming and H. Grobe for helping in sample collection. The isotopic measurements were carried out at the stable-isotopic laboratory at Bremen University. We gratefully acknowledge M. Segl and her team for performing the measurements. We thank U. Röhl for her technical support on the MSCL. Discussions with W.H. Berger and C. Waldmann have been most helpful. The manuscript was improved by the comments of H. Kuhnert, R. Huber and G. Crawford. This work was funded by the 'Paläoklima' BMBF-grant 03F0131A.

2.9 REFERENCES

Barnes, D.J. and Devereux, M.J. 1988: Variations in skeletal architecture associated with density banding in the hard coral *Porites*. *J. Exp. Mar. Biol. Ecol.* 121, 37-54.

Bjerknes, J. 1964: Atlantic air-sea interaction. *Adv. Geophys.* 10, 1-82.

Bodungen, B.v., Jickells, T.D., Smith, S.R., Ward, J.A.D. and Hillier, G.B. 1982: The Bermuda Marine Environment. Final report of the Bermuda inshore waters, Investigations 1975-1980. *BBSR Special Publication* 18, 123pp.

Cayan, D. 1992: Latent and sensible heat flux anomalies over the northern oceans: Driving the sea surface temperature. *J. Phys. Oceanogr.* 22, 859-881.

Chalker, B.E. and Barnes, D.J. 1990: Gamma-densitometry for measurement of skeletal density. *Coral Reefs* 9, 11-23.

Deser, C. and Blackmon, M.L. 1993: Surface climate variations over the North Atlantic Ocean during winter 1900-1989. *J. Clim.* 6, 1743-1753.

Dickson, R., Lazier, J., Meincke, J., Rhines, P. and Swift, J. 1996: Long-term coordinated changes in the convective activity of the North Atlantic. *Progr. Oceanogr.* 37, 207-262.

Dodge, R.E., Aller, R.C. and Thompson, J. 1974: Coral growth related to resuspension of bottom sediments. *Nature* 247, 574-577.

Dodge, R.E. and Thompson, J. 1974: The natural radiochemical and growth records in contemporary corals from the Atlantic and the Caribbean. *Earth Planet. Sci. Lett.* 23, 313-322.

Dodge, R.E. and Vaisnys, J.R. 1975: Hermatypic coral growth banding as an environmental recorder. *Nature* 258, 706-708.

Epstein, S., Buchsbaum, R., Lowenstam, H. and Urey, H.C. 1953: Revised carbonate-water isotopic temperature scale. *Geol. Soc. Am. Bull.* 64, 1315-1325.

Evans, H.B. 1965: GRAPE - A device for continuous determination of material density and porosity. *SPWLA 6th Annual Logging Symposium* 2, B1-B5.

Hansen, D.V. and Bezdek, H.F. 1996: On the nature of decadal anomalies in North Atlantic sea surface temperature. *J. Geophys. Res.* 101, C4, 8749-8758.

Highsmith, R.C. 1979: Coral growth rates and environmental control of density banding. *J. Exp. Mar. Biol. Ecol.* 37, 105-125.

Hurrell, J.W. 1995: Decadal trends in the North Atlantic Oscillation: Regional temperature and precipitation. *Science* 269, 676-679.

Hurrell, J.W. 1996: Influence of variations in extratropical wintertime teleconnections on Northern Hemisphere temperature. *Geophys. Res. Lett.* 23, 6, 665-668.

Klein, R., Pätzold, J., Wefer, G. and Loya, Y. 1993: Depth related timing of density band formation in *Porites* spp. corals from the Red Sea inferred from X-ray chronology and stable isotope composition. *Mar. Ecol. Progr. Ser.* 97, 99-104.

Knutson, D.W., Buddemeier, R.W. and Smith, S.V. 1972: Coral chronometers: Seasonal growth bands in reef corals. *Science* 177, 270-272.

Kushnir, Y. 1994: Interdecadal variations in North Atlantic sea surface temperature and associated atmospheric conditions. *J. Clim.* 7, 141-157.

Logan, A. and Tomascik, T. 1991: Extension growth rates in two coral species from high latitude reefs of Bermuda. *Coral Reefs* 3, 155-160.

Logan, A., Yang, L. and Tomascik, T. 1994: Linear skeletal extension rates in two species of *Diploria* from high latitude reefs in Bermuda. *Coral Reefs* 13, 225-230.

Mc Cartney, M. 1997: Is the Ocean at the helm? *Nature* 388, 521-522.

Menzel, D.W. and Ryther, J.H. 1961: Annual variation in primary production of the Sargasso Sea off Bermuda. *Deep Sea Res.* 7, 282-288.

Michaels, A.F., Knap, A.H., Dow, R.L., Gundersen, K., Johnson, J.J., Sorensen, J., Close, A., Knauer, G.A., Lohrenz, S.E., Asper, V.A., Tuel, M. and Bidigare, R. 1994: Seasonal patterns of ocean biogeochemistry at the JGOFS Bermuda Atlantic Time-Series Study Site. *Deep-Sea Res.* 41, 7, 1013-1038.

Molinari, R.L., Mayer, D.A., Festa, J.F. and Bezdek, H.F. 1997: Multiyear variability in the near surface temperature structure of the mid-latitude western North Atlantic Ocean. *J. Geophys. Res.* 102, C2, 3267-3278.

Morris, B., Barnes, J., Brown, F. and Markham, J. 1977: The Bermuda Marine Environment. A report of the Bermuda inshore waters, Investigations 1976-1977. *BBSR, Special Publication* 15, 199pp.

Muscatine, L., Porter, J.W. and Kaplan, I.R. 1989: Resource partitioning by reef corals as determined from stable isotope composition. *Mar. Biol.* 100, 185-193.

Rogers, J.C. 1984: The Association between the North Atlantic Oscillation and the Southern Oscillation in the Northern Hemisphere. *Mon. Weath. Rev.* 112, 1999-2015.

Siegel, D.A., Itturiaga, R., Bidigare, R.R., Smith, R.C., Pak, H., Dickey, T.D., Marra, J. and Baker, K.S. 1990: Meridional variations in the spring time phytoplankton community in the Sargasso Sea. *J. Mar. Res.* 48, 379-412.

Sutton, R.T. and Allen, M.R. 1997: Decadal predictability of North Atlantic sea surface temperature and climate. *Nature* 388, 563-567.

Taylor, R.B., Barnes, D.J. and Lough, J.M. 1993: Simple models of density band formation in massive corals. *J. Exp. Mar. Biol. Ecol.* 167, 109-125.

Tomascik, T. and Sander, F. 1985: Effects of eutrophication on reef building corals. 1. Growth rate of the reef building coral *Montastrea annularis*. *Mar. Biol.* 87, 143-155.

Wellington, G.M. and Glynn, P.W. 1983: Environmental influences on skeletal banding in Eastern Pacific (Panama) corals. *Coral Reefs* 1, 215-222.

Whitmarsh, R.B. 1971: Precise sediment density determination by gamma-ray attenuation. *J. Sed. Petr.* 41, 882-883.

Woodruff; S.D., Slutz, R.J., Jenne, R.L. and Steurer, P.M. 1987: A Comprehensive Ocean-Atmosphere Data Set. *Bull. Am. Meteorol. Soc.* 68, 1239-1250.

Woodshole Oceanographic Institute and Bermuda Biological Station for Research 1988: Station S off Bermuda: Physical measurements, 1954-1991, *Library of Congress Catalogue*, 88-51552.

3 North Atlantic climate variability since AD 1350 recorded in $\delta^{18}O$ and skeletal density of Bermuda corals

S. Draschba, J. Pätzold, G. Wefer

Fachbereich Geowissenschaften

Universität Bremen

Postfach 330 440

D-28334 Bremen

Germany

Submitted to 'Geologische Rundschau'

3.1 ABSTRACT

The reconstruction of the climatic history during the past several hundred years requires a sufficient geographical coverage of combined climate proxy-series. Especially, in order to identify causal connections between the atmosphere and the ocean, the including of marine records into composite climate time series, is of fundamental importance.

We present two skeletal $\delta^{18}O$ chronologies of coral skeletons of *Diploria labyrinthiformis* from Bermuda fore-reef sites covering periods in the nineteenth and twentieth century and compare them to instrumental temperature data. Both time series are demonstrated to display sea surface temperature (SST) variability on inter-annual to decadal time scales.

On the basis of a specific modern $\delta^{18}O$ versus instrumental SST calibration we reconstruct a time series of SST anomalies between AD 1350 and 1630 covering periods during the Little Ice Age. The application of the coral $\delta^{18}O$ versus temperature relationship leads to estimates of past SST variability which are comparable to the magnitude of modern variations. Parallel to $\delta^{18}O$ chronologies we present time series of skeletal bulk density. Coral $\delta^{18}O$ and skeletal density reveal a strong similarity during Little Ice Age, confirming the reliability of both proxy climate indicators.

The past coral records, presented in this study, share features with a previously published climate proxy record from Bermuda and a composite time series of reconstructed Northern Hemisphere summer temperatures. The coral proxy data presented here can represent a valuable contribution to elucidate northern Atlantic subtropical climate variation during the past several centuries.

3.2 INTRODUCTION

The oceanic-atmospheric system of low latitudes is a fundamental component in the global climate system. Understanding the mechanisms and forcings of climate variability on a long-term perspective will open further insights for the predictability of natural climate changes and will allow to assess anthropogenic impact. Of particular relevance are climatic variations of the last few centuries including the period referred to as Little Ice Age.

There is some disagreement about the actual start and ending of the Little Ice Age depending on the type of measurement. Porter (1986) defines the duration between the end of the Middle Ages at around AD 1250 until 1920, whereas Lamb (1977) confines the Little Ice Age to 1550 to 1850. However, there is agreement about the fact that it lasted for centuries and that conditions were cooler than the present century. So, the question arises whether the recent warming of the twentieth century belongs to natural climate fluctuations or is forced by human activity.

Unfavorably, instrumental climate observations, especially of low latitudes, are rare and seldom span more than a few decades. Furthermore, for the oceans that cover approximately 70% of the globe-surface, climate data are even more sparse and for vast areas of the tropical oceans instrumental information is devoid. In order to obtain a broader picture of past climate variability including the period of Little Ice Age, non-instrumental records from which climate conditions can be deduced have to be obtained. Among the most powerful climate-sensitive proxy indicators are those derived from the skeletons of long-lived hermatypic reef corals. Proxy data such as the stable isotope composition of the skeleton and skeletal growth parameters enable the detection of past high-frequency climate variations in low latitudes.

Physical controls on the stable oxygen isotope composition of marine carbonates are sea surface temperature and the isotopic composition of the ambient seawater (Epstein *et al.*, 1953). The $\delta^{18}O$ of the seawater underlies changes due to rainfall or evaporation and here sea surface salinity serves as a measure for the extent of isotopic dilution with isotopically light rainfall (Fairbanks *et al.*, 1992). Therefore, variability in coral $\delta^{18}O$ primarily reflects changes in temperature (e.g. Pätzold, 1984, Crowley *et al.*, 1997) or changes in sea surface salinity (e.g. Cole and Fairbanks, 1990; Tudhope *et al.*, 1995) or yields information on a composite signal (e.g. Carriquiry *et al.*, 1993; Wellington *et al.*, 1996).

Comparable to tree rings, the corals lay down alternating sub-annual skeleton-bands of high and low density (Knutson *et al.*, 1972). This banding pattern yields an excellent basis for a reliable stratigraphic backbone of coral records. Various studies demonstrated that environmental changes influence the growth and density patterns of coral skeletons. Ecological factors that were considered in this context include temperature (e.g. Lough *et al.*, 1996) and light (e.g. Taylor *et al.*, 1993). Other studies found relations between coral growth behavior and sedimentation rates (Brown *et al.*, 1986), growth depth (Logan and Tomascik,

1991; Klein *et al.*, 1993), the latitude of the reef location, nutrient supply and wave energy (Logan *et al.*, 1994), and the gametogenesis of polyps (Wellington and Glynn, 1983).

Former studies on the skeletons of *D. labyrinthiformis* from Bermuda showed that the density of annual bands yield information on SST (Draschba *et al.*, submitted). *D. labyrinthiformis* most sensitively responds to its environment during the winter months. Therefore, variations in annual skeletal density primary are a strong indicator for changes in winter SST conditions and they can serve as a supportive SST proxy.

The present study focuses on the reconstruction of sea surface temperature variations at Bermuda. The reconstruction is based on stable oxygen isotope and skeletal density records of three long-lived colonies of *Diploria labyrinthiformis*. We introduce stable oxygen isotope chronologies covering periods in the nineteenth and twentieth century and compare the proxy records to instrumental temperature time series. Coral $\delta^{18}O$ delivers confidential estimates of the temperature signature of the ambient seawater. Furthermore, we present a time series of reconstructed SST anomalies obtained by stable oxygen isotope and skeletal density of the climate history from Bermuda. The records span periods during the Little Ice Age from 1350 to 1630. The evaluation of the past coral records is based on the calibration of the modern $\delta^{18}O$ time series with instrumental climate data.

3.3 ENVIRONMENTAL SETTING OF THE STUDY AREA

The Bermuda islands are located at the western margin of the Sargasso Sea in the North Atlantic at 32°20´N, 64°50´W (Figure 3.1). The Archipelago has a subtropical climate system, supported by warm water transported north by the Gulf Stream. The climatological setting of the islands is dominated by a strong seasonality (Bermuda Environmental Scenario, 1974). Following the seasonal cycle in solar irradiance with 240 gcal cm^{-2} day^{-1} in December and 670 gcal cm^{-2} day^{-1} in July, the mean seasonal variance of sea surface temperatures is between 19°C in February and 26°C in August (Bermuda Environmental Scenario, 1974).

During summer, a strong stratification of the upper water column leads to oligotrophic conditions in the surface waters (Siegel *et al.*, 1990). During the transition to winter an increased mixing and surplus with inorganic nutrients occurs within the upper 100 to 400 m of

the water column (Michaels *et al.*, 1994). Salinity experiences low seasonal fluctuations with average minimum values of 36.2‰ in August and maximum salinity of 36.6‰ in April. Mean annual sea surface salinity is remarkably constant with an average inter-annual variability of 0.25‰ (Bermuda Environmental Scenario, 1974).

3.4 MATERIALS AND METHODS

Three high columnar coral colonies of *D. labyrinthiformis* were recovered at the northern and northeastern fore-reef rim of the Bermuda platform in July 1993. BDA 210 was collected at North East Breakers and BDA 221 and BDA 215 were recovered at Kitchen Shoals (Figure 3.1). All well-preserved colonies grew in approximately 25 m water depth under comparable open water conditions with negligible island effect. After sampling the corals were rinsed from polyp tissue and sectioned longitudinally into slabs of 5 mm uniform thickness, parallel to the axis of maximum growth. X-radiographs were assessed from the skeleton slices to expose density banding. Chronologies were achieved by counting the well developed density couplets.

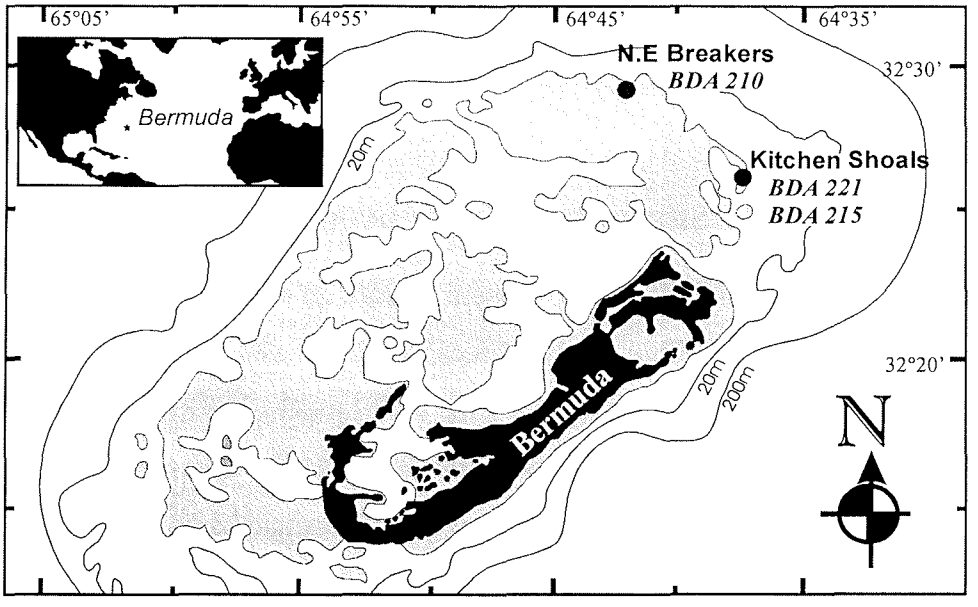

Figure 3.1 Map of the Bermuda Islands and sampling sites of *D. labyrinthiformis* colonies at North East Breakers (BDA 210, 32°30′2′′N/ 64°42′0′′W) and Kitchen Shoals (BDA 221, BDA 215, 32°28′2′′N/ 64°34′5′′). Shaded areas mark water depths ≤ 5m.

BDA 210 revealed continuous growth between 1825 and 1993 whereas BDA 215 and BDA 221 contain hiatuses. The bases of the colonies, that were separated from the upper living parts by algal growth, were ^{14}C dated by AMS in the Leibnitz Laboratory in Kiel. Precision of Dating came to ±30 years. The stratigraphy obtained from ^{14}C-dating was confirmed by the strong correspondence of the present proxy time series with a continuous 800-year coral skeletal chronology from Bermuda, presented by Pätzold *et al.* (1998) (see Figure 3.3c). Table 3.1 shows the time series of stable oxygen isotope composition and skeletal density presented in this study.

Table 3.1 List of time series of triennial coral $\delta^{18}O$ and annual skeletal density obtained from three large coral colonies of *D. labyrinthiformis* from Bermuda.

Record	Sampling location	Water depth [m]	Skeletal density measurements	$\delta^{18}O$ Chronology [year AD]
BDA 210a	NE Breakers	25	–	1832-1904
BDA 221a	Kitchen Shoals	25	–	1856-1920
BDA 221b	Kitchen Shoals	25	+	1514-1630
BDA 215c	Kitchen Shoals	27	+	1430-1505
BDA 215d	Kitchen Shoals	27	+	1350-1424
BDA 215d2	Kitchen Shoals	27	–	1398-1422

Sampling for isotope analysis was restricted to the exothecae because different skeletal elements in *D. labyrinthiformis* are subject to different fractionation effects (Pätzold, 1992). Stable isotope records with triennial sampling resolution (BDA 210a, BDA 221a, b and BDA 215c, d) were obtained by cutting sticks of 2 x 2 mm cross-section, including several decades of exothecal growth increments. The carbonate sticks were soaked in epoxy resin to avoid uncontrolled breaking of the filigree samples. The resin has no influence on the oxygen isotope results. Using a 100 µm blade, the sticks were cut into triennial segments at the center of every third low density band. The subsamples were ground and homogenized. In order to permit an estimation of the reproducibility, a short section was sampled on a parallel trace of profile BDA 215d, using the same procedure described above. The powdered aragonite samples were analyzed for oxygen isotope ratios on a Finnigan MAT 251 micro mass spectrometer with an automatic carbonate preparation device (Kiel Device). The oxygen

isotope ratios are reported in standard δ notation relative to the PDB isotopic standard. Average measurement precision was ±0.07‰ for $\delta^{18}O$.

The translation from a reference axis that represents the distance from the top of the colony into a time axis was achieved by chronologically attributing each sampling segment to the growth sequence seen in the X-radiographs. For triennial sampling resolution, each measurement was allocated the central year of the three-year window.

Absolute bulk density measurements were carried out by γ-densitometry on a Multi Sensor Core Logger with a Cs^{137} source and 1 mm collimator (Geotek Ltd., UK). The method is based upon the attenuation of a gamma photon beam, depending on the thickness and density of the skeletal material. The application on coral skeleton density was first introduced by Chalker and Barnes (1990). Due to considerable small annual growth rates of 3 to 4mm in *D. labyrinthiformis,* the method does not always detect distinguishable seasonal cycles of density variation but allows to calculate annual mean skeletal bulk density values.

For the allocation of a time axis on absolute bulk density records, high resolution optic density measurements were processed on adjacent profiles. Relative optic density measurements were obtained from contact prints of X-radiograph images. Gray values were measured along the growth axis using the image analysis software OPTIMAS (Bioscan Inc., UK). Annual growth increments are represented by 15 to 20 gray values and clearly display seasonal density banding which allow dating by counting the density cycles. On visual comparison, optic and gamma density time series coincide in detail. Based on the optic density chronology Gamma densitometry profiles were assigned to years by peak-to-peak assignment with the time series of optic density.

3.4.1 Climate data

Monthly mean air temperatures between 1856 and 1930 are acquired from Bermuda Botanical Gardens (Macky, 1952). For comparison of Bermuda air temperatures with SST data, the instrumental records of COADS (Comprehensive Ocean-Atmosphere Dataset, Woodruff *et al.*, 1987) was used. The data set provides monthly SSTs (1889 to 1997) for grid box areas of 2° latitude by 2° longitude obtained by trade ships. Bermuda lies close to the demarcation line of two grid boxes (center at 32°N, 65°W; 32°N, 63°W) and the mean of both grid areas was calculated. Approximately biweekly sea surface salinity measurements since 1954 were

obtained from the Hydrostation S approximately 22 km south of the archipelago (WOODS Hole Oceanographic Institute and Bermuda Biological Station for Research, 1988).

3.5 RESULTS AND DISCUSSION

3.5.1 88-years of coral $\delta^{8}O$ during the last century

The results of coral $\delta^{18}O$ records measured in BDA 210a and BDA 221a with triennial sampling resolution are illustrated in Figure 3.2 (a, b). The coral records cover periods during the 19th and 20th century. We compared the coral oxygen isotope records to air temperature data measured at Bermuda Botanical Gardens (Figure 3.2c).

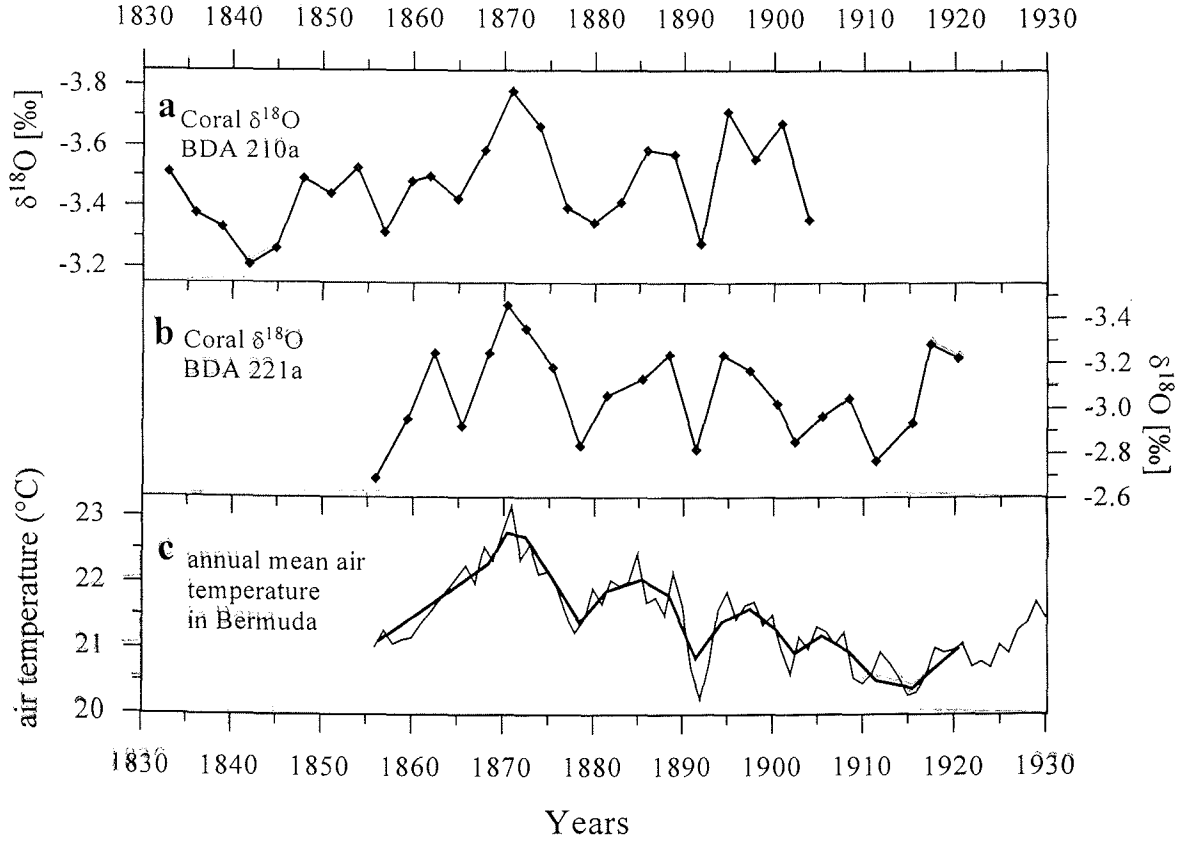

Figure 3.2a-c Time series of triennial stable oxygen isotope composition of BDA 210a and BDA 221a (a, b), covering periods during the 19th and 20th century, and a record of annual mean Bermuda air temperatures (c). Three-year means of climate data are drawn in bold.

Due to small annual growth rates of 3 to 4 mm combined with a complex skeleton architecture of *D. labyrinthiformis*, resolving the $\delta^{18}O$ signal on sub-annual time scales is crucial. Therefore, we concentrate on extracting SST variability by integrating several years of skeletal growth. The availability of instrumental climate data allow a comparison with the coral signal and will support the interpretation of reconstructed past temperature anomalies. The use of air temperatures is justified by the strong long-term correspondence between Bermuda SST (COADS) of a 2° latitude by 2° longitude area and Bermuda air temperature during a 40-year period. On a three-year running mean between 1890 and 1930 the temperature records favorably correspond yielding a correlation of r = +0.90 (n = 27) and the following linear regression relation:

$$SST_{triennial} = 0.58 * T[°C] + 10.38 \qquad T°C = \text{air temperature} \qquad (1)$$

We state that the coral $\delta^{18}O$ signal is dominantly reflecting SST conditions. Between 1954 and 1987 the typical seasonal range of sea surface salinity at Bermuda was 0.4‰ and mean inter-annual salinity changes were 0.25‰. On both, seasonal and inter-annual time scales, SST and sea surface salinity are inversely related accounting for an additive effect on coral $\delta^{18}O$. Fairbanks *et al.* (1992) determined a $\delta^{18}O$ versus salinity slope of 0.11 for western Atlantic surface waters. Seasonal salinity variations at Bermuda would therefore introduce a seasonal isotope amplitude of 0.044‰ and inter-annual variations would account for 0.0275‰ in $\delta^{18}O_{seawater}$. Hence, the salinity effect on the isotopic pool of the ambient sea-water is considered a negligible background signal and variations in coral $\delta^{18}O$ can be attributed to be primarily driven by changes in SST.

Both coral $\delta^{18}O$ records shown in Figure 3.2 are in good agreement with the time series of local air temperature variations. The $\delta^{18}O$ chronologies document a general cooling trend beginning in 1870 until 1915. Slightly higher temperatures in the mid-1880s and mid-1890s and lower than average temperatures in the late 1870s, early 1890s and early 1900 are recorded in the $\delta^{18}O$ records.

A high statistical agreement is given between three-year means of Bermuda air temperatures (bold line, Figure, 3.2c) and BDA 221a $\delta^{18}O$ with r = -0.79 (n = 22) and BDA 210a $\delta^{18}O$ with r = -0.68 (n = 18). Weaker correlation results from regression analysis between coral $\delta^{18}O$ and seasonal air temperature extremes. Mean winter temperatures were calculated from December

to February and mean summer conditions were calculated from June to August (not shown here). Based on lower correlations between coral $\delta^{18}O$ and seasonal air temperature regimes we suggest that the stable isotope records are representative for climate variability of years as a whole and temperature estimates are not biased towards a particular season.

A specific empirical relationship for triennial $\delta^{18}O$ versus SST values with respect to the 1856 to 1920 period was established by calibration of coral $\delta^{18}O$ against Bermuda air temperatures under consideration of the SST versus air temperature relationship given by equation (1). Linear regression between annual mean air temperature and coral $\delta^{18}O$ result in identical regression slopes but slightly different offsets. The best approximation for empirical SST is given by:

$$SST_{triennial} = ((-1.8\ \delta^{18}O)+16.0)\ 0.58 + 10.38 \qquad (2)$$

During kinetic temperature dependent fractionation in marine aragonitic skeletons determined by Grossman and Ku (1986) an increase of 1°C SST accounts for a decrease of 0.23‰ in $\delta^{18}O$. Most studies on scleractinian corals that established $\delta^{18}O$ versus temperature calibration on a seasonal basis, report relationships that range between 0.16 to 0.22‰ $\delta^{18}O$ per 1°C (e.g. Leder *et al.*, 1996). In comparison, inferred from the relationship (2) our results indicate that 1°C SST is responsible for 0.95‰ $\delta^{18}O$.

Finding a plausible explanation for the extreme slope of the relation is crucial. There must be amplifying influences that either would have a methodological source or would be of external or biologic origin. Based on previous studies on stable isotope composition of the skeletons of *D. labyrinthiformis* we exclude the hypothesis that the species is subject to elementary different vital fractionation responses than observed for other scleractinian coral species. (e.g. Keith and Weber, 1965a; Nozaki *et al.*, 1978). In order to seek a possible reason for the amplified $\delta^{18}O$ versus temperature relation in sea-water-$\delta^{18}O$, salinity would have to reveal inter-annual variations in the magnitude of approximately 6‰. However, inter-annual or long-term salinity variations in such vast dimensions can be excluded for the subtropical North Atlantic.

To consider possible methodological sources, the detection of climate variability on a triennial time scales is unlikely to be affected by coral growth mechanisms that operate on time scales

much shorter than the temporal sample integration. The sampling technique should equally minimize smoothing and distortion of the isotopic record due to complex coral growth, calyx architecture and calcification at depth within the tissue layer as described by Juillet-Leclerc *et al.* (1997). However, in annual bulk sampling strategies, distortions may appear where seasonal skeletal growth rates are constant and skeletal banding produces different carbonate accumulation rates throughout the year. Then, an integrative sampling approach will over-represent carbonate that was deposited during the period of high density band formation. The question remains to the quantitative isotope signal effect of varying proportions of skeletal material, carrying different temperature signals.

In summary, the considerable amplification of the specific $\delta^{18}O$ versus temperature relation can not be clarified at this point. At the same time it might be considered as a benefit since small changes in temperature result in comparably large changes in coral $\delta^{18}O$. Furthermore, the $\delta^{18}O$ versus temperature relationship is consistent in both colonies. Hence, despite the low level of sampling resolution the quality of resolving climate information on pentadal to decadal time scale is confidential and the climate signal is registered with a high susceptibility. We employ the specific triennial $\delta^{18}O$ versus temperature calibration for the reconstruction of past long-term SST variability by equivalently sampled triennial coral $\delta^{18}O$ time series.

3.5.2 Little Ice Age coral records

Determining the principle climatic characteristics of the last several hundred years, some attention has been given to climate variability of the low latitude North Atlantic. There is historical (Lamb, 1979) and proxy evidence (Pätzold *et al.*, 1998; Keigwin, 1996) for the LIA in the subtropical North Atlantic, which indicate that temperatures were cooler by 1 to 1.5°C, compared to recent annual average conditions. For example, Pätzold *et al.* (1998) introduced an 800-year Bermuda record of coral growth that has been interpreted in terms of cooling of this magnitude, which was induced at least partly by an enhancement of wind-driven vertical mixing and heat flux changes in the surface waters (see Figure 3.3c).

We present three records of coral $\delta^{18}O$ and skeletal density from Bermuda that cover a major portion of the Little Ice Age (Figure 3.3a, b). The chronologies span periods between 1350 and 1630 (BDA 221b, BDA 215c, BDA 215d). We applied the specific empirical coral $\delta^{18}O$

versus temperature relationship given in equation (2) to the past coral records. Figure 3.3a displays records of reconstructed SST anomalies relative to the mean.

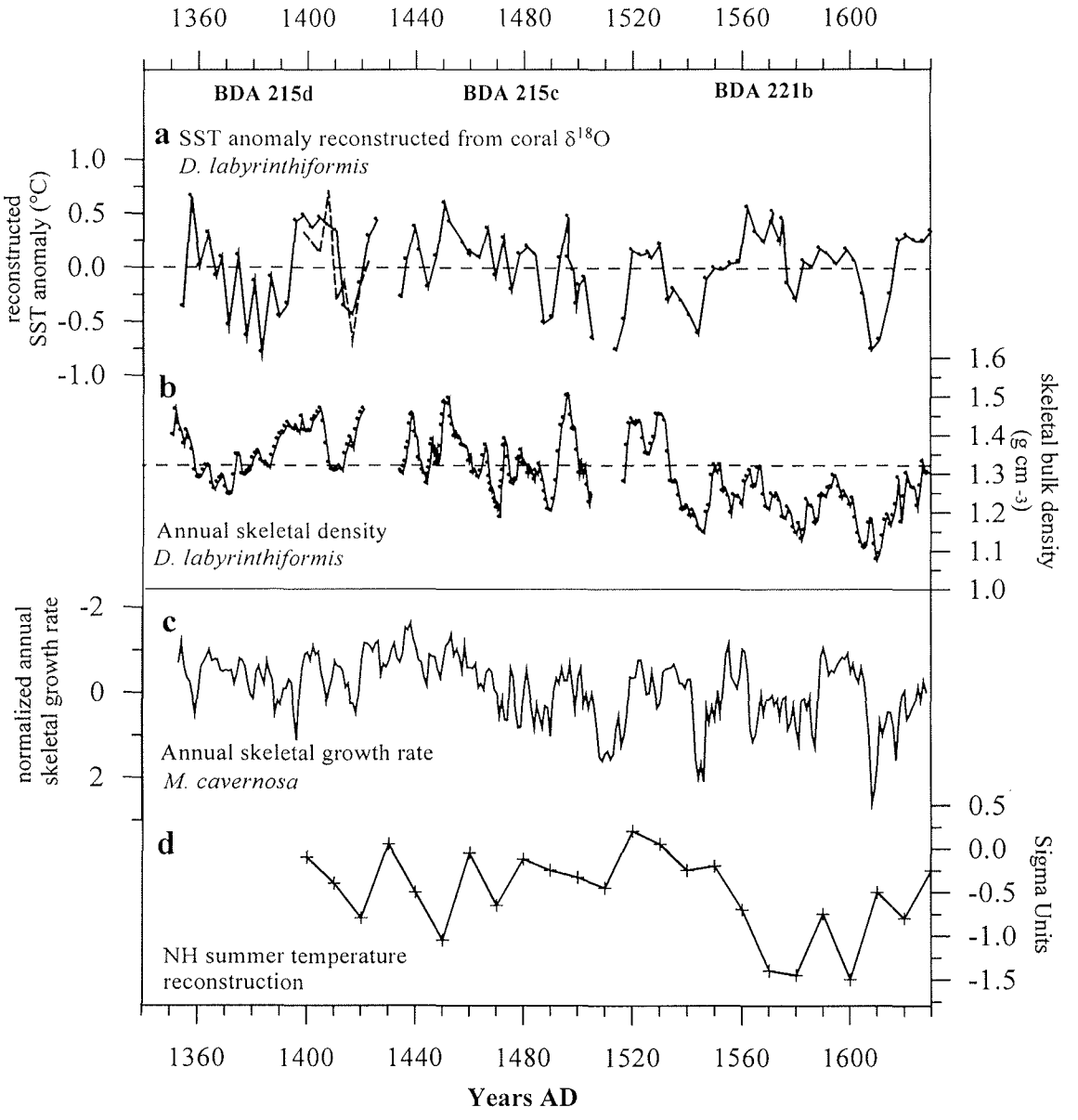

Figure 3.3 Time series of normalized reconstructed SST anomalies calculated from triennial stable oxygen isotope composition in BDA 215d, BDA 215c and BDA 221b (Figure 3.3a). A short replicate profile of BDA 215d is shown in the dashed curve. Figure 3.3b displays time series of annual skeletal bulk density in *D. labyrinthiformis*. Figure 3.3c shows a record of normalized annual growth rates (3-point Gauss-filtered) in the skeleton of a large colony of *M. cavernosa* from Bermuda (after Pätzold *et al.*, 1998). Note that the axis of growth rates is turned up side down. Figure 3.3d shows the normalized Northern Hemisphere summer temperature anomaly reconstruction after Bradley and Jones (1993).

The reproducibility of the sampling procedure was tested on a short parallel profile (dashed line with open circles) adjacent to the profile of BDA 215d. The replicate profile covers the period from 1398 to 1422 with triennial sampling resolution. The statistical agreement between the two chronologies of BDA 215d is r = +0.73 (n = 9). Such correlation illustrates that the parallel $\delta^{18}O$ profiles synchronously display an external influence, which is temperature.

The first chronology (BDA 215d) starts in 1350 indicating a decreasing temperature trend in the mid fourteenth century with a remarkable high fluctuations until the early 1380s (Figure 3.3a). Interrupted by a short period with considerably depressed temperatures around 1420, increasing temperature conditions are indicated until 1422. The second profile (BDA 215c) initiates in 1430 with an increasing SST trend that reaches a maximum in the 1450s followed by generally decreasing temperatures with a sharp depression around 1490. anomalous high temperatures are recorded around 1495 and a strong decrease is recorded until 1505. The third section (BDA 221b) again starts with a rising trend in 1514 and yields four prevailing warm sections centered in the 1520s, 1560s, 1590s and the 1620s. Those warm phases are interrupted by short cold periods around 1545, 1580 and 1610.

Calculating absolute temperatures from coral $\delta^{18}O$, individual fractionation effects of different coral individuals (BDA 215 and BDA 221) could be the source of misleading absolute temperature estimates. Therefore, we want to refrain from the representation of absolute temperatures and focus on estimates of the long-term temperature anomalies.

In Figure 3.3a, the range of coral $\delta^{18}O$ totally varies for 1.37‰ in BDA 215d, 1.32‰ in BDA 215c and 1.24‰ in BDA 221b. Application of the empirical coral $\delta^{18}O$ versus temperature equation (2) (0.95‰ per 1°C) coral $\Delta\delta^{18}O$ lead to triennial ΔSST estimates of 1.44°C in BDA 215d, 1.39°C in BDA 215c and 1.31°C in BDA 221b. In comparison, in the period between 1907 and 1991, three-year mean SST (COADS) revealed a total range of 1.38°C. Hence, the long-term temperature variability during Little Ice Age, calculated from the coral $\delta^{18}O$ records amounts to the order of 20th century temperature variations.

As a further proxy for changes in SST, skeletal density was investigated in the past coral records. Annual density values were calculated from the bulk density records (one measurement each millimeter) by averaging the three to four bulk density values that were attributed to one years growth by the linear share they represent (Figure 3.3b).

In a previous study on skeletal density of *D. labyrinthiformis* from Bermuda it could be shown that skeletal density of annual bands reveal a strong response to changes in water temperature (Draschba *et al.*, submitted). The corals secrete annual bands of enhanced density in response to higher than normal temperatures. The skeletal density records of *D. labyrinthiformis* from Bermuda were found to predominantly reflect a particular season of the year. They respond most sensitively to wintertime conditions. For comparison, during the twentieth century, climate data from Bermuda exhibit a strong correspondence between winter SST and annual mean SSTs with r = +0.76 (n=90) (calculated from COADS). Therefore, we suggest that the temperature signal recorded in skeletal density can be extrapolated to the climatic year as a whole and skeletal density is representative for annual average conditions in most years.

We compare skeletal density time series to the $\delta^{18}O$ chronologies as a further and supportive SST proxy. On a visual comparison, triennial values of $\delta^{18}O$ and annual skeletal density reveal strong similarity (Figure 3.3a, b). In the time series of BDA 215d (AD 1350 to 1421) skeletal density averages 1.36 g cm^{-3} with a total range between 1.24 g cm^{-3} and 1.36 g cm^{-3}. In BDA 215c (AD 1430 to 1506) the average density is 1.33 g cm^{-3} and values range between 1.20 g cm^{-3} and 1.50 g cm^{-3}. BDA 221b (AD 1516 to 1628) reveals an average density of 1.25 g cm^{-3} and the total range is between 1.07 g cm^{-3} and 1.45 g cm^{-3}. In general, the average density values of the time series reveal a constant declining trend between the mid 14th century and the early 17th century. The ranges of skeletal bulk density observed here are comparable to values measured in modern chronologies of *D. labyrinthiformis* (Draschba *et al.*, submitted). The statistical agreement between the three-year means of skeletal density and triennial $\delta^{18}O$ SST proxy series is r = -0.79 (n = 23) in BDA 215d, r = -0.64 (n = 29) in BDA 215c and r = -0.53 (n = 36) in BDA 221b. This strong covariance between both proxies clearly supports the credibility of the reconstructed SST pattern.

Figure 3.3c shows a time series between 1350 and 1630 of normalized annual skeletal growth rates of a colony of *Montastrea cavernosa* from Bermuda, presented by Pätzold *et al.* (1998). The colony grew in 8 m water depth at the northern fore-reef rim of the Bermuda platform. Since the colony of *M. cavernosa* reveals continuous growth for 800 years, it cloud serve as an additional stratigraphic marker for the discontinuous coral proxy records of *D. labyrinthiformis* discussed in this study. The coral time series of annual growth rate (Figure 3.3c) was interpreted in terms of a proxy for changes in water temperature and nutrient

supply (Pätzold *et al.*; 1998). While the correspondence between the coral $\delta^{18}O$ and skeletal density records and the annual growth rate record is small between 1350 and 1424 (BDA 215d), the time series fit very well during the periods between 1430 and 1505 (BDA 215c) and between 1514 and 1630 (BDA 221b). Therefore, the quality of the proxy information on temperature variability in Bermuda during parts of the Little Ice Age is mutually confirmed. In view of the fact that we considered three independent climate proxies, which additionally register the climate information on slightly different time scales, such high correlation is remarkable.

Bradley and Jones (1993) introduced a time series of reconstructed Northern Hemisphere summer temperature anomalies between AD 1400 to 1970 (Figure 3.3d). The composite proxy record was reconstructed by combining tree-ring records, documentary records and glacier melt records.

Our coral time series of reconstructed SST anomalies at share features with the summer Northern Hemisphere composite record. For instance, the decade before 1420 is cold in the Northern Hemisphere record (Figure 3.3d). Analogously, our coral records indicate uncommonly cold conditions between 1410 and 1420 (Figure 3.3a, b). The three time series of skeletal density (Figure 3.3b) imply a general decline of temperatures between 1350 and 1610. Comparably, a steady decrease of Northern Hemisphere temperatures between 1400 until the early seventeenth century is reported by Bradley and Jones (1993). Furthermore, the decade 1600 to 1609 is indicated as exceptionally cold in the Northern Hemisphere record. With a slight time shift, the coral $\delta^{18}O$ and skeletal density records reveal coinciding low temperatures during this period recording particular low temperatures during the first decade of the seventeenth century.

The short growth interruption occurring in BDA 215 (1422 to 1430) might be an expression of unfavorably cold conditions near Bermuda, too cold for reef coral growth. The same might have been the case for the hiatus occurring in BDA 221 after 1630. In the Northern Hemisphere composite record, Bradley and Jones (1993) report the period between 1570 and 1730 to represent the coldest period during the last 500 years.

Little correlation is given between the entire overlapping time series of the composite summer Northern Hemisphere and the Bermuda proxy-record. However, not necessarily we would

have to expect a consistent homogeneity between the seasonally specific composite record of the Northern Hemisphere and the Bermuda record which we believe is largely reflecting annual mean climate variations. Furthermore, the coherence of climatic variability between Bermuda and the Northern Hemisphere as a whole might be variable with time. Due to changes in the atmospheric and oceanic circulation patterns climatic anomalies are subject to considerable geographic variability (Briffa and Jones, 1993). Furthermore, temporal changes in the relation can be apparent.

In summary, our coral $\delta^{18}O$ and skeletal density proxy time series fit into the most recent picture of the nature of Little Ice Age. Formerly it was presumed that Little Ice Age was characterized by a prevailing, several hundred-year-long cold interval that was globally more or less uniform. Now, the available data begin to suggest that the climate revealed both, warm and cold anomalies, which were asynchronous between regions and also varied in importance geographically (Bradley and Jones, 1993). Evidence for such fluctuations can be useful for elucidating the processes that control climate change.

3.6 CONCLUSIONS

Triennial values of $\delta^{18}O$ in the skeletons of *D. labyrinthiformis* deliver reliable and comparative estimates of SST anomalies during periods of the nineteenth and twentieth century. They provide the calibration frame for the reconstruction of SST anomalies during periods of the Little Ice Age. Despite small growth rates in of *D. labyrinthiformis* the applied triennial sampling resolution for $\delta^{18}O$ is well valid in order to assess reliable temperature variations at Bermuda.

At the moment no conceivable elucidation can be given for a possible origin of the specific $\delta^{18}O$ versus temperature relationship found by our calibration where $\Delta 1°C$ SST accounts for almost $\Delta 1‰$ $\delta^{18}O$. Still, the temperature dependence of $\delta^{18}O$ could be shown to be identical in two different coral colonies giving evidence for the robustness of the relation were changes in SST are registered with extraordinary high sensitiveness.

The application of the empirical relationship calibrated between modern coral $\delta^{18}O$ and SST data delivers values for the long-term range of SST anomalies during Little Ice Age that are

comparable to modern conditions. The proxy information derived from $\delta^{18}O$ and skeletal density in *D. labyrinthiformis* and a time series of annual growth rates in an exemplar of *M. cavernosa* is mutually supported by the strong similarity of the time series.

During Little Ice Age the $\delta^{18}O$ and density time series shares some characteristic features with a composite time series of reconstructed summer temperatures of the Northern Hemisphere. The contribution of the coral proxy indices of climatic variation is to increase the understanding of natural climate changes in the subtropics. In turn, the coral derived data may provide further proxy information for the reconstruction of large-scale spatial connections of global atmospheric and oceanic conditions of the current millennium.

3.7 ACKNOWLEDGEMENTS

We thank T. Bickert, B. Flemming and H. Grobe for helping in sample collection. The isotopic measurements were carried out at the stable-isotopic laboratory at Bremen University. We acknowledge M. Segl and her team for performing the measurements. We thank U. Röhl for her technical support on the MSCL. This work was funded by the 'Paläoklima' BMBF-grant 03F0131A.

3.8 REFERENCES

Bermuda Environmental Scenario 1974: *US Naval Weather Service Detachment,* Asheville, New York, 199pp.

Bradley, R.S. and Jones, P.D. 1993: Little Ice Age summer temperature variations: their nature and relevance to recent global warming trends. *The Holocene* 3, 367-376.

Briffa, K.R. and Jones, P.D. 1993: Global surface air temperature variations during the twentieth century. Part 2: Implications for large-scale, high frequency paleoclimatic studies. *The Holocene* 3, 82-93.

Brown, B., Le Tissier, M., Howard, L.S., Charuchinda, M. and Jackson J.A. 1986: Asynchronous deposition of dense skeletal bands in *Porites lutea. Mar. Biol.* 93, 83-89.

Carriquiry, J.D., Risk, M.J. and Schwarcz, H.P. 1993: Stable isotope geochemistry of corals from Costa Rica as proxy indicator of the El Nino/ Southern Oscillation (ENSO). *Geochim. Cosmochim. Acta* 58, 335-351.

Chalker, B.E. and Barnes, D.J. 1990: Gamma-densitometry for measurement of skeletal density. *Coral Reefs* 9, 11-23.

Cole, J.E. and Fairbanks, R.G. 1990: The Southern Oscillation recorded in the $\delta^{18}O$ of corals from Tarawa Atoll. *Paleoceanography* 5, 669-683.

Crowley, T.J., Quinn, T.M., Taylor, F.W., Henin, C. and Joannot, P. 1997: Evidence for a volcanic cooling in a

335-year coral record from New Caledonia. *Paleoceanography* 12, 633-639.

Draschba, S., Pätzold, J. and Wefer, G. 1998: North Atlantic climate variability recorded in growth chronologies of hermatypic corals from a high latitude reef of Bermuda. Submitted to *The Holocene.*

Epstein, S., Buchsbaum, R., Lowenstam, H. and Urey, H.C. 1953: Revised carbonate-water isotopic temperature scale. *Geol. Soc. Am. Bull.* 64, 1315-1325.

Fairbanks, R.G., Charles, C.D. and Wright, J.D. 1992: Origin of global meltwater pulses. In: Taylor, R.E. (Ed.) *Radiocarbon after four decades.* Springer, Berlin Heidelberg, New York, 473-500.

Grossman, E.L. and Ku, T. 1986: Oxygen and carbon isotope fractionation in biogenic aragonite: temperature effects. *Chem. Geol.* 59, 59-74.

Jones, P.D. and Bradley, R.S. 1992: Climatic variations over the last 500 years. In: Bradley, R.S. and Jones, P.D. (Eds.) *Climate since AD 1500.* Routledge, London, pp 649-665.

Juillet-Leclerc, A., Montaggioni, L.F., Pichon, M. and Gattuso, J.P. 1997: Effects of calcification patterns on the oxygen isotope composition of the skeleton of the scleractinian coral *Acropora formosa. Oceanol. Acta* 20, 1-14.

Keigwin, L.D. 1996: The Little Ice Age and Medieval Warm Period in the Sargasso Sea. *Science* 274, 1504-1508.

Keith, M.L. and Weber, J.N. 1965: Systematic relationships between carbon and oxygen isotopes in carbonates deposited by modern corals and algae. *Science* 150, 498-501.

Klein, R., Pätzold, J., Wefer, G. and Loya, Y. 1993: Depth related timing of density band formation in *Porites* spp. corals from the Red Sea inferred from X-ray chronology and stable isotope composition. *Mar. Ecol. Prog. Ser.* 97, 99-104.

Knutson, D.W., Buddemeier, R.W. and Smith, S.V. 1972: Coral chronometers: Seasonal growth bands in reef corals. *Science* 177, 270-272.

Lamb, H.M. 1977: *Climate, Present Past and Future.* Menthuen, London, 835pp.

Leder, J.J., Swart, P.K., Szmant, A.M. and Dodge, R.E. 1996: The origin of variations in the isotopic record of scleractinian corals: 1 Oxygen. *Geochim. Cosmochim. Acta* 60, 2857-2870.

Logan, A. and Tomascik, T. 1991: Extension growth rates in two coral species from high latitude reefs of Bermuda. *Coral Reefs* 3, 155-160.

Logan, A., Yang, L. and Tomascik, T. 1994: Linear skeletal extension rates in two species of *Diploria* from high latitude reefs in Bermuda. *Coral Reefs* 13, 225-230.

Lough, J.M., Barnes, D.J. and Taylor, R.B. 1996: The potential of massive corals for the study of high-resolution climate variations in the past millennium. In: Jones, P.D., Bradley, R.S. and Jouzel, J. (Eds.) *Climatic variations and forcing mechanisms of the last 2000 years.* Springer, Berlin Heidelberg New York, pp 355-371.

Macky, W.A. 1952: Bermuda Temperatures. *Bermuda Meteorological Office*, Technical Note 4, Bermuda Press, Hamilton, 27pp.

Michaels, A.F., Knap, A.H., Dow, R.L., Gundersen, K., Johnson, J.J., Sorensen, J., Close, A., Knauer, G.A., Lohrenz, S.E., Asper, V.A., Tuel, M. and Bidigare, R. 1994: Seasonal patterns of ocean biogeochemistry at the JGOFS Bermuda Atlantic Time-Series Study Site. *Deep-Sea Res.* 41, 7, 1013-1038.

Nozaki, Y., Rye, D.M., Turekian, K.K. and Dodge, J.E. 1978: A 200-year record of carbon-13 and carbon-14 variations in a Bermuda coral. *Geophys. Res. Lett.* 5, 825-828.

Pätzold, J. 1984: Growth rhythms recorded in the stable isotopes and density bands in the reef coral *Porites lobata* (Cebu, Philippines). *Coral Reefs* 3, 87-90.

Pätzold, J. 1992: variation of the stable oxygen and carbon isotopic fractionation within skeletal elements of reef building corals from Bermuda. *Proc 7th Int. Coral Reef Symp.*, Guam, 1, 13595-13601.

Pätzold, J., Bickert, T., Flemming, B., Grobe, H. and Wefer, G. 1998: Holozänes Klima des Nordatlantiks rekonstruiert aus massiven Korallen von Bermuda. *Natur und Museum*, in press.

Porter, S.C. 1986: Pattern and forcing of Northern Hemisphere glacier variations during the last millennium. *Quatern. Res.* 26, 27-48.

Siegel, D.A., Itturiaga, R., Bidigare, R.R., Smith, R.C., Pak, H., Dickey, T.D., Marra, J. and Baker, K.S. 1990: Meridional variations in the spring time phytoplankton community in the Sargasso Sea. *J. Mar. Res.* 48, 379-412.

Taylor, R.B., Barnes, D.J. and Lough, J.M. 1993: Simple models of density band formation in massive corals. *J. Exp. Mar. Biol. Ecol.* 167, 109-125.

Tudhope, A.W., Shimmield, G.B., Chilcott, C.P., Jebb, M., Fallick, A.E. and Dalgleish, A.N. 1995: Recent changes in climate in the far western equatorial Pacific and their relationship to the Southern Oscillation; oxygen isotope records from massive corals, Papua New Guinea. *Earth Planet. Sci. Lett.* 136, 575-590.

Wellington, G.M. and Glynn, P.W. 1983: Environmental influences on skeletal banding in Eastern Pacific (Panama) corals. *Coral Reefs* 1, 215-222.

Wellington, G.M., Dunbar, R.B. and Merlen, G. 1996: Calibration of stable oxygen isotope signatures in Galapagos corals. *Paleoceanography* 11, 467-480.

Woodruff, S.D., Slutz, R.J., Jenne, R.L. and Steurer, P.M. 1987: A Comprehensive Ocean-Atmosphere Data Set. *Bull. Am. Meteorol. Soc.* 68, 1239-1250.

Woodshole Oceanographic Institute and Bermuda Biological Station for Research 1988: Station S off Bermuda: Physical measurements, 1954-1991. *Library of Congress Catalogue*, pp 1-51552.

4 WINTER MIXING PROCESSES RECORDED BY $\delta^{13}C$ IN BERMUDA CORALS

S. DRASCHBA, J. PÄTZOLD, G. WEFER

Fachbereich Geowissenschaften

Universität Bremen

Postfach 330 440

D-28334 Bremen

Germany

Submitted to 'Palaeogeography, Palaeoclimatology, Palaeoecology'

4.1 ABSTRACT

High resolution stable isotope ($\delta^{13}C$ and $\delta^{18}O$) records of two recent specimens of *Montastrea cavernosa* and one recent specimen of *Diploria labyrinthiformis*, collected from Bermuda fore-reef locations, are presented. We further introduce multi-century stable isotope chronologies of *D. labyrinthiformis* between AD 1350 and 1630.

In the modern records, two coral species reveal no species-specific differences in $\delta^{13}C$. A strong connection between the coral $\delta^{13}C$ signal and the convective activity of the surrounding seawater near Bermuda is indicated by high correlations between seasonal and interannual records of skeletal $\delta^{13}C$ and the maximum mixed layer depth in winter. We attribute the fact that coral $\delta^{13}C$ is coincident with convective activity to a response to nutrient availability in the upper water column.

Two aspects lead to the conclusion that the seasonal skeletal $\delta^{13}C$ variability does not display the solar irradiance cycle. First, comparison between seasonal coral $\delta^{13}C$ and $\delta^{18}O$ defines the occurrence of lowest $\delta^{13}C$ during fall and highest $\delta^{13}C$ during spring, leading light extremes by a quarter year. Second, seasonal carbon isotope variation in two corals from deep water (40m) is twice as high as in a coral from intermediate water depth (19m). The robust connection between coral $\delta^{13}C$ and winter mixing depth suggests that the corals from Bermuda can serve as a high resolution marine proxy for the history of hydrographic convective activity in the North Atlantic subtropical gyre.

On inter-annual time scales the skeletons of both modern and past coral records reveal simultaneous depletions in ^{13}C and ^{18}O. Such connection between coral $\delta^{13}C$ and $\delta^{18}O$ is given by the coupling between minimum winter temperatures, i.e. coral $\delta^{18}O$, and the excess of vertical convection in winter, monitored in $\delta^{13}C$. The time series of past coral $\delta^{13}C$, that cover periods during Little Ice Age, can deliver implements for the reconstruction of inter-annual variability in the regional and North Atlantic-scale hydrographic circulation pattern.

4.2 INTRODUCTION

The geochemical composition of reef coral skeletons can provide very high resolution proxy information for the reconstruction of past oceanic conditions. Especially the stable carbon and oxygen isotope composition ($\delta^{13}C$ and $\delta^{18}O$) of their skeletons have been proven to be sensitive monitors of the marine environment. $\delta^{18}O$ serves as a measure of sea surface temperature (Fairbanks and Dodge, 1979; Pätzold, 1984; Crowley *et al.*, 1997) and sea surface salinity (Cole and Fairbanks, 1990; Linsley *et al.*, 1994; Tudhope *et al.*, 1995).

The interpretation of coral $\delta^{13}C$ is more complicated. The commonly held opinion is that skeletal $\delta^{13}C$ is largely mediated by fractionation processes during photosynthesis of the endosymbiotic zooxanthellae, the trophic state of the coral animal and the $\delta^{13}C$ of the surrounding seawater (Goreau, 1977; Swart, 1983; Swart *et al.*, 1996). Especially variations in climatic and oceanic conditions which may define some form of physiological limit for the corals will be registered in the stable isotopic composition of their skeletons.

In the western subtropical Atlantic, the seasonal cycle of the convective activity of the oceans surface layer is one of the most striking characteristics of the hydrographic circulation pattern (Dickson *et al.*, 1996). The excess of convective mixing that occurs in the late winter largely controls the seasonal cycle of temperature and nutrient distribution near Bermuda (Spitzer and Jenkins, 1989; Michaels *et al.*, 1994). Nutrients supplied from deeper water drive net production in the euphotic zone and in turn promote zooplankton blooms (Menzel and Ryther, 1960, 1961; Siegel *et al.*, 1990). The later form a heterotrophic food source of coral polyps. The depth of the mixed surface layer and hence the intensity of water overturn that usually reaches a maximum in February, can considerably vary from year to year.

This inter-annual variability is argued to be closely connected to forcing by the North Atlantic Oscillation (NAO) (Michaels *et al.*, 1994), the mutual weakening and strengthening of the Subtropical High and the Iceland Low (Bjerknes, 1964; Kushnir, 1994; Hurrell, 1995, 1996; Dickson *et al.*, 1996). Low index states of the NAO promote an increase in convective activity at Bermuda due to a southward retraction of the zone of maximum wind stress in the North Atlantic (Dickson and Namias, 1976; Rogers, 1990). The NAO has recently gained much attention because of its role as the dominant atmospheric influence on the climate of the

Atlantic sector and surrounding continents on inter-annual to decadal time scales. Although the hydrographic pattern in the low latitudes of Bermuda only reveals an integral part of the NAO, the reconstruction of oceanic conditions near Bermuda by coral proxy information can deliver implements for the understanding of the large scale atmospheric circulation modes.

This study examines the stable carbon isotope composition of reef coral skeletons to reflect changes in the hydrographic pattern near Bermuda which modulates overall biomass production of the region. We present $\delta^{13}C$ data from one modern specimen of *Diploria labyrinthiformis* and two modern specimens of *Montastrea cavernosa* from intermediate and deep habitats of Bermuda fore-reefs. We further introduce multi-century records of coral $\delta^{13}C$ data between AD 1350 and 1630, covering periods during early Little Ice Age. These records, measured on two large colonies of *D. labyrinthiformis* can contribute to describe the temporal nature of hydrographic variability in the subtropical North Atlantic surface ocean far prior to the development of instrumental climate information. Even though the stable isotope records of the Bermuda corals display local conditions, it was suggested that the hydrographic conditions are likely to be representative for vast areas of the subtropical gyre due to relatively rapid horizontal circulation (Jenkins, 1982).

4.3 ENVIRONMENTAL SETTING

Bermuda is located in the northwestern Sargasso Sea (32°20´N, 64°50´W), the large mid-Atlantic, oligotrophic gyre bounded on the west by the Gulf Stream. The climatological year in Bermuda is divided into two distinct seasons and generally is moderated by the ocean. Northern Hemisphere summer lasts from May to October and winter lasts from November to April. Seasonal maxima in irradiance and air temperature are reached in June and July, respectively, and precede seasonal maximum water temperature that generally occurs in August. Winter minimum water temperatures occur in February. Average monthly sea surface temperature ranges between 18°C and 28°C (Bermuda Environmental Scenario, 1974).

In general, the water clarity is very high in the Sargasso Sea. The amount of light that penetrates the water column to the depth in which the corals grew is dependent on the seasonal cycle in netto irradiance, modified by cloud cover, and the transparency in the water column. Though irradiance is highest in June, the 1% compensation level for light, offshore Bermuda, reaches a second maximum in October due to high water transparency by low concentration of dispersed material. In comparison, the transparency of the upper water column is lowered during spring relative to fall by phytoplankton blooms (Bodungen *et al.*, 1982).

The water column is well mixed by wind action from January to March bringing a large supply of nutrients to the surface. The depth of the mixed layer shows a winter maximum each February but the depth can considerably vary from year to year between 50 and 400m. Winter mixing is followed by a rapid stabilization to a shallow summer mixed layer. The summer surface water is characterized by strong thermal stratification and oligotrophic conditions. In transition to winter, surface water cooling erodes the seasonal thermocline allowing wind-induced mixing in December and January, leading to a new increase in surface nutrient concentrations (Morris *et al.*, 1977; Spitzer and Jenkins, 1989; Michaels *et al.*, 1994). As a consequence of the nutritional cycle, driven by vertical mixing and consumption in the upper water column, oceanic plankton populations generally show low abundance and species diversity during summer and early fall, whereas winter and early spring populations are more diverse and abundant (Menzel and Rhyther, 1960; 1961).

4.4 MATERIALS AND METHODS

The investigated coral colonies were sampled at the northern fore-reef slope of the Bermuda platform, an area with open water conditions and negligible island effect. Specimens included the hermatypic reef coral species *Montastrea cavernosa* and *Diploria labyrinthiformis*. The colonies were collected from a depth range of 19 to 38 m. Figure 4.1 gives an overview over the sampling locations.

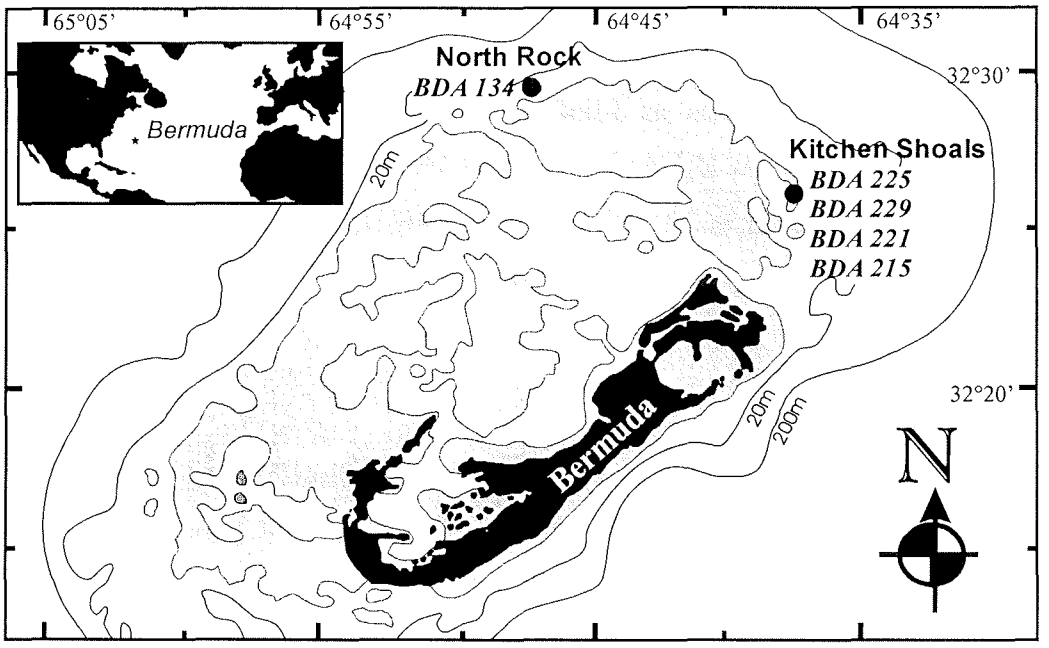

Figure 4.1 Location map of the Bermuda Islands and sampling sites of the coral colonies at North Rock (BDA 134) and Kitchen Shoals (BDA 225, BDA 229, BDA 215, BDA 221). Shaded areas mark water depths ≤ 5m.

The coral heads were sectioned along the axis of maximum growth, slabbed to a thickness of 5 mm and X-radiographs of the coral slabs were taken. The X-radiographs exhibited well defined seasonal banding pattern of the coral skeletons. The annual skeletal density couplets were assigned ages from the known collection date at the colony surfaces.

Profiles of stable oxygen and carbon isotopes of the coral skeletons were taken with seasonal and triennial sampling resolution. For isotopic analysis with seasonal resolution (BDA 134, BDA 225, BDA 229), small sticks were cut from the skeleton slices. The sticks with approximately 2 mm cross-section and several cm in length started at the colony surface and followed the dominant growth axis. Pätzold (1992) detected a pronounced variability in the isotopic composition between different skeletal elements in colonies of *Diploria* and *Montastrea*, respectively. Hence, sampling was restricted to the exothecae of the skeletons. In order to avoid breaking of the filigree sampling sticks they were soaked in Epoxy resin, which does not influence stable isotope measurements. Using an universal machine tool, aragonite samples were grinded from the cross-section of the sticks in steps of 150 μm.

Usually, the annual growth rate was 2.5 to 3 mm. Hence average sampling resolution is 17 to 20 per year. The age model of high resolution isotope profiles is based on fixing of seasonal $\delta^{18}O$ extremes on instrumental temperature extremes with known date and by assigning ages to intermediate values by linear interpolation according to their spatial distances along the sampling profile.

Stable isotope profiles with triennial sampling resolution (BDA 215, BDA 221) were obtained by cutting sticks of exothecal skeleton material, following the growth direction. Using a 100 µm blade the sticks were cut into triennial segments at the center of every third low density increment. The bulk-subsamples were ground and homogenized.

The coral colonies BDA 215 and BDA 221 revealed discontinuous growth from the bases to the tops of the colonies. The bases of the colonies were ^{14}C dated by AMS in the Leibnitz Laboratory in Kiel. Precision of dating came to ±30 years.

The stratigraphy of the present chronologies was confirmed by a strong correspondence to a continuous 800-year skeletal growth rate chronology of a colony of *Montastrea cavernosa* from Bermuda, presented by Pätzold *et al.* (1998). Their record was interpreted in terms changes in sea surface temperature and an enhancement of wind-driven vertical mixing and nutrient supply in the surface waters.

Stable isotope records with triennial sampling resolution were assigned ages by allocation of each measurement by the central year of the three-year window. Table 4.1 summarizes the time series of stable oxygen and carbon isotope composition, presented in this study.

Table 4.1 List of coral colonies from Bermuda study sites and the investigated periods of time.

Record	Species	Sampling location	Depth [m]	$\delta^{13}C$ chronology [years AD]	sampling resolution
BDA 134	*M. cavernosa*	North Rock	19	1969 - 1982	seasonal
BDA 225	*M. cavernosa*	Kitchen Shoals	38	1884 - 1993	"
BDA 229	*D. labyrinthiformis*	Kitchen Shoals	38	1980 - 1992	"
BDA 215	*D. labyrinthiformis*	Kitchen Shoals	25	1350 - 1505	triennial
BDA 221	*D. labyrinthiformis*	Kitchen Shoals	27	1514 - 1630	"

The powdered aragonite samples were processed by an automated carbonate preparation device (Kiel device) attached to a Finnigan MAT 251 mass spectrometer. Errors of replicate measurements of an internal laboratory standard (Solnhofen limestone), calibrated against the NBS-19 standard, were for ±0.03‰ $\delta^{13}C$ and ±0.06‰ for $\delta^{18}O$. The stable isotope data are reported relative to PDB.

Environmental data for comparison with our stable isotope results were measured bimonthly at the Hydrostation S, situated 25 km southeast of Bermuda. Bacastow *et al.* (1996) provided measurements of surface ocean water $\delta^{13}C$ between 1984 and 1993. Michaels *et al.* (1994) calculated a time series of mixed layer depth at Hydrostation S between 1957 and 1991.

4.5 RESULTS

4.5.1 Seasonal variation of coral $\delta^{13}C$

The high resolution stable oxygen and carbon isotope records of two specimens of *M. cavernosa* and one specimen of *D. labyrinthiformis* cover the period between 1969 and 1993 (Figure 4.2). The $\delta^{13}C$ records of the two different coral species reveal no specific differences.

The skeletal isotopic compositions reveal clear seasonal cycles. This confirms the annual character of density band couplets. Changes in the oxygen isotopic composition of the seawater can be deduced from changes in sea surface salinity. Salinity reveals negligible variability on seasonal and inter-annual time scales near Bermuda. Hence, variations in coral $\delta^{18}O$ can be attributed to be primarily driven by changes in sea surface temperature.

The temporal relationship between skeletal $\delta^{18}O$ and $\delta^{13}C$ sinusoidal curves strongly follow a pattern of a time shift. In all coral colonies $\delta^{18}O$ minima, which reflect seasonal maximum temperatures in August, precede $\delta^{13}C$ minima by several samples. In general, linear regression yields weak but statistically significant positive correlation between seasonal $\delta^{18}O$ and $\delta^{13}C$, reflecting the phase shift between the two records. Lagged correlation analysis performed on $\delta^{18}O$ versus $\delta^{13}C$ time series could closer define the phase shift between the stable isotopes. This time shift accounts for eight to ten weeks in all corals. This indicates that $\delta^{13}C$

composition reaches most negative values in the last quarter of the year, i.e. October to November, as also indicated by visual comparison of both isotope time series. Correspondingly, highest $\delta^{13}C$ values occur during spring, i.e. April to May.

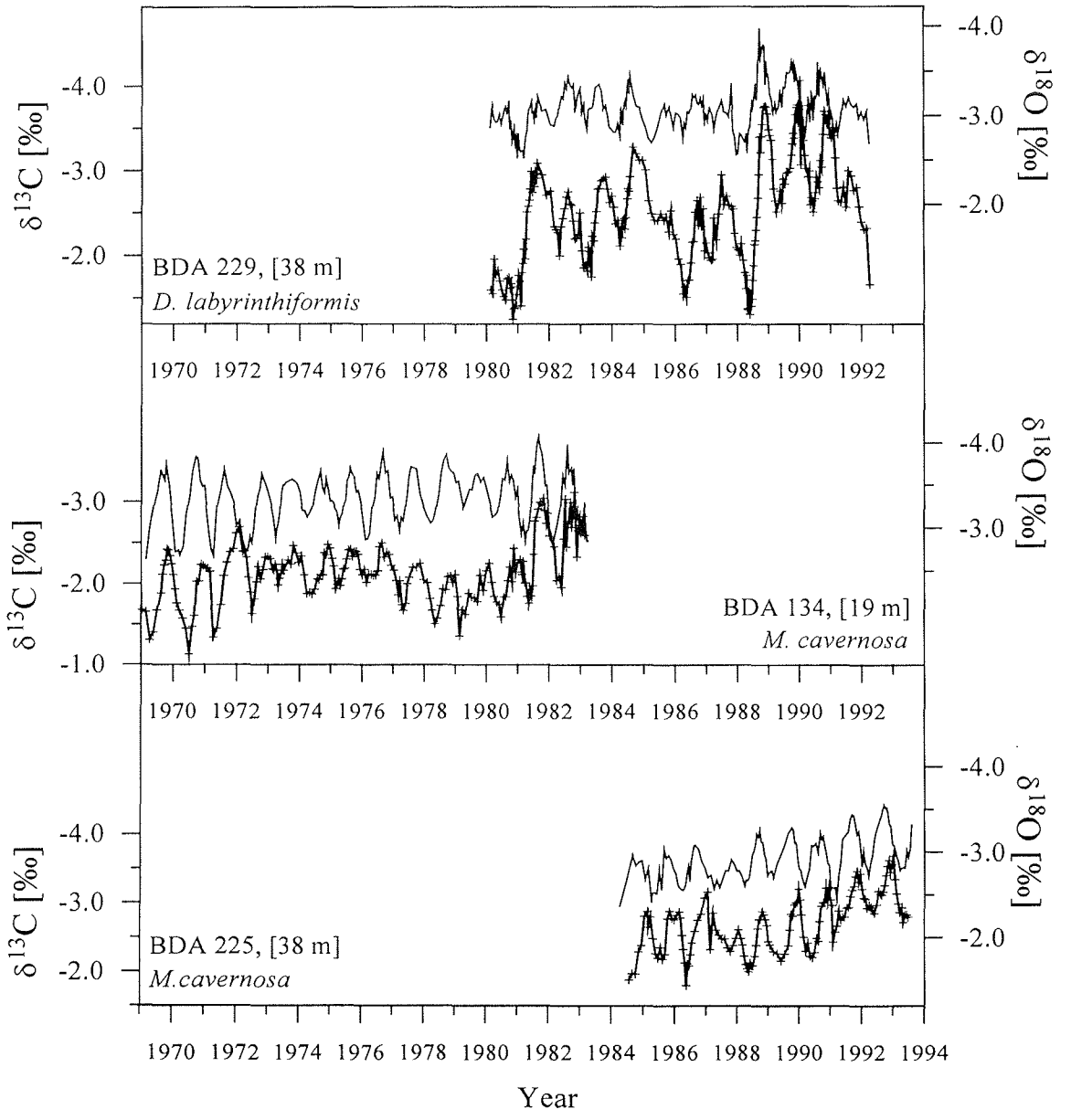

Figure 4.2 High resolution time series of coral $\delta^{13}C$ and $\delta^{18}O$ from the skeletons of *Diploria labyrinthiformis* (BDA 229) and *Montastrea cavernosa* (BDA 134 and BDA 225). The records are plotted with the positive isotope axis downward. Sampling points are indicated by crosses on $\delta^{13}C$ profiles.

The average seasonal range of skeletal carbon isotope values is 1.4‰ in BDA 229, 1.4‰ in BDA 225 and 0.7‰ in BDA 134 (Figure 4.2). In comparison, the seasonal $\delta^{13}C$ signal measured in the sea surface water at Hydrostation S near Bermuda reveals an average amplitude of 0.2‰ to 0.3‰ (Bacastow *et al.*, 1996).

Astonishingly, the seasonal signature of stable carbon composition of the seawater near Bermuda is inversely related to the isotopic cycles observed in the corals. Lowest $\delta^{13}C_{seawater}$ values occur in winter and early spring in response to vertical mixing with deeper and colder water. This sub-surface water is depleted in ^{13}C due to remineralization of organic matter within the lower seasonal thermocline. Without the counteracting effect of the $\delta^{13}C$ composition of the seawater, the average seasonal amplitude of coral $\delta^{13}C$ would be even greater. At the same time the seasonal pattern of $\delta^{13}C_{seawater}$ is predicted to have only a small effect on seasonal coral $\delta^{13}C$ variations.

4.5.2 Inter-annual variability of coral $\delta^{13}C$

In Figure 4.3 annual mean coral $\delta^{13}C$ values compared to data of the maximum winter depth of the mixed layer at Bermuda (after Michaels *et al.*, 1994) are shown. Mean skeletal $\delta^{13}C$ values are -2.49‰ in BDA 229, -2.15‰ in BDA 134, and -2.69‰ in BDA 225. Hence, both deeper living corals from 38m water depth are slightly more depleted in ^{13}C than the coral from intermediate water depth of 19m.

Superimposed on the coral $\delta^{13}C$ records is the linear trend. All skeletal $\delta^{13}C$ records register a decreasing trend that accounts for a relative depletion in $\delta^{13}C$ for 0.083‰ per year in BDA 229, 0.019‰ per year in BDA 134 and 0.088‰ per year in BDA 225. Bacastow *et al.* (1996) calculated the ^{13}C Suess effect of the ocean at the Bermuda offshore location Hydrostation S between 1984 and 1993 to be -0.022‰ $\delta^{13}C$ (± 0.002‰) per year. The trend reflects the isotopic dilution of the ocean reservoir with anthropogenically combusted fossil fuels, which are isotopically lighter. The decreasing $\delta^{13}C$ tendencies in the corals from the deep environments (BDA 225 and BDA 229), however, are about four times higher than the ^{13}C Suess effect.

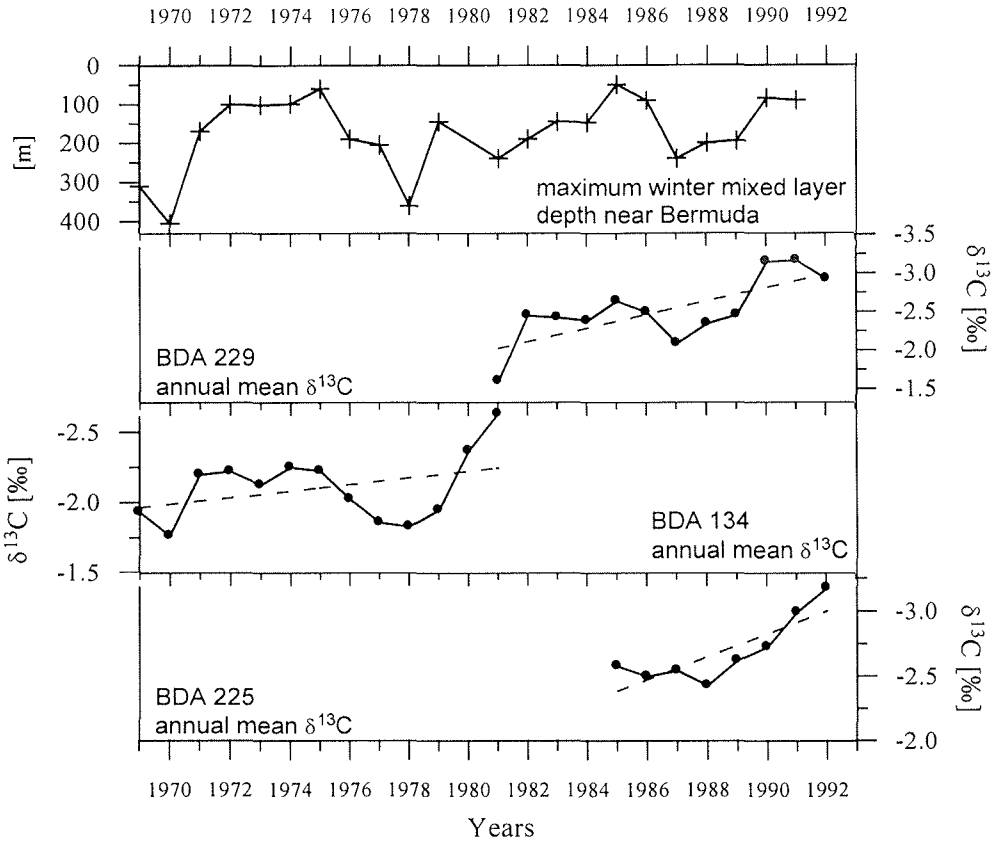

Figure 4.3 Time series of annual mean coral $\delta^{13}C$ calculated from high resolution $\delta^{13}C$ records shown in Figure 4.2. The linear trend is superimposed on each record (dashed line). The data are compared to the maximum winter mixed layer depth near Bermuda (redrawn after Michaels *et al.*, 1994).

A statistically significant and positive relation ($p \leq 0.05$) between annual mean $\delta^{13}C$ and $\delta^{18}O$ is monitored by all corals (not shown here). The relation is strongest in BDA 225 with $r = 0.64$ ($n = 9$) and weaker but still statistically significant in BDA 229 with $r = 0.35$ ($n = 12$) and BDA 134 with $r = 0.31$ ($n = 13$).

Most interestingly, Figure 4.3 reveals a strong convariation of annual mean coral $\delta^{13}C$ with the maximum mixed layer depth in winter (after Michaels *et al.*, 1994). The correlation coefficients are shown in Table 4.2a. The low $\delta^{13}C$ values registered in BDA 134 are coincident with a prolonged phase of shallow winter thermocline during the mid-1970s. This phase is enveloped by years of deep mixing in 1970 and 1978 in which the coral recorded

higher skeletal $\delta^{13}C$. BDA 229 records an decreasing $\delta^{13}C$ trend between 1981 and 1985, which is coincident with a decrease in winter mixed layer depth at Bermuda. The $\delta^{13}C$ records of BDA 229 and BDA 225 strongly resemble, displaying positive $\delta^{13}C$ values in 1987 and 1988 and a constant decrease hereafter. Most crucial is the fact that years in which deep convective mixing occurs (which indicates dilution of surface waters with isotopically depleted deeper water) high annual mean $\delta^{13}C$ is registered by the corals. In fact, Bacastow *et al.* (1996) measured low $\delta^{13}C_{seawater}$ values in 1988, coincident with deep mixing, and high $\delta^{13}C_{seawater}$ values in 1990, coincident with shallow mixing, at Hydrostation S. Like on seasonal time-scales, the inter-annual carbon isotopic signature of the ambient seawater is opposite to the inter-annual record of coral $\delta^{13}C$. However, average inter-annual variation in $\delta^{13}C_{seawater}$ on average only accounts for approximately 0.06‰. We refrained from correcting our coral $\delta^{13}C$ data for the $\delta^{13}C$ effect of seawater since the variability of carbon isotopic composition in the ambient water is small relative to variations in coral $\delta^{13}C$.

Table 4.2 Correlation coefficients between maximum mixed layer depth in winter (MLD) versus (a) annual mean coral $\delta^{13}C$, and (b) versus coral $\delta^{13}C$ data that are assigned with dates from February until May. Bold marked coefficients are statistically valid ($p \leq 0.05$).

	a Correlation between MLD / annual mean $\delta^{13}C$	**b Correlation between MLD / winter mean $\delta^{13}C$**	**n**
BDA 229	**0.77**	**0.53**	11
BDA 134	**0.73**	0.47	12
BDA 225	0.42	0.17	7

As the mixed layer reaches a maximum in winter and the corals carry a responding signal of convective activity, it could be expected that correlation between coral $\delta^{13}C$ and the maximum mixed layer depth is strongest during the winter months and the following period. The period from February until May is the time that is mostly influenced by mixing. In contrast to this assumption, correlation between winter mixed layer depth and the stable carbon isotope values that are assigned with dates from February until May, reveals a lower coefficient than

correlation with annual mean coral $\delta^{13}C$ given above (Table 4.2b). This indicates that the corals carry a signal that integrates the hydrographic conditions of the year as a whole and is not biased towards a particular season.

4.5.3 Coral $\delta^{13}C$ between AD 1350 and 1630

In Figure 4.4 the triennial stable carbon and oxygen isotope composition of coral records that cover periods during early Little Ice Age (BDA 215a, b and BDA 221) is illustrated. The coral records reveal strong variability in both stable carbon and oxygen isotopic composition. Total variation of coral $\delta^{13}C$ ranges between +1.6‰ to -1.70‰ in BDA 215a, +1.96‰ to -1.67‰ in BDA 215b, and +1.18‰ to -1.50‰ in BDA 221, respectively. The mean values of the past coral $\delta^{13}C$ records are considerably higher compared to the three recent $\delta^{13}C$ records from comparable off-shore reef environments. BDA 215a reveals a $\delta^{13}C$ mean of -0.36‰, BDA 215b of -0.85‰ and BDA 221 of -0.52‰.

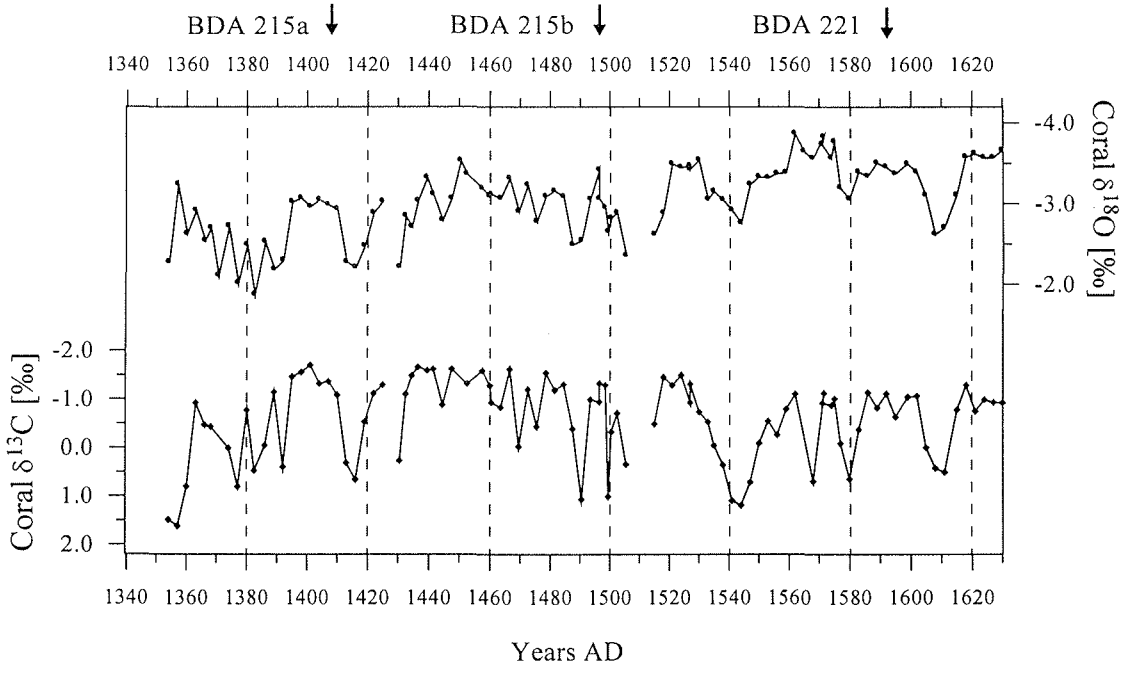

Figure 4.4 Time series between 1350 and 1630 of triennial coral $\delta^{13}C$ and $\delta^{18}O$ values from the skeletons of two colonies of *Diploria labyrinthiformis* (BDA 215a, b and BDA 221). The record of BDA 215 reveals a short interruption between 1416 and 1425. Note that the records are plotted with the positive isotope axis downward.

The first chronology (BDA 215a, AD 1350 to 1424) starts with very high $\delta^{13}C$ values and registers a generally decreasing trend until 1400. High $\delta^{13}C$ occur again during the second decade of the fifteenth century. BDA 215b (AD 1430 to 1505) shows a generally increasing $\delta^{13}C$ trend, with strong variability during the last two decades. BDA 221 (AD 1514 to 1630) is characterized by prolonged periods of low coral $\delta^{13}C$ around 1520, 1555, 1590 and 1620. These phases last for at least two decades and are interrupted by shorter periods of relatively high coral $\delta^{13}C$ around 1540, 1567, 1580 and 1610.

The most striking feature is the strong similarity between coral $\delta^{13}C$ and $\delta^{18}O$. Linear correlation between both isotopes is $r = 0.74$ ($n = 24$) in BDA 215a, $r = 0.69$ ($n = 30$) in BDA 215b and $r = 0.71$ ($n = 43$) in BDA 221.

Moreover, visual comparison suggests that the strongest correlation between the isotope records is given in the high range of coral $\delta^{13}C$ and $\delta^{18}O$ values, where $\delta^{18}O$ indicates low temperatures. This is supported in correlation graphs where the upper range of $\delta^{13}C$ versus $\delta^{18}O$ reveals smaller scatter of values compared to the low range of $\delta^{13}C$ versus $\delta^{18}O$. This leads to the suggestion that coral $\delta^{13}C$ displays an environmental signal that is coupled to sea surface water temperature and that the response to this signal is most sensitive during events that supply cold water to the surface.

4.6 DISCUSSION

Being largely unaffected by island effects, the Bermuda fore-reef corals presented in this study uniquely deliver the opportunity to study environmental conditions that are representative for typical open ocean conditions in the subtropical North Atlantic.

Such coralline records that are not influenced by local coastal processes are necessary to reveal changes in the near-surface hydrographic, and in turn ecological, conditions. The striking correspondence between interannual changes in coral $\delta^{13}C$ and the convective activity demonstrates the monitoring potential of the Bermuda corals.

4.6.1 Effects on stable carbon isotope fractionation

Despite researchers have sought to find a generally applicable interpretation of stable carbon isotopic composition of hermatypic reef coral skeletons, it is still the subject of much controversy (e.g. Swart, 1983; Wefer and Berger, 1991; Carriquiry, 1993; Swart *et al.*, 1996). Informative reviews of vital fractionation processes are given by Swart *et al.* (1983), McConnaughey (1989), Aharon (1991) and McConnaughey *et al.* (1996).

In order to seek for an explanation for the seasonal and inter-annual coral $\delta^{13}C$ observed in our results we first want to focus on the role of light. Two alternative models that concentrate on light and in turn of photosynthetic activity are available for the interpretation of the $\delta^{13}C$ of hermatypic coral skeletons. The commonly favored hypothesis summarized by Goreau (1977) is based on the experimental observation that skeletal $\delta^{13}C$ increases with the depth of the coral habitat (Land *et al.*, 1975; Weber *et al.*, 1976; Fairbanks and Dodge, 1979; Bosscher, 1992). These studies showed that deeper living corals are consistently enriched in ^{12}C in comparison to shallow living individuals. This was attributed to a decrease in algal photosynthetic activity in deeper water and hence a decrease of preferential uptake of ^{12}C during photosynthesis. Consequently, the internal carbon pool from which the corals calcify becomes less depleted in ^{12}C resulting in lower $\delta^{13}C$ values of coral skeletons (Weber and Woodhead, 1972; Goreau, 1977).

On the other hand, Erez (1978) suggested that increasing rates of photosynthesis relative to respiration provide an increasing portion of metabolic CO_2 and hence ^{12}C into the internal carbon pool which is incorporated into the coral skeleton.

On seasonal time-scales the coral $\delta^{13}C$ signal observed in our study can not be attributed to the seasonal cycle in light availability at Bermuda. There is an approximately two to three months lag between the seasonal coral $\delta^{13}C$ and the light cycle at Bermuda. Furthermore, the seasonal $\delta^{13}C$ range observed in both deep living individuals (BDA 229 and BDA 225) is twice as high relative to the coral from intermediate water depth (BDA 134). This finding contradicts the "carbon insolation model" introduced by Fairbanks and Dodge (1979). They predicted that seasonal $\delta^{13}C$ variability decreases with depth due to an attenuation of the seasonal variability in light intensity.

Applying the ^{12}C fractionation model of Goreau (1977), the rationale for the seasonal distribution of coral $\delta^{13}C$ would be high photosynthesis during spring resulting in coral ^{12}C depletion. In turn, we would have to deduce a decreasing influence of photosynthesis during fall producing a decrease in the P/R rate. However, the seasonal availability of light does not coincide with this pattern. Bodungen *et al.* (1982) reported a reduction in light intensity during spring relative to fall due to a reduction in water transparency by phytoplankton blooms. Analogously, on inter-annual time scales the hypothesis of Goreau (1977) will lead to the interpretation that during years with effective winter mixing the corals $\delta^{13}C$ signal is increased by photosynthesis. This rationale is in contrast to our results since it is least conceivable that photosynthesis dominates during years when deep winter mixing has driven phytoplankton blooms to reduce water transparency.

Concentrating on light as the possible triggering factor for coral $\delta^{13}C$ our data appear to favor the model of Erez (1978). However, we favor the idea that illumination can not solely explain our coral $\delta^{13}C$ data. Further fractionation processes must be responsible for the specific seasonal and inter-annual $\delta^{13}C$ pattern observed in our corals.

Swart (1983) discussed the trophic capacity of the coral animal to modify the metabolism and in turn isotopic fractionation effects. The seasonal timing of high and low coral $\delta^{13}C$ extremes during spring and fall, respectively, temporally coincide with the occurrence and lack of nutrients in the upper water column. High nutrient levels in the ambient upper water column during spring are provided by the convective mixing and low nutrient levels occur during fall due to the preceded consumption by phytoplankton. Analogously, on inter-annual time scales, we find high coral $\delta^{13}C$ values in response to deep convective mixing and enhanced dissolved organic matter and zooplankton levels (Menzel and Ryther, 1960, 1961; Siegel *et al.*, 1990). Because of the striking correspondence between coral $\delta^{13}C$ and external carbon source availability we suggest that the coral $\delta^{13}C$ signal displays some form of variability that is coupled to the uptake of external carbon sources and the trophic state of the animal.

Fairbanks and Dodge (1979) investigated the stable carbon composition of an individual of *Montastrea annularis* from 3m water depth from the Bermuda platform. They interpreted the seasonal $\delta^{13}C$ signal to be regulated by the seasonal cycle in light intensity. As discussed

above, such connection is opposite to our findings. Possibly the clue is the difference in growth depth between the corals studied here and by Fairbanks and Dodge (1979). The corals observed here flourished in intermediate (19m) and deeper (38m) water depths. Supported by the results of Kinsey (1985) and Porter (1985) it is most conceivable that our deeper living corals reveal a considerable reliance on heterotrophy and are not self-sufficiently autotrophic as it might have been the case for the individual observed by Fairbanks and Dodge (1979). Hence, the internal calcification pool of deeper corals is expected to partly reflect varying rates of autotrophy versus heterotrophic uptake of diet.

A certain crucial point, however, is the fact that a coral $\delta^{13}C$ signal that is strongly generated by the heterotrophic capacity is expected to display a decrease in coral $\delta^{13}C$ in response to increased heterotrophy. This is given by the fact that a diet consisting of dissolved organic matter and zooplanktonic prey (-17% to -22‰ $\delta^{13}C$; Goreau, 1977; Muscatine *et al.*, 1989) is isotopically much lighter than the photosynthate of intracellular zooxanthellae (-13.5‰ $\delta^{13}C$; Goreau, 1977). With respect to this prerequisite, the availability of dissolved organic matter and zooplanktonic prey at Bermuda is vice versa to the seasonal and inter-annual variability seen in our coral $\delta^{13}C$ signals.

It is important to recall at this point that the pathways of stable isotope fractionation in hermatypic corals are manifold and contain a larger complexity as discussed so far. Besides the factors of illumination or the nutritional status of the animal, resource partitioning between the algal and animal components of the symbiotic system will additionally alter the internal carbon pool (Muscatine *et al.*, 1989). In order to satisfy the photosynthetic demand for bicarbonate from the internal carbon pool, a considerable amount of CO_2 has to be replaced from external seawater bicarbonate (Goreau, 1977). Muscatine *et al.* (1989) suggested that during the diffusive pathway into the coral tissue seawater bicarbonate might be exposed to additional fractionation processes. However, the relative contributions of metabolic i.e. respiratory carbon and bicarbonate from seawater and, more important, how these relative proportions in the internal carbon pool vary with time are still unknown (Pearse-Buchsbaum, 1970; Dustan, 1982).

In our past coral $\delta^{13}C$ records between 1350 and 1630, we observe relatively high mean $\delta^{13}C$ values between -0.36‰ and -0.85‰ $\delta^{13}C$. For comparison, the modern annual mean $\delta^{13}C_{seawater}$ near Bermuda is 1.4‰ $\delta^{13}C$, where recent stable carbon isotopic composition of the seawater is expected to be slightly lower compared to pre-industrial time, due to the surface ocean $\delta^{13}C$ Suess effect (Bacastow *et al.*, 1996). The high coral $\delta^{13}C$ values observed in this study may result from the uptake of bicarbonate from seawater at a considerable rate.

With respect to our results it is important to notice that algal blooms will progressively increase the ^{13}C-concentration of the ambient seawater due to the preferential uptake of ^{12}C. There exists close internal cycling within the reef ecosystem, so that the carbon dioxide for which the corals compete will be isotopically heavier during phases of high biomass productivity in response to convective mixing. Based on this scenario we suggest that the corals internal carbon pool can be generated towards higher isotopic composition during periods of high primary productivity, enabled by strong convective mixing. Possibly, coral $\delta^{13}C$ displays variations in seawater $\delta^{13}C$, i.e. competitive pathways of carbon cycling that are characteristic for the reef environment.

Besides the importance of the $\delta^{13}C$ signature of the surrounding seawater, Spero *et al.* (1997) reported an effect of the concentration of dissolved inorganic carbon [CO_3^{2-}] in seawater on the stable carbon isotope composition in symbiotic foraminifera (e.g. *Orbulina universa*). Their results show that shell $\delta^{13}C$ decreases by 0.006‰ as the carbonate ion concentration increases by 1μmol kg^{-1}. In Bermuda, [CO_3^{2-}] is low during winter (210μmol kg^{-1}) and high during summer (260μmol kg^{-1}) (Bates *et al.*, 1996). If a comparable effect would account for hermatypic corals, although not quantitatively investigated, 0.3‰ of the seasonal amplitude observed in our $\delta^{13}C$ could be due to the carbonate ion effect.

Another important fact is that the overall photosynthetic capacity of the symbiotic zooxanthellae is not only dependent on light availability but can also be regulated by the number of zooxanthellae, the amount of photosynthetic pigments, and the size of photosynthetic units (Dustan, 1982). Hermatypic corals are able to regulate the internal cycling of carbon between the symbiotic partners by either promotion or reduction of zooxanthellae density (Titlyanov *et al.*, 1996). Consequently, changes in the buildup and ingestion of zooxanthellae by the coral host will alter the isotopic composition of the internal

carbon pool. Such active regulation of photosynthetic capacity by the coral host has been shown to be influenced by the nutritional state of the animal (Titlyanov *et al.*, 1996). It is conceivable that the corals observed in this study actively reduced or increased the number of their zooxanthellae during times of low or high nutrient availability, respectively. Such behavior will lead to a change in net photosynthesis of zooxanthellae and possibly in the fraction of external carbon sources taken up by the corals. Invoking the hypothesis of Goreau (1977), an increase in photosynthesis alters skeletal $\delta^{13}C$ towards higher values, yielding the corals response to an optimal supply with nutrients.

In summary, the origin of the coral response to mixed layer depth can not definitely be clarified at this point. The processes that can lead to stable carbon fractionation and the metabolic pathways are numerous and yet not fully understood. Despite these complexities involved, we observe that variable environmental conditions lead to physiologically related $\delta^{13}C$ anomalies in the coral skeletons. The response to convective activity at Bermuda is analogous in three recent coral individuals, and reveals consistency on seasonal and inter-annual time scales. Hence, the integrity of the coral proxy information is maintained. We predict that the same processes have generated the coral $\delta^{13}C$ time series covering periods during Little Ice Age. The past coral $\delta^{13}C$ records may represent a tool to gain insight into the history of convective activity at Bermuda. The quality of the oceanic proxy information is hereby mutually confirmed by the consistency of a strong positive relationship between $\delta^{18}O$ and $\delta^{13}C$ in both the recent and past coral records.

4.6.2 Connections between coral $\delta^{18}O$ and $\delta^{13}C$ signals

Especially for the $\delta^{13}C$ time series covering periods during Little Ice Age we observe a strong positive relationship between coral $\delta^{13}C$ and $\delta^{18}O$. The significance of the strong positive correlation suggests some kind of a causal linkage of the influences affecting both isotopes. Given that coral $\delta^{13}C$ increases with increasing winter mixing depth and coral $\delta^{18}O$ decreases with temperature we can search for an interpretation of the positive relation between both isotopes. Maximum depth of the winter mixed layer, used here for correlation with coral $\delta^{13}C$,

can be considered an indicator for the strength of surface water overturn but does not say anything about the duration and the total amount of water mixed into the surface layer. On the other hand, variations in winter temperature are closely coupled with the overall amount of winter convective activity (Bacastow *et al.*, 1996). The variability in minimum temperature may be an excellent indicator for total mixing from deeper water that has a colder signature. Hence, minimum temperature should tend to represent the integral of the mixing process. This rationale is supported by the synoptic atmospheric surface forcing model presented by Doney (1996). The model allows the detection of a signal in sea surface temperature in response to convective activity near Bermuda. The close coupling between sea surface temperature and the process of mixing is reflected in the significant relation between coral $\delta^{13}C$ and $\delta^{18}O$. The correlation is consistent in both the modern and past coral records indicating that the processes that regulate fractionation of both stable isotopes prevailed.

We conclude that the variability in $\delta^{13}C$, observed in modern and past chronologies of Bermuda corals, reflect the varying degrees of convective activity in the western subtropical gyre. Of particular relevance is the fact that the coupling between coral $\delta^{18}O$ and $\delta^{13}C$ signals seems to be strongest during years, which are characterized by low temperatures coincident with deep mixing, respectively. Such increase in winter mixed layer depth and synchronous chilling of the surface ocean obeys atmospheric forcing that is characterized by a low index state of the North Atlantic Oscillation (Dickson *et al.*, 1996) where the ocean coincidentally responses to an increase in storminess in the low latitude North Atlantic (Rogers, 1990). So far there is not such high resolution marine proxy information on the hydrographic history in the North Atlantic subtropical gyre as presented in the $\delta^{13}C$ records between the fourteenth and the seventeenth century. The data provided by the skeletons of *D. labyrinthiformis* and *M. cavernosa* may contribute to elucidate the periodicity and strength of extreme states of the North Atlantic Oscillation system.

4.7 CONCLUSIONS

Our thrust is to illustrate the opportunity to apply Bermuda reef corals as recorders of inter-annual variability in the convective activity in the low-latitude North Atlantic. Comparisons between three recent records of skeletal $\delta^{13}C$ and the maximum mixed layer depth in winter suggests a robust connection between the coral signal and the convective activity of the surrounding seawater.

Comparison of seasonal and interannual $\delta^{13}C$ composition of the coral skeletons can not be explained by changes in light availability, regulating the photosynthetic activity. We suggest that the corals observed here were not self-sufficiently autotrophic but relied on heterotrophic food sources at a considerable rate. Hence, the signal of winter mixing depth carried by coral $\delta^{13}C$ can most likely be interpreted as a response to nutrient availability in the upper water column. Possibly the corals actively regulate the density of their endosymbiotic zooxanthellae in response to extant nutrient supply.

Modern and past coral records were proved to reveal close coupling between processes that generate both skeletal $\delta^{13}C$ and $\delta^{18}O$. Such coupling is given by the fact that especially variations in winter temperature are closely connected with the overall amount of winter convective activity in the subtropical gyre.

The time series of coral $\delta^{13}C$ that cover periods during Little Ice Age can be used to reconstruct regional and North Atlantic-scale hydrographic changes far prior to the establishment of instrumental data sets.

4.8 ACKNOWLEDGMENTS

We thank T. Bickert, B. Flemming and H. Grobe for helping in sample collection. The isotopic measurements were carried out at the stable-isotopic laboratory at Bremen University. We acknowledge M. Segl and her team for performing the measurements. Comments on the manuscript by H. Kuhnert were most helpful. This work was funded by the 'Paläoklima' BMBF-grant 03F0131A.

4.9 REFERENCES

Aharon, P. 1991: Recorders of reef environment histories: Stable isotopes in corals, giant clams, and calcareous algae. *Coral Reefs* 10, 71-90.

Bacastow, R.B., Keeling, C.D., Lueker, T.J. and Wahlen, M. 1996: The ^{13}C Suess effect in the world surface oceans and its implications for oceanic uptake of CO_2: Analysis of observations at Bermuda. *Global Biochem. Cycles* 10, 335-346.

Bates, N.R., Michaels, A.F. and Knap, A.H. 1996: Seasonal and interannual variability of oceanic carbon dioxide species at the U.S. JGOFS Bermuda Atlantic Time-series Study (BATS) site. *Deep Sea Res.* 2, 43, 347-383.

Bermuda Environmental Scenario 1974: *US Naval Weather Service Detachment.* Asheville, New York, 199pp.

Bjerknes, J. 1964: Atlantic air-sea interaction. *Adv. Geophys.* 10, 1-82.

Bodungen, B.v., Jickells, T.D., Smith, S.R., Ward, J.A.D. and Hillier, G.B. 1982: The Bermuda Marine Environment. Final report of the Bermuda inshore waters, Investigations 1975-1980. *BBSR Special Publication* 18, 123pp.

Boscher, H. 1992: *Growth potential of coral reefs and carbonate platforms.* Ph.D. dissertation, Vrije Universiteit Amsterdam, Vrije University Press, 160pp.

Carriquiry, J.D., Risk, M.J. and Schwarcz, H.P. 1993: Stable isotope geochemistry of corals from Costa Rica as proxy indicator of the El Nino/ Southern Oscillation (ENSO). *Geochim. Cosmochim. Acta* 58, 335-351.

Cole, J.E. and Fairbanks, R.G.1990: The Southern Oscillation recorded in the $\delta^{18}O$ of corals from Tarawa Atoll. *Paleoceanography* 5, 669-683.

Crowley, T.J., Quinn, T.M., Taylor, F.W., Henin, C. and Joannot, P. 1997: Evidence for a volcanic cooling in a 335-year coral record from New Caledonia. *Paleoceanography* 12, 633-639.

Dickson, R.R. and Namias, J. 1976: North American influences on the circulation and climate of the North Atlantic sector. *Mon. Weath. Rev.* 104, 1256-1265.

Dickson, R.R., Lazier, J., Meincke, J., Rhines, P. and Swift, J. 1996: Long-term coordinated changes in the convective activity of the North Atlantic. *Progr. Oceanogr.* 37, 207-262.

Doney, S.C. 1996: A synoptic atmospheric surface forcing data set and physical upper ocean model for the U.S. JGOFS Bermuda Atlantic Time-Series Study (BATS) Site. *J. Geophys. Res.*, C, 101, 25615-25634.

Dustan, P. 1982: Depth-dependent photoadaption by zooxanthellae of the reef coral *Montastrea annularis. Mar. Biol.* 68, 253-264.

Erez, J. 1978: Vital effect on stable-isotope composition seen in foraminifera and coral skeletons. *Nature* 273, 199-202.

Fairbanks, R.G. and Dodge, R.E. 1979: Annual periodicity of the $^{18}O/^{16}O$ and $^{13}C/^{12}C$ ratios in the coral *Montastrea annularis. Geochim. Cosmochim. Acta* 43, 1009-1020.

Goreau, T.J. 1977: Coral skeleton chemistry: physiological and environmental regulation of stable isotopes and trace metals in *Montastrea annularis. Proc. Royal Soc., London* B196, 291-315.

Hurrell, J.W. 1995: Decadal trends in the North Atlantic Oscillation: Regional temperature and precipitation. *Science* 269, 676-679.

Hurrell, J.W. 1996: Influence of variations in extratropical wintertime teleconnections on Northern Hemisphere temperature. *Geophys. Res. Lett.* 23, 6, 665-668.

Jenkins, W.J. 1982: On the climate of a subtropical gyre: decadal scale variations in water mass renewal in the Sargasso Sea. *J. Mar. Res.* 40, 265-290.

Kinsey, D.W. 1985: Metabolism, calcification and carbon production. 1. System level studies. *Proc. 5th Int. Coral Reef Congr.*, Tahiti, 4, 505-526.

Kushnir, Y. 1994: Interdecadal variations in North Atlantic sea surface temperature and associated atmospheric conditions. *J. Clim.* 7, 141-157.

Land, L.S., Lang, J.C. and Smith, B.N. 1977: Preliminary observations on the carbon isotopic composition of some reef coral tissues and symbiotic zooxanthellae. *Limnol. Oceanogr.* 20, 283-287.

Linsley, B.K., Dunbar, R.B., Wellington, G.M. and Mucciarone, D.A. 1994: A coral-based reconstruction of Intertropical Convergence Zone variability over central America since 1707. *J. Geophys. Res.* 99, 9977-9994.

McConnaughey, T. 1989: ^{13}C and ^{18}O isotopic disequilibrium in biological carbonates. 2: In vitro simulation of kinetic isotope effects. *Geochim. Cosmochim. Acta* 53, 163-171.

McConnaughey, T., Burdett, J., Whelan, J.F. and Paull, C.K. 1996: Carbon isotopes in biological carbonates: Respiration and photosynthesis. *Geochim. Cosmochim. Acta* 61, 611-622.

Menzel, D.W. and Ryther, J.H. 1960: The annual cycle of primary production in the Sargasso Sea off Bermuda. *Deep-Sea Res.* 6, 351-367.

Menzel, D.W. and Ryther, J.H. 1961: Annual variation in primary production of the Sargasso Sea off Bermuda. *Deep Sea Res.* 7, 282-288.

Michaels, A.F., Knap, A.H., Dow, R.L., Gundersen, K., Johnson, J.J., Sorensen, J., Close, A., Knauer, G.A., Lohrenz, S.E., Asper, V.A., Tuel, M. and Bidigare, R. 1994: Seasonal patterns of ocean biogeochemistry at the JGOFS Bermuda Atlantic Time-Series Study Site. *Deep-Sea Res.* 41, 7, 1013-1038.

Morris, B., Barnes, J., Brown, F. and Markham, J. 1977: The Bermuda Marine Environment. A report of the Bermuda inshore waters, Investigations 1976-1977. *BBSR Special Publication* 15, 199pp.

Muscatine, L., Porter, J.W. and Kaplan, I.R. 1989: Resource partitioning by reef corals as determined from stable isotope composition. *Mar. Biol.* 100, 185-193.

Pätzold, J. 1984: Growth rhythms recorded in the stable isotopes and density bands in the reef coral *Porites lobata* (Cebu, Philippines). *Coral Reefs* 3, 87-90.

Pätzold, J. 1992: variation of the stable oxygen and carbon isotopic fractionation within skeletal elements of reef building corals from Bermuda. *Proc. 7th Int. Coral Reef Symp.*, Guam 1, 13595-13601.

Pätzold, J.., Bickert, T., Flemming, B., Grobe, H. and Wefer, G. 1998: Holozänes Klima des Nordatlantiks rekonstruiert aus massiven Korallen von Bermuda. *Natur und Museum*, in press.

Pearse-Buchsbaum, V. 1970: Incorporation of metabolic CO_2 into coral skeletons. *Nature* 228, 383.

Porter, J.W. 1985: The maritime weather of Jamaica: It's effects on annual carbon budgets of the massive reef-building coral *Montastrea annularis*. *Proc. 5th Int. Coral Reef Congr., Tahiti*, 6, 363-379.

Rogers, J.C. 1990: Patterns of low-frequency monthly sea-level pressure variability (1899-1986) and associated wave-cyclone frequencies. *J. Climatol.* 3, 1364-1379.

Siegel, D.A., Itturiaga, R., Bidigare, R.R., Smith, R.C., Pak, H., Dickey, T.D., Marra, J. and Baker, K.S. 1990: Meridional variations in the spring time phytoplankton community in the Sargasso Sea. *J. Mar. Res.* 48, 379-412.

Spero, H.J., Bijma, J., Lea, D.W. and Bemis, B.E. 1997: Effect of seawater carbonate concentration on foraminiferal carbon and oxygen isotopes. *Nature* 390, 497-500.

Spitzer, W.S. and Jenkins, W.J. 1989: Rates of vertical mixing, gas exchange and new production: Estimates from seasonal gas cycles in the upper ocean near Bermuda. *J. Mar. Res.* 47, 169-196.

Swart, P.K. 1983: Carbon and oxygen isotope fractionation in scleractinian corals: a review. *Earth-Science Rev.* 19, 51-80.

Swart, P.K., Leder, J.J., Szmant, A.M. and Dodge, R.E. 1996: The origin of variations in the isotopic record of scleractinian corals: 2. Carbon. *Geochim. Cosmochim. Acta* 60, 2871-2885.

Titlyanov, E.A., Titlyanova, T.V., Leletkin, V.A., Tsukahara, J., Van Woesik, R. and Yamazato, K. 1996: Degradation of zooxanthellae and regulation of their density in hermatypic corals. *Mar. Ecol. Progr. Ser.* 139, 167-178.

Tudhope, A.W., Shimmield, G.B., Chilcott, C.P., Jebb, M., Fallick, A.E. and Dalgleish, A.N. 1995: Recent changes in climate in the far western equatorial Pacific and their relationship to the Southern Oscillation; oxygen isotope records from massive corals, Papua New Guinea. *Earth Planet. Sci. Lett.* 136, 575-590.

Weber, J.N. and Woodhead, P.M.J. 1972: Temperature dependence of oxygen-18 concentration in reef coral carbonates. *J. Geophys. Res.* 77, 463-473.

Weber, J.N., Deines, P., White, E.W. and Weber, P.H. 1976: Seasonal high and low density bands in reef coral skeletons. *Nature* 255, 697-698.

Wefer, G. and Berger, W.H. 1991: Isotope paleontology: growth and composition of extant calcareous species. *Mar. Geol.* 100, 207-248.

5 SUMMARY OF RESULTS AND OUTLOOK

There is a great complexity of regional and seasonal temperature variability in the Northern Hemisphere, and thus a consequential need for a higher density of proxy records to indicate genuine hemispheric scale temperature change. In this thesis, climate proxy indicators of the skeletons of Bermuda corals have been investigated in three separate studies. The historical perspective is valuable because it provides insights into climate changes occurring on socially relevant time scales of years to centuries.

The following gives the main results of this thesis:

- The skeletons of coral colonies of the hermatypic reef coral *Diploria labyrinthiformis* monitor changes in their marine environment in form of variations in annual skeletal growth rates and density. Climatic influences on the coral skeletons are changes in sea surface temperatures and the extend of vertical mixing of the water column that occurs during winter. Furthermore, the skeletons monitor changes which are connected to fluctuations in the atmospheric North Atlantic Oscillation system.
- In *D. labyrinthiformis* from Bermuda, skeletal density is the more sensitive recorder of climatic influences, compared to annual growth rates.
- Correlation between skeletal growth parameters and seasonal values of climate indices (i.e. sea surface temperatures and the North Atlantic Oscillation Index) has demonstrated that the corals respond most sensitively to wintertime conditions. Especially skeletal density is an excellent proxy indicator for winter climate conditions in Bermuda.
- Coral skeletal $\delta^{18}O$ of *D. labyrinthiformis* has been used to reconstruct changes is sea surface temperatures in Bermuda. Triennial values of coral $\delta^{18}O$ reveal strong correlation to instrumental temperature data from Bermuda and deliver reliable and comparative estimates of sea surface temperature variations during periods of the 19th and 20th century.
- Estimates of sea surface temperature anomalies during periods of the Little Ice Age are derived from triennial coral $\delta^{18}O$. The Little Ice Age (AD 1350 to 1630) coral $\delta^{18}O$ records indicate long-term variations in sea surface temperatures which amount to the order of variations observed for the 20th century. Time series of annual skeletal density reveal a strong similarity with the temperature anomaly pattern, reconstructed from $\delta^{18}O$.
- The coral $\delta^{18}O$ and skeletal density time series observed in this thesis share characteristic features with previously published climate proxy series for Bermuda and the Northern

Hemisphere (Pätzold *et al.*, 1998; Bradley and Jones, 1993). The reconstructed temperature pattern achieved in this study, fits well into the most recent picture of the Little Ice Age.

- High resolution modern (1969 to 1992) time series of coral $\delta^{13}C$ of *D. labyrinthiformis* and *M. cavernosa* show a strong correlation with the extend of vertical ventilation of the water column near Bermuda, on both seasonal and inter-annual time scales. The signal of convecitve activity carried by the coral skeletons is suggested to reflect nutrient supply.
- The seasonal coral $\delta^{13}C$ signal of *D. labyrinthiformis* and *M. cavernosa* can not be attributed to the seasonal cycle in light availability in Bermuda. Light has earlier been interpreted as the major regulating factor for stable carbon isotope fractionation in hermatypic corals due to it's dominating effect on zooxanthellae photosynthesis.
- In both, modern annual (1969 to 1992), and past triennial (Little Ice Age, AD 1350 to 1630) stable isotope records, coral $\delta^{13}C$ and $\delta^{18}O$ exhibit a strong positive correlation. This association reflects the causal connection between the extend of winter convective activity (indicated by coral $\delta^{13}C$) and sea surface temperatures (revealed by coral $\delta^{18}O$) in the hydrographic pattern at Bermuda.

Bermuda represents a key-site for the reconstruction of natural climate variability of low latitudes in the North Atlantic, and with respect to it's location besides the Gulf Stream. A further extension of climate sensitive proxy records from this site is most beneficial. For example, the relatively fast and easy measurement of skeletal bulk density, and the applicability as a climate proxy encourages to a further establishment of this approach.

With respect to the $\delta^{18}O$ signal in the coral skeletons, a valuable approach in the future, is the supplementary measurement of Sr/Ca and Mg/Ca ratios in the skeletons. Such procedure can elucidate possible local salinity effects on skeletal $\delta^{18}O$, since both methods are independent of changes in salinity and are subject to only small vital effects.

Questions regarding the interpretation of coral $\delta^{13}C$ will gain considerable support by new findings about the coral-algal physiology. Symbiotic interaction and metabolism in hermatypic reef corals, which remains elusive until today, has to be further deciphered in order to strengthen $\delta^{13}C$ as a climate proxy indicator.

6 APPENDIX

Table 6.1 Analytical data of annual **skeletal bulk density** and annual **growth rates** in the skeletons of *D. labyrinthiformis* (BDA 210 and BDA 221) between 1857 and 1988. The stratigraphy is based on counting of annual density bands, starting at the top of the colony in 1993. Skeletal bulk density and annual growth rates were determined as described in the material and methods section of Chapter 2 and are used in that section.

Years	Annual skeletal density [g cm^{-3}] **BDA 210**	Annual growth rate [cm] **BDA 210**	Annual skeletal density [g cm^{-3}] **BDA 221**	Annual growth rate [cm] **BDA 221**
1857			1.236	0.31
1858	1.148	0.42	1.301	0.31
1859	1.171	0.41	1.351	0.31
1860	1.182	0.39	1.347	0.28
1861	1.199	0.32	1.273	0.28
1862	1.199	0.42	1.250	0.30
1863	1.166	0.41	1.236	0.33
1864	1.143	0.40	1.220	0.36
1865	1.113	0.39	1.207	0.42
1866	1.082	0.41	1.174	0.45
1867	1.053	0.42	1.134	0.53
1868	1.041	0.47	1.085	0.59
1869	0.996	0.53	1.095	0.52
1870	0.972	0.57	1.114	0.48
1871	1.002	0.46	1.170	0.49
1872	1.115	0.40	1.184	0.41
1873	1.145	0.38	1.204	0.39
1874	1.132	0.42	1.217	0.36
1875	1.075	0.40	1.215	0.32
1876	1.065	0.41	1.165	0.32
1877	1.029	0.39	1.152	0.32
1878	1.026	0.46	1.115	0.31
1879	1.045	0.42	1.133	0.41
1880	1.095	0.51	1.192	0.34
1881	1.061	0.42	1.180	0.38
1882	1.124	0.43	1.255	0.37
1883	1.123	0.42	1.265	0.37
1884	1.134	0.43	1.246	0.36
1885	1.135	0.40	1.209	0.36
1886	1.072	0.34	1.193	0.37
1887	1.042	0.36	1.219	0.28
1888	1.092	0.33	1.220	0.41
1889	1.152	0.34	1.229	0.32
1890	1.162	0.36	1.259	0.34
1891	1.125	0.38	1.267	0.32
1892	1.097	0.42	1.278	0.32
1893	1.077	0.34	1.285	0.33
1894	1.048	0.38	1.270	0.31
1895	1.062	0.39	1.250	0.35
1896	1.070	0.34	1.200	0.35
1897	1.083	0.38	1.176	0.31
1898	1.095	0.40	1.152	0.33
1899	1.070	0.41	1.159	0.32
1900	1.048	0.34	1.113	0.28
1901	0.999	0.41	1.080	0.50
1902	0.994	0.51	1.110	0.51
1903	1.049	0.38	1.146	0.43

Table 6.1 continued

Years	Annual skeletal density [g cm^{-3}] **BDA 210**	Annual growth rate [cm] **BDA 210**	Annual skeletal density [g cm^{-3}] **BDA 221**	Annual growth rate [cm] **BDA 221**
1904	1.076	0.42	1.179	0.40
1905	1.080	0.41	1.198	0.38
1906	1.101	0.42	1.198	0.37
1907	1.110	0.41	1.226	0.36
1908	1.112	0.43	1.205	0.33
1909	1.078	0.41	1.165	0.31
1910	1.015	0.46	1.114	0.35
1911	0.985	0.49	1.110	0.41
1912	1.008	0.46	1.179	0.42
1913	1.060	0.44	1.193	0.36
1914	1.053	0.41	1.216	0.31
1915	1.043	0.40	1.249	0.32
1916	1.020	0.42	1.248	0.33
1917	1.030	0.50	1.227	0.34
1918	0.981	0.51	1.212	0.35
1919	0.965	0.51	1.175	0.31
1920	0.996	0.50	1.220	0.41
1921	0.991	0.47	1.283	0.41
1922	1.070	0.48	1.290	0.37
1923	1.104	0.46	1.302	0.32
1924	1.112	0.41	1.272	0.33
1925	1.120	0.45	1.321	0.33
1926	1.122	0.42	1.258	0.34
1927	1.149	0.39	1.255	0.31
1928	1.132	0.39	1.263	0.30
1929	1.175	0.35	1.275	0.30
1930	1.202	0.35	1.288	0.34
1931	1.155	0.44	1.167	0.37
1932	1.097	0.44	1.220	0.39
1933	1.088	0.42	1.254	0.32
1934	1.100	0.43	1.246	0.29
1935	1.090	0.43	1.199	0.30
1936	1.101	0.42	1.282	0.31
1937	1.107	0.40	1.278	0.37
1938	1.092	0.40	1.231	0.33
1939	1.041	0.47	1.226	0.29
1940	1.007	0.51	1.090	0.41
1941	1.002	0.52	1.063	0.42
1942	1.051	0.43	1.188	0.40
1943	1.104	0.43	1.229	0.34
1944	1.154	0.43	1.235	0.35
1945	1.147	0.43	1.234	0.36
1946	1.130	0.45	1.204	0.37
1947	1.139	0.44	1.198	0.42
1948	1.179	0.45	1.272	0.33
1949	1.181	0.41	1.305	0.34
1950	1.253	0.39	1.315	0.36
1951	1.252	0.37	1.300	0.32
1952	1.247	0.38	1.327	0.35
1953	1.245	0.38	1.333	0.31
1954	1.218	0.40	1.366	0.31
1955	1.218	0.40	1.354	0.26
1956	1.206	0.40	1.376	0.29

Table 6.1 continued

Years	Annual skeletal density [g cm^{-3}] **BDA 210**	Annual growth rate [cm] **BDA 210**	Annual skeletal density [g cm^{-3}] **BDA 221**	Annual growth rate [cm] **BDA 221**
1957	1.193	0.41	1.350	0.31
1958	1.161	0.42	1.315	0.32
1959	1.113	0.42	1.294	0.34
1960	1.137	0.39	1.283	0.32
1961	1.157	0.37	1.295	0.33
1962	1.149	0.40	1.355	0.35
1963	1.152	0.36	1.331	0.37
1964	1.169	0.41	1.322	0.37
1965	1.202	0.41	1.310	0.41
1966	1.165	0.41	1.280	0.44
1967	1.175	0.48		
1968	1.109	0.51		
1969	1.107	0.48		
1970	1.162	0.47		
1971	1.182	0.48		
1972	1.209	0.41		
1973	1.229	0.42		
1974	1.265	0.41		
1975	1.253	0.43		
1976	1.217	0.42		
1977	1.205	0.41		
1978	1.206	0.44		
1979	1.235	0.42		
1980	1.222	0.36		
1981	1.294	0.34		
1982	1.325	0.37		
1983	1.295	0.33		
1984	1.275	0.34		
1985	1.320	0.35		
1986	1.237	0.37		
1987	1.261	0.33		
1988	1.353	0.34		

Table 6.2 Analytical data of high-resolution coral skeletal $\delta^{18}O$ [‰] and relative **optic density** in X-radiograph positives versus the distance from the colony top in BDA 210. The data were determined as described in the material and methods section of Chapter 2 and are used in that section.

Distance from colony top [mm]	$\delta^{18}O$ [‰] vs. PDB BDA 210
0.4	-3.59
0.6	-3.48
0.8	-3.16
1	-3.08
1.2	-3.26
1.4	-3.01
1.6	-3.29
1.8	-3.14
2	-3.34
2.2	-3.35
2.4	-3.43
2.6	-3.56
2.8	-3.68
3	-3.75
3.2	-3.78
3.4	-3.96
3.6	-3.81
3.8	-3.85
4	-3.42
4.2	-3.31
4.4	-3.34
4.6	-3.12
4.8	-3.18
5	-2.95
5.2	-3.04
5.4	-3.36
5.6	-3.56
5.8	-3.59
6	-3.37
6.2	-3.59
6.4	-3.46
6.6	-3.79
6.8	-3.64
7	-3.54

Distance from colony top [mm]	Optic density [gray-value] **BDA 210**
0.22	128
0.44	126
0.66	115
0.89	100
1.11	102
1.33	92
1.55	102
1.77	99
1.99	108
2.21	101
2.44	109
2.66	145
3.10	142
3.33	134
3.55	128
3.78	111
4.00	103
4.23	101
4.45	112
4.68	98
4.90	113
5.13	107
5.35	123
5.58	129
5.80	145
5.99	126
6.18	123
6.36	119
6.55	105
6.74	95
6.93	101
7.12	99
7.31	97
7.49	108

Continuation of Table 6.2

Distance from colony top [mm]	$\delta^{18}O$ [‰] vs. PDB BDA 210
7.2	-3.26
7.4	-3.09
7.6	-3.07
7.8	-3.35
8	-3.24
8.2	-3.20
8.4	-3.35
8.6	-3.51
8.8	-3.38
9	-3.55
9.2	-3.57
9.4	-3.29
9.6	-3.37
9.8	-3.20
10	-3.37
10.2	-3.32
10.4	-3.31
10.6	-3.29
10.8	-3.03
11	-2.96
11.2	-3.16
11.4	-3.38
11.6	-3.59
11.8	-3.65
12	-3.68
12.2	-3.56
12.4	-3.55
12.6	-3.40
12.8	-3.25
13	-3.22
13.2	-2.89
13.4	-3.19
13.6	-3.11
13.8	-3.16
14	-3.19

Distance from colony top [mm]	Optic density [gray-value] **BDA 210**
7.68	103
7.87	108
8.06	112
8.25	115
8.44	121
8.62	117
8.81	138
9.00	124
9.21	119
9.43	116
9.64	92
9.86	95
10.07	82
10.29	71
10.50	76
10.71	69
10.93	84
11.14	80
11.36	82
11.57	94
11.79	99
12.00	117
12.19	99
12.38	88
12.56	96
12.75	85
12.94	80
13.13	75
13.31	69
13.69	72
13.88	70
14.06	87
14.25	91
14.44	96
14.63	105

Table 6.3 Triennial skeletal stable oxygen isotope composition ($\delta^{18}O$ [‰]) in BDA 210a and BDA 221a. The stratigraphy is based on annual density banding. Each triennial stable isotope value was attributed to the central year of the three-year skeletal section that was sampled. The data cover the period between 1833 (BDA 210a) and 1920 (BDA 221a). The data were obtained as described in Chapter 3 and are used in that section.

:

Year	$\delta^{18}O$ [‰] vs. PDB BDA 210 a
1833	-3,51
1836	-3,38
1839	-3,33
1842	-3,21
1845	-3,26
1848	-3,49
1851	-3,44
1854	-3,53
1857	-3,32
1860	-3,48
1862	-3,50
1865	-3,42
1868	-3,59
1871	-3,78
1874	-3,66
1877	-3,40
1880	-3,35
1883	-3,41
1886	-3,59
1889	-3,57
1892	-3,28
1895	-3,71
1898	-3,56
1901	-3,67
1904	-3,36

Year	$\delta^{18}O$ [‰] vs. PDB BDA 221 a
1856	-2,69
1859	-2,95
1862	-3,24
1865	-2,92
1868	-3,24
1870	-3,45
1872	-3,35
1875	-3,18
1878	-2,83
1881	-3,06
1885	-3,13
1888	-3,24
1891	-2,82
1894	-3,24
1897	-3,17
1900	-3,02
1902	-2,85
1905	-2,96
1908	-3,04
1911	-2,76
1915	-2,93
1917	-3,28
1920	-3,22

Table 6.4 Data of **annual skeletal density** [g cm^{-3}] and skeletal stable oxygen (δ^{18}**O**) and carbon (δ^{13}**C**) isotopic composition in BDA 215a, BDA 215b and BDA 221b. A short parallel profile of coral δ^{18}O was measured in BDA 215a. The stratigraphy (Year AD) is based on AMS ^{14}C dating and counting of skeletal bands. The data cover the period between 1351 and 1630. Data of skeletal density were obtained as described in Chapter 2, and stable isotope data as described in Chapter 3 and 4. Records of annual skeletal density and triennial coral δ^{18}O are shown in Chapter 3 and data of triennial coral δ^{18}O and δ^{13}C are shown in Chapter 4.

BDA 215 a

Year AD	Annual skeletal density [g cm^{-3}]	δ^{18}O [‰] vs. PDB	δ^{18}O [‰] vs. PDB	δ^{13}C [‰] vs. PDB
1351	1.400			
1352	1.466			
1353	1.428			
1354	1.411	-2.27		1.49
1355	1.376			
1356	1.411			
1357	1.389	-3.23		1.61
1358	1.361			
1359	1.308			
1360	1.289	-2.62		0.80
1361	1.292			
1362	1.307			
1363	1.320	-2.91		-0.92
1364	1.320			
1365	1.273			
1366	1.259	-2.53		-0.47
1367	1.276			
1368	1.287	-2.70		-0.43
1369	1.294			
1370	1.263			
1371	1.246	-2.10		-0.21
1372	1.248			
1373	1.294			
1374	1.349	-2.71		0.01
1375	1.349			
1376	1.298			
1377	1.297	-2.01		0.80
1378	1.304			
1379	1.310			
1380	1.339	-2.48		-0.78
1381	1.351			
1382	1.358			
1383	1.333	-1.86		0.47
1384	1.327			
1385	1.328			
1386	1.315	-2.52		-0.05
1387	1.345			
1388	1.366			
1389	1.388	-2.18		-1.14
1390	1.401			
1391	1.406			
1392	1.421	-2.29		0.39
1393	1.432			
1394	1.420			
1395	1.415	-3.02		-1.46
1396	1.423			

Table 6.4 (BDA 215a) continued

Year AD	Annual skeletal density [g cm^{-3}]	$\delta^{18}O$ [‰] vs. PDB	$\delta^{18}O$ [‰] vs. PDB	$\delta^{13}C$ [‰] vs. PDB
1397	1.408			
1398	1.448	-3.06	-2.98	-1.56
1399	1.411			
1400	1.411			
1401	1.412	-2.96	-2.90	-1.70
1402	1.438			
1403	1.447			
1404	1.459	-3.05	-2.71	-1.32
1405	1.469			
1406	1.434			
1407	1.377	-2.98	-3.35	-1.37
1408	1.329			
1409	1.310			
1410	1.308	-2.93	-2.39	-1.09
1411	1.312			
1412	1.320			
1413	1.309	-2.27	-2.55	0.31
1414	1.351			
1415	1.373			
1416	1.394	-2.20	-1.95	0.66
1417	1.368			
1418	1.413			
1419	1.440	-2.47	-2.53	-0.53
1420	1.457			
1421	1.468			
1422	1.465	-2.88	-2.72	-1.12

BDA 215 b

Year AD	Annual skeletal density [g cm^{-3}]	$\delta^{18}O$ [‰] vs. PDB	$\delta^{18}O$ [‰] vs. PDB	$\delta^{13}C$ [‰] vs. PDB
1432		-2.85		-1.12
1433	1.305			
1434	1.307	-2.72		-1.50
1435	1.309			
1436	1.347	-3.04		-1.68
1437	1.403			
1438	1.451			
1439	1.431	-3.33		-1.61
1440	1.394			
1441	1.336			
1442	1.308	-3.12		-1.63
1443	1.298			
1444	1.295			
1445	1.352	-2.80		-0.89
1446	1.371			
1447	1.350			
1448	1.337	-3.07		-1.63
1449	1.397			
1450	1.468			
1451	1.484	-3.54		-1.45
1452	1.495			
1453	1.436			
1454	1.397	-3.37		-1.33
1455	1.400			
1456	1.395			
1457	1.374	-3.19		-1.59

Table 6.4 (BDA 215 b) continued

Year AD	Annual skeletal density [g cm^{-3}]	$\delta^{18}O$ [‰] vs. PDB	$\delta^{18}O$ [‰] vs. PDB	$\delta^{13}C$ [‰] vs. PDB
1458	1.371			
1459	1.350			
1460	1.346	-3.12		-0.93
1461	1.302			
1462	1.309			
1463	1.291	-3.06		-0.83
1464	1.306			
1465	1.346			
1466	1.344	-3.32		-1.62
1467	1.282			
1468	1.256			
1469	1.228	-2.90		-0.03
1470	1.216			
1471	1.243			
1472	1.339	-3.23		-1.20
1473	1.383			
1474	1.318			
1475	1.276	-2.78		-0.43
1476	1.278			
1477	1.311			
1478	1.341	-3.09		-1.54
1479	1.343			
1480	1.328			
1481	1.300	-3.16		-1.19
1482	1.316			
1483	1.298			
1484	1.295	-3.09		-1.31
1485	1.311			
1486	1.302			
1487	1.266	-2.49		-0.39
1488	1.230			
1489	1.207			
1490	1.204	-2.54		1.07
1491	1.232			
1492	1.281			
1493	1.356	-3.05		-1.00
1494	1.424			
1495	1.443			
1496	1.502	-3.42		-0.95
1497	1.450			
1498	1.414	-2.95		-1.29
1499	1.389	-2.65		1.01
1500	1.300			
1501	1.329			
1502	1.308	-2.89		-0.72
1503	1.268			
1504	1.223			
1505	1.248	-2.36		0.34

BDA 221b

Year AD	Annual skeletal density [g cm^{-3}]	$\delta^{18}O$ [‰] vs. PDB	$\delta^{18}O$ [‰] vs. PDB	$\delta^{13}C$ [‰] vs. PDB
1514		-2.62		-0.49
1515				
1516	1.275			
1517	1.279	-2.88		-1.46

Table 6.4 (BDA 221b) continued

Year AD	Annual skeletal density [g cm^{-3}]	$\delta^{18}O$ [‰] vs. PDB	$\delta^{18}O$ [‰] vs. PDB	$\delta^{13}C$ [‰] vs. PDB
1518	1.373			
1519	1.430			
1520	1.442	-3.49		-1.29
1521	1.428			
1522	1.435			
1523	1.435	-3.45		-1.50
1524	1.391			
1525	1.352			
1526	1.351	-3.42		-1.31
1527	1.376			
1528	1.394			
1529	1.454	-3.54		-0.74
1530	1.454			
1531	1.452			
1532	1.437	-3.05		-0.53
1533	1.356			
1534	1.279			
1535	1.278	-3.15		-0.05
1536	1.281			
1537	1.242			
1538	1.206	-3.04		0.35
1539	1.209			
1540	1.216			
1541	1.190	-2.91		1.09
1542	1.204			
1543	1.186			
1544	1.161	-2.76		1.19
1545	1.153			
1546	1.147			
1547	1.199	-3.24		0.71
1548	1.216			
1549	1.295			
1550	1.322	-3.33		-0.09
1551	1.304			
1552	1.322			
1553	1.254	-3.32		-0.55
1554	1.260			
1555	1.241			
1556	1.197	-3.37		-0.26
1557	1.244			
1558	1.240			
1559	1.240	-3.38		-0.79
1560	1.221			
1561	1.279			
1562	1.292	-3.86		-1.11
1563	1.309			
1564	1.266			
1565	1.270	-3.65		-0.64
1566	1.315			
1567	1.317			
1568	1.245	-3.56		0.69
1569	1.214			
1570	1.208			
1571	1.247	-3.73		-0.93
1572	1.240			

Table 6.4 (BDA 221b) continued

Year AD	Annual skeletal density [g cm^{-3}]	$\delta^{18}O$ [‰] vs. PDB	$\delta^{18}O$ [‰] vs. PDB	$\delta^{13}C$ [‰] vs. PDB
1573	1.247			
1574	1.230	-3.56		-0.87
1575	1.187			
1576	1.184	-3.77		-1.01
1577	1.213			
1578	1.198			
1579	1.160	-3.20		-0.09
1580	1.145			
1581	1.170			
1582	1.129	-3.06		0.64
1583	1.153			
1584	1.233			
1585	1.217	-3.40		-0.37
1586	1.215			
1587	1.172			
1588	1.179	-3.34		-1.14
1589	1.241			
1590	1.246			
1591	1.241	-3.50		-0.82
1592	1.263			
1593	1.265			
1594	1.295	-3.45		-1.11
1595	1.291			
1596	1.266			
1597	1.238	-3.37		-0.64
1598	1.253			
1599	1.239			
1600	1.218	-3.49		-1.04
1601	1.236			
1602	1.185			
1603	1.144	-3.39		-1.07
1604	1.120			
1605	1.108			
1606	1.115	-3.10		0.00
1607	1.171			
1608	1.181			
1609	1.115	-2.62		0.42
1610	1.076			
1611	1.092			
1612	1.138	-2.70		0.50
1613	1.179			
1614	1.192			
1615	1.167	-3.10		-0.78
1616	1.190			
1617	1.220			
1618	1.290	-3.58		-1.29
1619	1.173			
1620	1.240			
1621	1.300	-3.62		-0.75
1622	1.278			
1623	1.264			
1624	1.262	-3.57		-0.99
1625	1.215			
1626	1.269			
1627	1.331	-3.57		-0.93
1628	1.301			
1629	1.303			
1630	1.302	-3.66		-0.92

Table 6.5 Analytical data of high-resolution coral skeletal stable oxygen (δ^{18}**O** [‰]) and carbon isotope (δ^{13}C [‰]) composition in BDA229, BDA 134 and BDA 225. The time axis was established by fixing seasonal δ^{18}O extremes on instrumental temperature extremes (with known date), and by assigning ages to intermediate values by linear interpolation. The data cover the period between 1969 and 1993. They were obtained as described in Chapter 4 and are used in that section.

Time	δ^{18}O [‰] vs. PDB BDA 229	δ^{13}C [‰] vs. PDB BDA 229
1980.12	-2.87	-1.60
1980.18	-3.11	-1.55
1980.24	-2.97	-1.96
1980.30	-2.93	-1.78
1980.36	-2.94	-1.83
1980.42	-3.02	-1.70
1980.48	-2.92	-1.60
1980.54	-3.00	-1.52
1980.60	-3.10	-1.48
1980.66	-3.04	-1.73
1980.72	-3.17	-1.74
1980.75	-2.85	-1.62
1980.79	-2.95	-1.67
1980.82	-2.71	-1.48
1980.85	-2.75	-1.25
1980.89	-2.85	-1.37
1980.92	-2.69	-1.39
1980.96	-2.75	-1.54
1980.99	-2.52	-1.63
1981.03	-2.81	-1.77
1981.06	-2.62	-1.70
1981.10	-2.60	-1.41
1981.13	-2.61	-1.80
1981.17	-2.61	-1.91
1981.20	-2.52	-2.08
1981.23	-2.70	-1.96
1981.27	-2.78	-2.19
1981.30	-2.83	-2.51
1981.33	-3.02	-2.58
1981.37	-3.08	-2.65
1981.40	-3.12	-2.78
1981.44	-3.16	-2.99
1981.47	-3.04	-2.74
1981.50	-3.04	-2.96
1981.54	-2.97	-2.81
1981.57	-3.09	-2.97
1981.60	-2.98	-2.91
1981.64	-3.22	-3.09
1981.77	-3.05	-2.95
1981.91	-3.07	-2.71
1982.04	-2.91	-2.76
1982.18	-2.89	-2.34
1982.23	-2.97	-2.31
1982.28	-3.01	-2.28
1982.34	-3.12	-2.00

Time	δ^{18}O [‰] vs. PDB BDA 134	δ^{13}C [‰] vs. PDB BDA 134
1969.15	-2.65	-1.65
1969.26	-3.01	-1.31
1969.38	-3.24	-1.40
1969.49	-3.41	-1.67
1969.61	-3.67	-1.88
1969.73	-3.56	-2.23
1969.77	-3.74	-2.28
1969.82	-3.62	-2.42
1969.87	-3.50	-2.41
1969.92	-3.32	-2.34
1969.97	-3.13	-2.25
1970.02	-2.91	-2.11
1970.07	-2.73	-1.93
1970.11	-2.73	-1.76
1970.16	-2.74	-1.72
1970.21	-2.69	-1.67
1970.31	-2.77	-1.57
1970.41	-3.16	-1.45
1970.51	-3.36	-1.13
1970.61	-3.66	-1.47
1970.71	-3.83	-1.60
1970.78	-3.82	-2.03
1970.85	-3.55	-2.23
1970.92	-3.48	-2.22
1970.99	-3.49	-2.19
1971.05	-3.19	-2.19
1971.12	-2.94	-2.16
1971.19	-2.75	-2.15
1971.26	-2.68	-1.34
1971.38	-3.24	-1.44
1971.49	-3.44	-1.74
1971.60	-3.69	-2.10
1971.70	-3.48	-2.26
1971.80	-3.40	-2.39
1971.90	-3.30	-2.43
1972.00	-3.03	-2.62
1972.10	-3.09	-2.69
1972.20	-2.85	-2.39
1972.30	-2.72	-2.32
1972.36	-2.76	-2.08
1972.42	-2.90	-1.90
1972.48	-2.83	-1.63
1972.54	-3.00	-1.81
1972.60	-3.23	-2.02
1972.66	-3.39	-2.21

Time	δ^{18}O [‰] vs. PDB BDA 225	δ^{13}C [‰] vs. PDB BDA 225
1984.25	-2.37	-1.99
1984.46	-2.65	-1.88
1984.66	-2.96	-1.97
1984.76	-2.84	-1.97
1984.86	-2.88	-2.29
1984.95	-2.89	-2.38
1985.05	-2.68	-2.81
1985.15	-2.80	-2.65
1985.25	-2.40	-2.80
1985.27	-2.51	-2.48
1985.34	-2.53	-2.26
1985.42	-2.51	-2.20
1985.49	-2.78	-2.35
1985.57	-2.55	-2.18
1985.65	-3.03	-2.25
1985.72	-2.93	-2.77
1985.80	-2.95	-2.88
1985.87	-2.91	-2.78
1985.95	-2.80	-2.76
1986.02	-2.74	-2.83
1986.10	-2.60	-2.87
1986.17	-2.57	-2.79
1986.25	-2.55	-2.33
1986.29	-2.57	-2.13
1986.34	-2.62	-1.80
1986.38	-2.76	-2.12
1986.43	-2.83	-2.08
1986.47	-2.65	-2.25
1986.51	-2.89	-2.37
1986.56	-2.98	-2.42
1986.60	-3.07	-2.48
1986.65	-3.08	-2.59
1986.75	-3.03	-2.75
1986.85	-2.89	-2.84
1986.95	-2.82	-3.08
1987.05	-2.70	-3.16
1987.15	-2.73	-2.32
1987.25	-2.57	-2.85
1987.34	-2.66	-2.61
1987.43	-2.58	-2.53
1987.52	-2.68	-2.48
1987.62	-2.78	-2.48
1987.71	-2.78	-2.35
1987.80	-2.91	-2.29
1987.89	-2.86	-2.38

Table 6.5 continued

Time	$\delta^{18}O$ [‰] vs. PDB BDA 229	$\delta^{13}C$ [‰] vs. PDB BDA 229
1982.39	-3.22	-2.34
1982.45	-3.20	-2.44
1982.50	-3.37	-2.55
1982.55	-3.32	-2.69
1982.61	-3.43	-2.75
1982.66	-3.35	-2.61
1982.72	-3.32	-2.59
1982.77	-3.36	-2.41
1982.83	-3.04	-2.20
1982.88	-3.20	-2.21
1982.94	-3.27	-2.24
1982.99	-3.32	-2.50
1983.05	-3.04	-2.06
1983.10	-3.12	-1.86
1983.16	-2.94	-1.89
1983.22	-2.86	-1.82
1983.26	-3.07	-2.10
1983.30	-3.09	-2.05
1983.34	-3.09	-1.75
1983.38	-3.11	-2.23
1983.42	-3.20	-2.17
1983.47	-3.32	-2.39
1983.51	-3.33	-2.52
1983.55	-3.34	-2.78
1983.59	-3.36	-2.79
1983.66	-3.29	-2.88
1983.72	-3.07	-2.90
1983.79	-3.12	-2.93
1983.86	-3.03	-2.79
1983.92	-2.87	-2.62
1983.99	-2.85	-2.70
1984.05	-2.82	-2.57
1984.12	-2.82	-2.37
1984.19	-2.91	-2.41
1984.25	-2.78	-2.12
1984.29	-3.07	-2.34
1984.32	-3.04	-2.21
1984.35	-2.90	-2.41
1984.38	-3.14	-2.44
1984.41	-3.18	-2.31
1984.44	-3.13	-2.45
1984.48	-3.32	-2.67
1984.51	-3.42	-2.79
1984.54	-3.25	-2.76
1984.57	-3.45	-2.93
1984.67	-3.23	-3.28
1984.76	-3.11	-3.20
1984.86	-3.10	-3.13
1984.96	-2.97	-3.12
1985.06	-2.88	-3.01
1985.15	-2.75	-2.64
1985.25	-2.70	-2.50
1985.35	-2.77	-2.41
1985.45	-2.88	-2.41
1985.55	-3.03	-2.49

Time	$\delta^{18}O$ [‰] vs. PDB BDA 134	$\delta^{13}C$ [‰] vs. PDB BDA 134
1972.73	-3.45	-2.06
1972.79	-3.63	-2.17
1972.86	-3.55	-2.32
1972.94	-3.48	-2.33
1973.02	-3.38	-2.31
1973.09	-3.27	-2.18
1973.17	-3.11	-2.17
1973.24	-2.88	-2.24
1973.29	-3.00	-2.16
1973.33	-3.08	-1.98
1973.38	-3.20	-2.06
1973.42	-3.42	-2.12
1973.47	-3.50	-2.24
1973.51	-3.50	-2.16
1973.56	-3.53	-2.22
1973.60	-3.54	-2.29
1973.75	-3.57	-2.24
1973.83	-3.55	-2.47
1973.92	-3.52	-2.37
1974.00	-3.43	-2.26
1974.09	-3.21	-2.34
1974.17	-3.20	-2.11
1974.26	-3.13	-1.88
1974.34	-3.19	-1.90
1974.42	-3.25	-1.87
1974.51	-3.44	-1.93
1974.59	-3.56	-2.06
1974.67	-3.67	-2.05
1974.73	-3.46	-2.11
1974.79	-3.41	-2.38
1974.85	-3.57	-2.35
1974.91	-3.46	-2.48
1974.97	-3.31	-2.43
1975.03	-3.32	-2.31
1975.09	-3.29	-2.22
1975.14	-3.22	-1.94
1975.20	-3.19	-1.99
1975.27	-3.03	-2.06
1975.32	-3.13	-1.98
1975.37	-3.16	-2.06
1975.42	-3.28	-2.18
1975.47	-3.31	-2.19
1975.52	-3.55	-2.30
1975.57	-3.59	-2.41
1975.62	-3.70	-2.42
1975.68	-3.63	-2.33
1975.74	-3.61	-2.40
1975.80	-3.42	-2.39
1975.86	-3.44	-2.36
1975.92	-3.34	-2.18
1975.99	-3.22	-2.11
1976.05	-3.06	-2.17
1976.11	-2.87	-2.02
1976.18	-2.87	-2.11
1976.25	-2.94	-2.11

Time	$\delta^{18}O$ [‰] vs. PDB BDA 225	$\delta^{13}C$ [‰] vs. PDB BDA 225
1987.97	-2.78	-2.49
1988.06	-2.77	-2.61
1988.15	-2.71	-2.48
1988.24	-2.60	-2.23
1988.29	-2.67	-2.10
1988.33	-2.67	-2.04
1988.38	-2.69	-2.00
1988.43	-2.82	-2.13
1988.48	-2.96	-2.09
1988.53	-3.01	-2.09
1988.58	-3.07	-2.22
1988.63	-3.20	-2.39
1988.67	-3.17	-2.63
1988.72	-3.25	-2.76
1988.77	-3.12	-2.77
1988.82	-3.11	-2.88
1988.87	-2.97	-2.83
1988.92	-2.91	-2.76
1988.97	-2.72	-2.68
1989.02	-2.75	-2.44
1989.06	-2.77	-2.39
1989.11	-2.78	-2.33
1989.16	-2.70	-2.29
1989.28	-2.86	-2.26
1989.40	-2.96	-2.16
1989.52	-3.07	-2.26
1989.64	-3.21	-2.38
1989.76	-3.28	-2.84
1989.81	-3.26	-2.81
1989.85	-3.11	-2.98
1989.90	-3.11	-3.00
1989.95	-2.93	-3.01
1989.99	-2.80	-3.21
1990.04	-2.79	-3.05
1990.09	-2.70	-2.83
1990.13	-2.64	-2.50
1990.18	-2.60	-2.30
1990.25	-2.71	-2.42
1990.32	-2.79	-2.23
1990.39	-3.07	-2.21
1990.46	-3.06	-2.28
1990.53	-3.10	-2.49
1990.60	-2.99	-2.44
1990.68	-3.21	-2.73
1990.72	-3.14	-2.96
1990.77	-3.17	-3.00
1990.82	-3.06	-3.01
1990.87	-2.98	-3.22
1990.91	-2.86	-3.04
1990.96	-2.84	-3.22
1991.01	-2.55	-3.05
1991.06	-2.58	-2.97
1991.10	-2.57	-2.43
1991.15	-2.58	-2.57
1991.20	-2.46	-2.67

Table 6.5 continued

Time	$\delta^{18}O$ [‰] vs. PDB BDA 229	$\delta^{13}C$ [‰] vs. PDB BDA 229
1985.65	-3.13	-2.41
1985.72	-3.01	-2.45
1985.80	-3.10	-2.28
1985.87	-3.02	-2.53
1985.95	-2.87	-2.25
1986.02	-3.03	-2.20
1986.10	-3.02	-1.96
1986.17	-2.98	-1.90
1986.25	-2.75	-1.56
1986.30	-2.92	-1.63
1986.35	-2.87	-1.51
1986.40	-3.05	-1.71
1986.45	-3.03	-1.72
1986.50	-3.08	-1.92
1986.55	-3.24	-2.16
1986.60	-3.21	-2.16
1986.65	-3.23	-2.51
1986.70	-3.14	-2.65
1986.75	-3.13	-2.35
1986.80	-3.19	-2.68
1986.85	-3.12	-2.34
1986.90	-3.19	-2.55
1986.95	-2.94	-2.06
1987.00	-3.02	-2.15
1987.05	-2.95	-2.04
1987.10	-3.09	-1.97
1987.15	-3.06	-1.95
1987.20	-3.01	-1.96
1987.25	-2.85	-2.44
1987.32	-3.00	-2.18
1987.40	-3.10	-2.49
1987.48	-3.17	-2.95
1987.56	-3.05	-2.60
1987.64	-3.04	-2.69
1987.72	-2.99	-2.59
1987.80	-3.37	-2.58
1987.86	-2.83	-2.54
1987.91	-2.78	-2.26
1987.96	-2.56	-2.09
1988.02	-2.58	-2.07
1988.07	-2.80	-2.00
1988.13	-2.79	-2.14
1988.18	-2.75	-1.95
1988.23	-2.71	-1.80
1988.26	-2.73	-1.61
1988.29	-2.81	-1.77
1988.32	-2.58	-1.38
1988.35	-2.76	-1.37
1988.38	-2.86	-1.60
1988.41	-2.86	-1.31
1988.44	-2.97	-1.41
1988.46	-3.14	-1.49
1988.49	-3.10	-1.71
1988.52	-3.19	-1.88
1988.55	-3.26	-2.13

Time	$\delta^{18}O$ [‰] vs. PDB BDA 134	$\delta^{13}C$ [‰] vs. PDB BDA 134
1976.32	-3.24	-2.11
1976.40	-3.34	-2.10
1976.47	-3.63	-2.16
1976.54	-3.57	-2.45
1976.62	-3.80	-2.50
1976.67	-3.89	-2.32
1976.75	-3.65	-2.38
1976.82	-3.67	-2.36
1976.90	-3.36	-2.23
1976.98	-3.36	-2.17
1977.05	-3.10	-2.04
1977.13	-3.14	-1.87
1977.21	-2.98	-2.04
1977.27	-3.12	-1.74
1977.33	-3.09	-1.67
1977.39	-3.23	-1.76
1977.45	-3.40	-2.00
1977.51	-3.61	-2.08
1977.57	-3.71	-2.14
1977.63	-3.71	-2.20
1977.74	-3.69	-2.20
1977.86	-3.40	-2.25
1977.97	-3.25	-2.05
1978.09	-3.14	-2.01
1978.21	-3.06	-1.82
1978.29	-3.09	-1.67
1978.38	-3.22	-1.50
1978.46	-3.38	-1.58
1978.54	-3.65	-1.73
1978.63	-3.80	-1.93
1978.71	-3.86	-1.92
1978.79	-3.70	-2.08
1978.87	-3.66	-2.09
1978.94	-3.65	-2.02
1979.02	-3.53	-2.11
1979.10	-3.55	-1.84
1979.18	-3.38	-1.35
1979.26	-3.24	-1.68
1979.35	-3.34	-1.62
1979.44	-3.45	-1.89
1979.53	-3.45	-1.84
1979.62	-3.62	-1.83
1979.72	-3.63	-1.78
1979.81	-3.54	-2.10
1979.91	-3.59	-1.92
1980.01	-3.45	-2.16
1980.10	-3.30	-2.25
1980.20	-3.13	-2.02
1980.28	-3.15	-1.85
1980.36	-3.19	-1.77
1980.43	-3.36	-1.75
1980.52	-3.58	-1.59
1980.59	-3.56	-1.84
1980.67	-3.78	-1.84
1980.74	-3.54	-2.20

Time	$\delta^{18}O$ [‰] vs. PDB BDA 225	$\delta^{13}C$ [‰] vs. PDB BDA 225
1991.26	-2.73	-2.88
1991.32	-2.87	-2.76
1991.38	-3.14	-2.79
1991.45	-3.17	-2.79
1991.51	-3.20	-2.93
1991.57	-3.23	-2.94
1991.63	-3.38	-3.10
1991.69	-3.44	-3.19
1991.74	-3.43	-3.24
1991.80	-3.33	-3.39
1991.85	-3.20	-3.47
1991.90	-3.24	-3.30
1991.96	-3.08	-3.42
1992.01	-2.82	-3.20
1992.06	-3.00	-3.07
1992.11	-2.85	-3.06
1992.17	-2.81	-2.93
1992.22	-2.71	-2.97
1992.28	-2.86	-2.94
1992.34	-2.96	-2.90
1992.40	-3.14	-2.85
1992.46	-3.23	-2.97
1992.52	-3.30	-3.17
1992.58	-3.37	-3.13
1992.64	-3.44	-3.12
1992.70	-3.55	-3.16
1992.75	-3.52	-3.26
1992.79	-3.51	-3.40
1992.84	-3.46	-3.54
1992.89	-3.32	-3.62
1992.94	-3.31	-3.45
1992.98	-3.09	-3.57
1993.03	-3.08	-3.69
1993.08	-3.01	-3.35
1993.13	-2.93	-3.14
1993.17	-2.88	-2.99
1993.22	-2.78	-2.86
1993.27	-2.81	-2.94
1993.33	-2.82	-2.72
1993.38	-2.81	-2.82
1993.44	-3.01	-2.83
1993.49	-2.94	-2.80

Table 6.5 continued

Time	$\delta^{18}O$ [‰] vs. PDB BDA 229	$\delta^{13}C$ [‰] vs. PDB BDA 229
1988.58	-3.37	-2.18
1988.61	-3.18	-2.30
1988.64	-3.27	-2.45
1988.67	-3.61	-2.68
1988.69	-3.65	-2.96
1988.72	-3.98	-3.40
1988.75	-3.66	-3.21
1988.78	-3.71	-3.40
1988.81	-3.77	-3.55
1988.84	-3.79	-3.75
1988.87	-3.79	-3.76
1988.90	-3.35	-3.76
1988.93	-3.61	-3.75
1988.96	-3.46	-3.67
1988.99	-3.47	-3.67
1989.02	-3.39	-3.49
1989.04	-3.24	-3.42
1989.07	-3.21	-3.36
1989.10	-3.18	-3.36
1989.13	-3.08	-3.13
1989.16	-3.04	-2.79
1989.22	-3.14	-2.65
1989.27	-3.05	-2.51
1989.33	-3.10	-2.61
1989.38	-3.30	-2.76
1989.43	-3.10	-2.61
1989.49	-3.32	-2.90
1989.54	-3.31	-2.84
1989.60	-3.49	-2.97
1989.65	-3.48	-2.99
1989.71	-3.49	-3.03
1989.76	-3.60	-3.19
1989.79	-3.52	-3.32
1989.82	-3.57	-3.44
1989.85	-3.38	-3.39
1989.88	-3.52	-3.66
1989.91	-3.47	-3.75
1989.94	-3.40	-3.78
1989.97	-3.33	-3.56
1990.00	-3.22	-3.73
1990.03	-3.29	-4.06
1990.06	-2.92	-3.07
1990.09	-3.01	-3.77
1990.12	-2.98	-3.48
1990.15	-2.99	-3.35
1990.18	-2.74	-3.18
1990.22	-2.82	-3.03
1990.25	-2.95	-3.02
1990.29	-3.22	-2.93
1990.32	-3.09	-3.00
1990.36	-2.93	-2.60
1990.39	-3.25	-2.68
1990.43	-3.22	-2.64
1990.46	-2.95	-2.51
1990.50	-3.22	-2.67

Time	$\delta^{18}O$ [‰] vs. PDB BDA 134	$\delta^{13}C$ [‰] vs. PDB BDA 134
1980.80	-3.62	-2.03
1980.87	-3.56	-2.43
1980.93	-3.36	-2.14
1981.00	-3.45	-2.26
1981.06	-3.12	-2.29
1981.13	-2.94	-2.11
1981.19	-3.06	-2.27
1981.26	-2.86	-2.01
1981.30	-2.97	-1.85
1981.34	-2.97	-1.76
1981.38	-3.05	-1.93
1981.42	-3.21	-1.85
1981.47	-3.50	-1.97
1981.51	-3.73	-2.36
1981.55	-3.63	-2.77
1981.59	-3.88	-2.80
1981.63	-4.00	-2.81
1981.68	-4.07	-2.91
1981.73	-3.94	-2.99
1981.78	-3.88	-2.97
1981.83	-3.70	-3.04
1981.88	-3.50	-2.89
1981.93	-3.50	-2.74
1981.98	-3.21	-2.87
1982.03	-2.99	-2.58
1982.09	-2.94	-2.46
1982.14	-2.81	-2.21
1982.29	-3.08	-2.04
1982.37	-3.23	-2.09
1982.44	-3.61	-1.96
1982.52	-3.51	-3.04
1982.59	-3.99	-2.69
1982.63	-3.65	-2.77
1982.67	-3.68	-3.00
1982.71	-3.70	-2.69
1982.76	-3.50	-2.82
1982.80	-3.70	-3.12
1982.84	-3.19	-2.85
1982.88	-3.08	-2.33
1982.92	-3.21	-2.65
1982.96	-3.06	-2.72
1983.01	-3.14	-2.62
1983.05	-2.96	-2.64
1983.09	-2.93	-2.83
1983.13	-3.30	-2.59

Table 6.5 continued

Time	$\delta^{18}O$ [‰] vs. PDB BDA 229	$\delta^{13}C$ [‰] vs. PDB BDA 229
1990.53	-3.20	-2.74
1990.57	-3.23	-2.92
1990.60	-3.61	-2.87
1990.64	-3.21	-2.80
1990.69	-3.54	-3.12
1990.73	-3.43	-3.04
1990.77	-3.35	-3.43
1990.82	-3.50	-3.70
1990.86	-3.31	-3.66
1990.90	-3.16	-3.56
1990.95	-3.25	-3.64
1990.99	-2.90	-3.42
1991.04	-3.04	-3.39
1991.08	-2.98	-3.51
1991.12	-2.82	-3.41
1991.17	-2.81	-3.15
1991.21	-2.90	-2.79
1991.25	-2.79	-2.64
1991.34	-2.96	-2.62
1991.42	-3.17	-2.80
1991.50	-3.11	-2.56
1991.59	-3.20	-3.00
1991.67	-3.12	-2.94
1991.75	-3.10	-2.77
1991.84	-3.14	-2.80
1991.92	-2.98	-2.57
1992.00	-3.04	-2.39
1992.08	-2.96	-2.30
1992.17	-3.05	-2.32
1992.25	-2.69	-1.66

Table 6.6 Annual mean values of coral skeletal stable oxygen ($\delta^{18}O$ [‰]) and carbon isotope ($\delta^{13}C$ [‰]) composition in BDA229, BDA 134 and BDA 225, calculated from the high-resolution data given in Table 6.5. The data cover the period between 1969 and 1992. They were obtained as described in Chapter 4 and are used in that section.

Year	Annual mean $\delta^{18}O$ [‰]vs. PDB **BDA 229**	Annual mean $\delta^{13}C$ [‰] vs. PDB **BDA 229**	Annual mean $\delta^{18}O$ [‰]vs. PDB **BDA 134**	Annual mean $\delta^{13}C$ [‰] vs. PDB **BDA 134**	Annual mean $\delta^{18}O$ [‰]vs. PDB **BDA 225**	Annual mean $\delta^{13}C$ [‰] vs. PDB **BDA 225**
1993						
1992	-3.01	-2.93			-3.17	-3.17
1991	-3.16	-3.16			-3.01	-2.99
1990	-3.32	-3.15			-2.92	-2.72
1989	-3.21	-2.46			-2.97	-2.62
1988	-2.99	-2.34			-2.91	-2.43
1987	-3.06	-2.09			-2.73	-2.54
1986	-2.92	-2.49			-2.79	-2.49
1985	-2.90	-2.64			-2.72	-2.58
1984	-3.11	-2.38				
1983	-3.19	-2.43				
1982	-2.90	-2.45	-3.35	-2.63		
1981	-2.91	-1.60	-3.44	-2.36		
1980			-3.43	-1.94		
1979			-3.48	-1.82		
1978			-3.47	-1.85		
1977			-3.34	-2.02		
1976			-3.38	-2.22		
1975			-3.36	-2.25		
1974			-3.38	-2.12		
1973			-3.34	-2.22		
1972			-3.14	-2.19		
1971			-3.19	-1.76		
1970			-3.21	-1.93		
1969			-3.35	-1.95		